HELIOS SOLAR STORM SCENARIO

Centre for
Risk Studies

UNIVERSITY OF CAMBRIDGE
Judge Business School

AIG

Research Project Team

Helios Solar Storm Scenario Project Lead
Dr Michelle Tuveson, *Executive Director*
Tamara Evan, *Coordinating Editor*

Helios Solar Storm Scenario Project Contributers
Dr Andrew Coburn, *Director of Advisory Board*
Professor Daniel Ralph, *Academic Director*
Simon Ruffle, *Director of Technology Research and Innovation*
Dr Edward Oughton, *Research Associate*
Dr Andrew Skelton, *Research Associate*
Jennifer Copic, *Research Assistant*
Viktorija Kesaite, *Research Assistant*
Jaclyn Zhiyi Yeo, *Research Assistant*

Cambridge Centre for Risk Studies Research Team
Dr Shahzeb Malik, *Research Associate*
Eireann Leverett, *Senior Risk Researcher*
Dr Louise Pryor, *Senior Risk Researcher*
Dr Duncan Needham, *Senior Risk Researcher*
Dr Jay Chan Do Jung, *Risk Researcher*
Dr Andrew Chaplin, *Risk Researcher*
Arjun Mahalingam, *Research Assistant*
Dr Ali Shaghaghi, *Research Assistant*
Jessica Tsang, *Research Assistant*
Shaheera Asante, *Editorial Assistant*

Consultant and Collaborators
Professor Richard Horne of the *British Antarctic Survey*
Dr Helen Mason, Assistant Director of Research, *University of Cambridge Department of Applied Mathematics and Theoretical Physics*
Dr Alan Thomson, *Head of Geomagnetism*, *British Geological Survey*
Professor Emeritus C. Trevor Gaunt, *University of Cape Town*

Cambridge Centre for Risk Studies
Website and Research Platform

http://risk.jbs.cam.ac.uk/

Helios Solar Storm
Technology Catastrophe Stress Test Scenario

Contents

Helios Solar Storm - Stress Test Scenario

1   Executive Summary

The study of solar eruptive phenomena has progressed over the centuries from scholarly recordings of astronomical events, such as sunspots, to advanced modelling of how solar activity may drive geophysical planetary responses, e.g., geomagnetic disturbances. However, there is still a great deal of uncertainty around the potential economic impacts of extreme space weather on modern society.

In this report, we provide a catastrophe scenario for a US-wide power system collapse that is caused by an extreme space weather event affecting Earth: the Helios Solar Storm scenario.

This scenario is a stress test for managers and policy-makers. Stress tests are important for understanding risk exposure across a spectrum of extreme systemic shocks such as those proposed in the Cambridge Taxonomy of Threats, which encompasses a dozen major classes of catastrophes. A suite of scenarios can be used as a basis for calibrating an organisation's inherent risk, vulnerability and resilience.

Helios Solar Storm Scenario

This scenario describes how an extreme space weather event can cause direct damage and indirect debilitation of high voltage transmission grids in the USA, resulting in power blackouts along with consequential insurance claims and economic losses. Over the past decade, there have been a number of analyses of the potential effects of extreme space weather on the electricity transmission network.[1] This report adds to this literature by providing a transparent economic analysis of the potential costs associated with such an event.

We estimate a range of US insurance industry losses resulting from three variants of the scenario which explore different damage distributions and restoration periods, culminating in losses between $55.0 and $333.7 billion. At the low end, this is roughly double the insurance payouts of either Hurricane Katrina or Superstorm Sandy, and similar to the total insured losses from all catastrophes in 2015.

Overall economic losses are evaluated from two perspectives. First, we estimate global supply chain disruption footprints that stem from suspended business and production activity directly caused by power outages in the US. This perspective provided a detailed industry sector breakdown of potential economic losses but does not account for the dynamic response of the economy. Global supply chain disruptions are conservatively estimated to range from $0.5 to $2.7 trillion across the three scenario variants.

Second we employ a global integrated economic model to estimate losses in global GDP over a five year period relative to a baseline projection – our standard loss metric referred to as GDP@Risk. Importantly, this perspective accounts for post-catastrophe dynamic responses in the global economy, including, for example, changes in monetary policy. For this reason our GDP@Risk estimates are lower than our estimated static losses from supply chain disruptions. The Helios Solar Storm has a global GDP@Risk ranging from $140 to $613 billion across the three scenario variants (representing between 0.15% and 0.7% of global GDP over the projected five year period).

Selection of a space weather scenario as a disruptor of infrastructure

Anomalous behaviour of US telegraph operations in the mid-1800s, especially during the 1859 Carrington Event, brought about the recognition that solar activity can affect human technology.

Although extreme space weather events include a variety of phenomena like Solar Particle Events (SPEs) and bursts of electromagnetic radiation from solar flares, it is very fast Carrington-sized Coronal Mass Ejections (CMEs) which are mostly associated with the geomagnetic disturbances (GMDs) that are severe enough to cause power grid failure. A severe CME has the potential to generate geomagnetically induced currents (GICs) that could cause permanent damage to Extra High Voltage (EHV) transformers. Such high value assets are not easy to procure and replace in the short-term.

Failure in these critical assets could cause system-wide instability issues leading to cascading failure across the electricity system, passed on to other critical interdependent infrastructures such as transportation, digital communications and our vital public health systems. This disruption could also cause considerable disruption to business activities.

---

[1]   See Space Studies Board, 2008; Organization for Economic Co-operation and Development, 2011; JASON, 2011; North American Electric Reliability Corporation, 2012; Cannon et al, 2013.

Our impact analysis is underpinned by some key methodological contributions which include deriving bottom- up, state-level restoration curves, which show how long it takes to restore the supply of electricity after the extreme space weather event, based on key risk factors including geomagnetic latitude and deep-earth ground conductivity. Disruptions in electricity supply are mapped to state-level industrial output by industrial sector, and are aggregated to the US national level. This yields direct economic loss estimates that are then fed into a global multiregional economic input-output model to assess domestic and international supply chain disruptions. These estimates are themselves a basis for applying a dynamic economic equilibrium model to gauge how the USA and its trading partners recover from this shock over time.

Variants of the scenario

The Helios Solar Storm scenario depicts a geomagnetic disturbance that generates GICs capable of damaging or even destroying EHV transformers. Through direct damage and indirect debilitation of the power grid, an extreme space weather event can cause immediate blackouts, leading to insurance payouts and supply chain interruptions. For the purposes of this report we only account for the **impact directly on the USA and indirectly on major trading partners**.

Beyond appealing to the scientific and industrial literature, the scope of the extreme space weather event and its expected consequences are based on workshops and interviews with subject matter specialists in space physics, economics, catastrophe modelling, actuarial science, and law; insurance specialists in property, casualty and space insurance; and key representatives from utility companies, government agencies, industry bodies, and engineering consultancies. However, the analysis and determination of impacts is our own and does not imply endorsement of these views by the specialists consulted.

This report proposes three scenario variants (S1, S2 & X1) to span the evidence and expert opinion on electrical damage inflicted by extreme space weather. The S1 variant is considered our basic or baseline scenario. It involves limited damage to EHV transformers in the US, with only 5% of those units suffering any damage, and restoration periods of moderate length. S1 represents an optimistic view that a massive geomagnetic storm would cause limited damage due to an initial grid collapse. This would isolate any further damage to the transmission network, allowing the grid to be re-started after the storm passes. The S2 variant assumes greater

damage levels but similar restoration times, reflecting uncertainty about how much damage the components of a power grid might be exposed to in extremis. The X1 scenario is deliberately extreme, and reflects the Kappenman (2010) perspective, with similar damage levels to the S2 scenario but with longer restoration periods.[2] The scenario is used to explore the upper bound for the economic and insurance loss estimates. Indeed, this is considered by some to reflect an overly pessimistic view of vulnerability of the electricity transmission system to GICs. Opponents of this perspective do not necessarily disagree with the long replacement times for damaged EHV transformers, but instead disagree with the severity of the damage distribution to the assets themselves.

This is a stress test, not a prediction

This report is one of a series of stress test scenarios that have been developed by the University of Cambridge Centre for Risk Studies to explore management processes for dealing with extreme shocks. It does not predict when a catastrophe may unfold. Indeed, it does not also provide definitive economic and insurance loss estimates, as there is still widespread disagreement between different schools of thought. It does however provide insight into the range of exposure that may be experienced based on different expert opinions of extreme space weather events.

An extreme space weather event

Spots on the surface of the Sun

A cluster of sun spots produces a relatively moderate CME, leading heliophysicists at the U.S. National Oceanic and Atmospheric Administration (NOAA) to predict a moderately sized geomagnetic storm in four days' time. Three days later, a second very large CME is thrown outwards towards Earth, accompanied by a massive solar flare that produces a radiation storm. This CME reaches a very high speed that is sustained in its path towards Earth due to the previous CME which has lowered the ambient solar wind density.

A Carrington-sized CME slams Earth

The front of the first and moderate CME is preceded by a 30-60 minute warning from space weather satellites. The second CME arrives on the heels of the first but travelling much faster and carrying much higher levels of energy. As the first CME is only moderate in size it is not deemed a major risk and utility operators do not implement their emergency plans.

By the time the second CME is detected there is not enough time to fully implement all mitigation

---

[2]   See JASON, 2011 for further details.

measures by the time it arrives at Earth. Satellites suffer significant damage from solar radiation. On Earth many EHV transformers are affected from the geomagnetic storm, particularly those in high geomagnetic latitudes. Some transformers are damaged or even destroyed, while others are tripped off by the network operators. Transformers are at greatest risk at locations with a high geomagnetic latitude and where there is a highly resistive deep-earth ground conductivity structure.

Restoration in the aftermath

The ability to restore power depends on availability of skilled engineers to assess and either re-set, commission repairs, or replace damaged units. Replacing severely damaged transformers can be slow – over a period of months – if many new units are required because of the bespoke nature of large capacity high voltage units and the limited stocks of such units. In the S1 scenario most of the affected population has power restored within a few hours while 15% of those affected remain without power for up to three months or longer. In the X1 scenario, more people are affected and some 10% of those lack power for a ten-month period.

Summary of impacts

Direct economic losses

The damage distributions resulting from the extreme space weather event in the S1 scenario show a quarter of US EHV transformers are tripped off-line with only 5% suffering any form of damage. The loss of these assets leads to a power outage initially affecting 90 million US citizens. The majority of those affected have power restored relatively quickly, with only 5% of the total US population being disconnected for more than three days. The US states most directly affected are Illinois and New York with direct losses from suspended economic activity of roughly $30 billion each in S1.

In both the S2 and X1 scenarios 33% of transformers are tripped off-line, 14% sustain minor damage, 3% sustain major damage and 0.2% are completely destroyed. The loss of these assets leads to a power outage initially affecting 145 million US citizens.

The difference in these scenarios is the time it takes for power to be restored. In the X1 scenario, with a significantly longer duration, 15% of the total US population remain disconnected for more than three days. Illinois and New York see direct economic losses of roughly $170 billion and $150 billion respectively in X1.

The total direct shock to value-added activities in the US economy as a result of power failure amounts to $220 billion for S1, $700 billion for S2 and $1.2 trillion for X1, corresponding to 1.4%, 4.6% and 8.1% of US GDP, respectively.

US and international supply chain impacts

The total indirect US supply chain shock is similar size to the direct shock. International supply chain shocks, stemming both upstream via US imports and downstream via US exports, are estimated to be roughly a quarter the size of the overall direct US shock. With overall supply chain disruptions estimated to be as high as $470 billion for S1, $1.5 trillion in S2 and $2.7 trillion in X1 (representing economic losses of 0.7%, 2.2% and 3.9% of global GDP, respectively), the economic impact of these scenario variants is likely to be very significant, potentially leading to major policy interventions such as interest rate adjustments and short-term stimulus measures.

At the industry sector level, US Manufacturing, with the largest gross value added (GVA) of $1.9 trillion, has both the greatest direct ($30 billion in S1 to $170 billion in X1) and indirect ($30 billion in S1 to $180 billion in X1) shocks, with indirect shocks having a roughly equal split between those that have been induced upstream and those induced downstream. China, Canada and Mexico, as the three largest trade partners of the US, collectively account for about a third of all indirect international supply chain impacts, ranging from $20 billion in S1 to $100 billion in X1.

GDP Losses over five years

The scenario variants characterise different shares of the US population experiencing power outage for different durations. We translate these restoration curves into more specific shocks in terms of private and government consumption, productivity (via hours worked), investment, exports, imports and confidence. These variable- specific shocks then become the basis for shocking the overall US economy, within the Global Economic Model (GEM) of Oxford Economics. The integrated economic model solves to find a state of equilibrium with associated deviations in US and global GDP from baseline projections.

In S1, the total estimated US GDP@Risk is $135 billion, or 0.15% of the five-year baseline GDP projection for the US economy, whereas the global GDP@Risk is $140 billion (0.03% of the global GDP projection). In X1, US GDP@Risk is $610 billion (0.7% of the US GDP projection), whereas the global GDP@Risk of $1.1 trillion is roughly a quarter of the five-year baseline global GDP projection.

Insurance losses

We estimate the range of US insurance industry losses for the scenarios described in this report to be between $55.0 billion and $333.7 billion. Just over 90% of this loss is from service interruption within property insurance policies for those that loss power. While only 1% is from direct physical property damage. Other insurance lines such as Space, Directors and Officers, Homeowners and Speciality contribute to total insured losses.

By comparison, Swiss Re studies estimate insurances losses from Hurricane Katrina and Superstorm Sandy as $45 and $35 billion, respectively (Swiss Re, 2006; Swiss Re 2013), and total insured losses from catastrophes in 2015 as $85 billion (Swiss Re, 2015).

Past events led to relatively short outages that would be within the waiting periods of most property insurance policies. However, the event contemplated in this report assumes a much longer outage that would extend beyond the typical waiting period.

Conclusion

This report contributes to the understanding of the range of economic and insurance impacts of extreme space weather, and makes a number of key methodological contributions relevant for future economic impact assessment. Understanding the economic impact of space weather risks can improve mitigation procedures and practices, and guide where limited resources should be allocated to improve economic resilience. Moreover, in industry it is not just electricity utility companies who are concerned with catastrophe scenarios; the potential losses to consumers of power and to insurance companies due to casualty and business interruption pay-outs are significant.

Narrowing the range of geomagnetic effects following a given solar event, specifically the systemic effect on the electricity transmission network and its key assets, is necessary. Moreover, ongoing work is needed to implement mitigation provisions and response plans which include the rollout of temporary generation facilities and short-term portable replacement transformers. This is consistent with a call by the US National Space Weather Action Plan (National Science and Technology Council, 2015) for improved assessment, modelling, and prediction of the impact of this threat on critical infrastructure systems. Given the uncertainty that exists in this area of research, what is required in the wake of this report is for space physicists, geophysicist and electrical engineers to work collaboratively on improving the estimation of the economic impacts of extreme space weather.

2   Introduction to Space Weather

What is space weather?

Space weather can be defined as disturbances of the upper atmosphere and near-Earth space that can disrupt a wide range of technological systems (Hapgood et al. 2012). It can arise from many different types of eruptive phenomena associated with solar activity taking place on the surface of the sun (often referred to as a 'solar storm'). On average, the Sun's magnetic activity follows an 11 year solar cycle, with variable minimum and maximum sunspot periods. Solar cycle 24 began in 2008 with minimal sunspot activity until 2010. We are now in the declining phase of the solar cycle where intense activity has previously been more prevalent than other periods (Juusola et al. 2015).

The strength and complexity of the Sun's evolving global magnetic field changes throughout the solar cycle, manifesting as regions of concentrated magnetic field in the photosphere known as sunspots. Through this cycle, the magnetic field in the solar atmosphere alters from a magnetically simple state to a magnetically complex configuration, leading to an increasing number of sunspots (Green and Baker, 2015). While there may be more solar activity during some parts of the solar cycle, solar eruptive phenomena are still the result of a random process. Therefore, there is the potential for this to cause an extreme space weather event affecting Earth at any time.

There are three primary forms of solar activity which drive extreme space weather, as shown in Figure 1.

- **Coronal Mass Ejections (CMEs)** – CMEs are massive explosions of billions of tonnes of charged particles and magnetic field thrown out into space (Webb and Howard, 2012).

- **Solar Proton Events (SPEs)** – SPEs are a huge increase in energetic particles, mainly of protons but also heavy ions, thrown out into space (Shea and Smart, 2012). They may be related to CMEs and solar flares.

- **Solar flares** – Solar flares are a rapid release of electromagnetic energy previously stored in inductive magnetic fields. Emitted radiation covers most of the electromagnetic spectrum, from radio waves to x- rays (Fletcher et al. 2011).

Extreme space weather results from these eruptive solar phenomena. When occurring in combination, Earth may first be bombarded with initial radiation (such as X-rays) from a solar flare from eight minutes after the event on the surface of the sun.
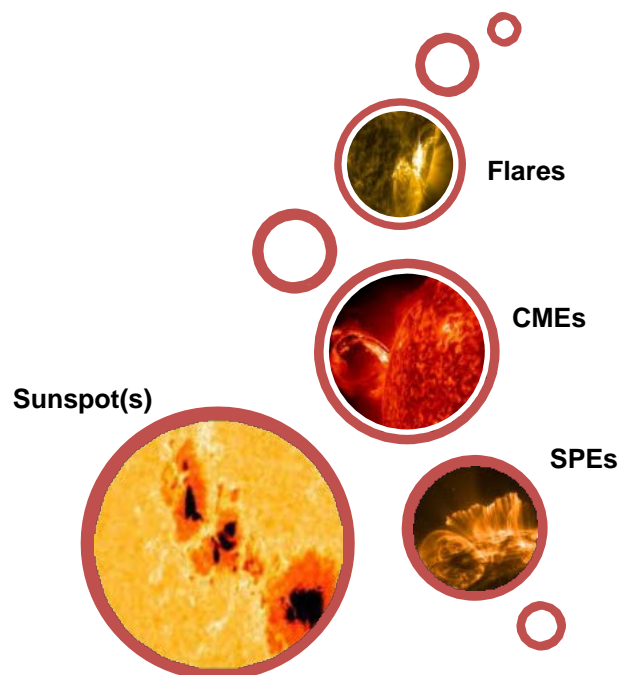
Figure 1: Sunspots are the beginning of various solar phenomena

A second barrage of very-high-energy protons (an SPE) may then arrive anywhere between tens-of-minutes later, and may last for days. The SPE may be followed by a large CME reaching Earth some 14.5 hours or more later. The magnetic field in the CME can cause an extreme geomagnetic storm that can also last for days. The storm drives huge electrical current at high latitudes and bright auroral displays.

CMEs are a key aspect of coronal and interplanetary dynamics, and, as they are associated with the vast majority of solar eruptive phenomena (Webb and Howard, 2012). Moreover, CMEs pose the main risk to Earth and its modern, technological society because large (1012kg), dense (100/cm3) and fast (>500kms-1) CMEs hitting Earth with a southward interplanetary magnetic field direction (Bz) can give rise to extreme geomagnetic disturbances (Möstl 2015; Temmer and Nitta, 2015; Balan et al. 2014). This has the potential to damage key electricity network assets and disrupt the aviation, satellites and GPS on which our economy and society depend. This is particularly problematic because failure in the power sector can cascade to other critical interdependent infrastructure systems, disrupting business activities and inducing a range of other economic and social consequences which can affect the global economy (Ouyang, 2014; Anderson et al. 2007; Haimes and Jiang, 2001; Rinaldi et al. 2001).
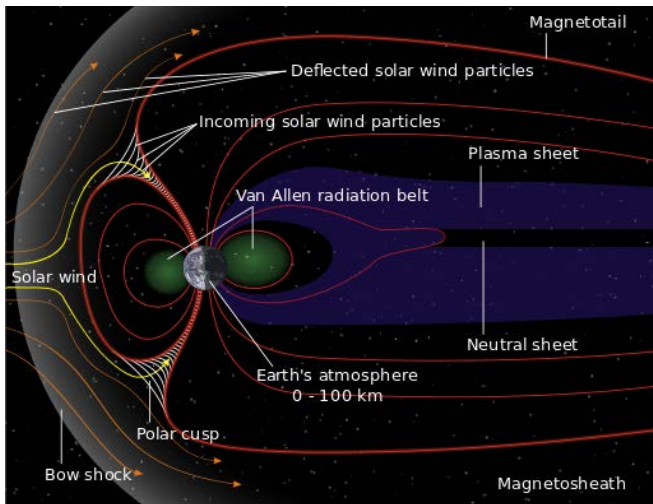
Figure 2: Structure of the magnetosphere. (Image: William Crochot**)**

Once a CME strikes Earth's magnetosphere (Figure 2) it can have a significant impact on the magnetic field and electrical currents that flow within it.[3] A powerful CME with a southward interplanetary magnetic field (relative to Earth's magnetic field) leads to the largest interaction effect. While the aurora are often seen during modest forms of geomagnetic activity, they are generally enhanced by large CMEs interacting with Earth's magnetic field, at which point the auroral band can expand equatorward to lower latitudes.

The aurorae are caused by bands of charged particles accelerated along Earth's magnetic field lines into the atmosphere, exciting atmospheric gases that then give off the light we see. Usually these auroae occur in the auroral oval regions encircling Earth's poles are indicative of geomagnetic activity. They can be altered in modest forms by the solar wind or in more extreme circumstances by a CME interacting with the planet's atmosphere. Figure 3 shows an example of aurorae in Norway in 2015.

Figure 3: Aurora over Tromsø, Ringvassøya, Norway (2015) (Photograph: Svein-Magne Tunli**)**

---

[3] For a broad overview designed for analysts unfamiliar magnetosphereic physics, see Eastwood et al. (2015).

New analysis of extreme events has shown that in-transit interaction between two closely released CMEs is one potential cause of nonlinear amplification (Liu et al. 2014). Preconditioning of the heliosphere by the first CME, leading to minimal deceleration of the second, greatly increases the ultimate impact on Earth. This was the case in July 2012 when a solar ejection narrowly missed Earth. Analysis of geomagnetic data strongly suggests that this dual occurrence led to previous extreme cases when aurorae were visible at very low latitudes (Vaquero et al. 2008). Given that aurora sightings are a proxy of geomagnetic activity, we know from the analysis of historical records that even low geomagnetic latitudes can be affected by this phenomenon when a severe deformation of Earth's magnetosphere occurs (Willis et al. 2005; Basurah, 2006; Ribeiro, 2011).

During a geomagnetic storm there are many rapid global-scale variations in Earth's field and current systems which occur repeatedly. These are known as substorms. They cause large changes in the time rate-of-change of the magnetic field at the surface (dB/dt). The rapid change in the magnetic field produces geomagnetically induced currents (GICs), which can flow into manmade structures including the electricity transmission network and oil pipelines.

Historical extreme space weather events affecting Earth

Historical accounts record auroral sightings going back millennia. We only have quantified ground-based magnetic data for storms from CMEs since the nineteenth century. A list of major storms since 1859 are summarised as follows (MacAlester and Murtagh, 2014):

1847 – First recorded storm caused "anomalous currents" on telegraph lines in the UK (Cade, 2013).

1859 - The Carrington Event caused significant disruption to telegraph systems (Boteler, 2006; Clauer and Siscoe, 2006).

1870 – A large storm produced aurora sightings as low as the Middle East (Vaquero et al 2008).

1872 – Aurora were sighted as low as 10-20° geomagnetic latitude (Silverman, 2008).

1882 – This storm caused disruption to several US telegraph systems and interrupted trading on the Chicago Stock Market (EIS Council, 2014).

1903 – A very severe storm causing interruption to telegraph systems and transatlantic cables. Switzerland suffered a power outage (EIS Council, 2014).

1909 – Numerous aurora sightings were seen as far south as the 30-35° geomagnetic latitude. There are reports that a telegraph line in Western Australia

functioned without batteries for 30 minutes (Silverman,1995).

1921 – Similar in size to the Carrington Event, a storm caused fires at several telegraph stations in Sweden(Karsberg et al. 1959).

1938 – Interruption to radio communications recorded in Southern Europe (Silverman, 2006).

1940 – Damage caused to the US telephone system (Harang, 1941), and reported effects on the electricity network (Davidson, 1940).

1958 – Transatlantic communications were disrupted between Newfoundland and Scotland (Anderson, 1978). There was a blackout in the Toronto area (Lanzerotti and Gregori, 1986).

1989 – It took only 90 seconds for the entire Quebec power grid to collapse. The well-documented Quebec power outage lasted nine hours (Bolduc, 2002).

2000 – The Bastille Day Event saw a very large CME and flare (Tsurutani et al. 2005).

2003 – The Halloween Storms included a mix of CMEs and flares leading to a one hour power outage in Sweden (Pulkkinen et al. 2005). This storm also led to a radio blackout of high frequency communications, as well as disruption to GPS systems (Bergeot et al. 2010).

Different measures of geomagnetic storms

There are a wide variety of metrics used to measure changes to Earth's magnetic field and these include the Dst, Kp, Ap, G and Dst_{MP} indices. Though there is debate over the best method of measuring geomagnetic activity, the time rate-of-change (dB/dt) of the geomagnetic field best represents the threat to Extra High Voltage (EHV) transformers and the electricity transmission network via geomagnetically induced currents (GICs). The time rate-of-change of the magnetic field is represented by dB/dt and is sometimes measured in nano-Teslas (per unit of time). This captures the rapid dynamic movement of electrical currents >90km above ground, which in the northern hemisphere usually takes place above 50° geomagnetic latitude (Thomson et al. 2011).

However, low-latitude regions are mostly affected by the intensification of the ring current, often represented by the Disturbance Storm Time (Dst) index (Sugiura, 1963), which is a widely used characterisation of geomagnetic activity (Banerjee et al. 2012). Dst_{MP} is a recent development of this, using the mean value of Dst during the main phase of a geomagnetic storm, to represent a high energy input in the magnetosphere-ionosphere system over a short duration (Balan et al. 2016). A negative Dst index value indicates that Earth's magnetic field is weakened, as specifically is the case during extreme geomagnetic activity.

Frequency

Each solar phenomenon (CME, SPE and flares) has a different probability and severity. It is essential that we deconstruct 'space weather' in this way because ultimately it is CMEs that drive the time rate-of-change (dB/dt) of the geomagnetic field, therefore affecting the threat to Extra High Voltage (EHV) transformers. Analysis of past solar cycles shows that CMEs far outnumber the frequency of SPEs and flares, hence why other studies have focused purely on this solar eruptive phenomena (Webb and Howard, 2012). Although, during extreme events, we would likely see a combination of all of these phenomena.

Extreme space weather events occur often, but do not necessarily always affect Earth. Many have reported on the powerful CME that erupted from the Sun on 23rd July 2012 but missed Earth (Intriligator et al. 2015; Temmer and Nitta, 2015; Liou et al. 2014; Baker et al. 2013; Ngwira et al. 2013). Baker et al. 2013 show that with an initial speed of 2500±500km/s, this event could be comparable with the largest events of the twentieth century (Dst~-500nT). The most extreme scenario (Dst=-1182nT) shows that this could have been a considerably larger geomagnetic disturbance than the Carrington Event had it hit Earth (Ibid.).[4]

With limited time series data, estimating the frequency of a very large 1-in-100 or 200 year event is challenging. This type of approach is ultimately required to develop robust estimates of the occurrence frequency of extreme space weather events and then quantify the potential consequences, in order to implement risk mitigation strategies. A range of estimates include (i) a probability of 4-6% of a Carrington-sized event taking place in the next decade (Kataoka, 2013), (ii) a 12% probability of a Carrington-sized event occurring every 79 years (Riley, 2012), and (iii) the likelihood that a Carrington-sized event could take place 1.13 times per century (Love et al. 2015).

Ultimately, a 100-year geomagnetic storm is identified as having a size greater than Carrington (Dst ≤-880 nT) (Love et al. 2015). In contrast, the July 2012 CME which missed Earth has been estimated as being much larger (Dst = -1182nT), and therefore Baker et al. (2013) propose that this be used as the archetypal extreme space weather event for scenario planning purposes. In terms of the dB/dt estimates for geomagnetic activity, Thomson et al. (2011) propose that we could see 1,000-4,000 nT/min (1-in-100 year event) and 1,000-6,000 nT/min (1-in-200 year event).

---

[4] Although the actual size of the Carrington Event is not necessarily conclusive (Saiz et al. 2016; Siscoe et al. 2006).

3   Ground-effects of Extreme Space Weather

Another research challenge is the estimation of the expected geographical footprint of an extreme geomagnetic storm. This section explores the geographical footprint of historical storms based on aurora sightings. We follow Pulkkinen et al. (2012) in that threshold geomagnetic latitude can be also investigated by means of low-latitude auroral observations to provide an indicative location of the auroral region. Indeed, records of aurora sightings are available for certain historical storms as consequently analysed, hence these can be used as a proxy for the geographic footprint of geomagnetic activity. The consequences of GICs on various systems are also summarised.

Geographical footprint

Most aurorae under normal conditions occur in the auroral oval, or the auroral zone between 65-85° geomagnetic latitude, around the magnetic poles (Feldstein, 1986). However, under extreme conditions when Earth's magnetosphere undergoes considerable deformation, the auroral band expands equatorward towards lower latitudes.

The Carrington Event of 1859 has traditionally been regarded as one of the largest global geomagnetic storms (Cannon et al. 2013). Analysis of auroral observations during the Carrington Event shows that they were seen as low as 20° geomagnetic latitude, as shown in Figure 4 (Green and Boardsen, 2006).

Silverman (2008) analyses historic aurora sightings for the storm of 4 February 1872 in order to determine the minimum geomagnetic latitude where aurorae occurred. Table 1 (page 10) summarises the geomagnetic latitude observations for different storms identified in the literature (Pulkkinen et al. 2012; Silverman and Cliver, 2001; Silverman, 1995; Green and Boardsen, 2006; Silverman, 2008).

Thomson et al. (2011) estimate that for a 1-in-100 year event, the maximum impact occurs between 53-62° geomagnetic latitude. Although, limited historical data is available, Pulkkinen et al. (2012) suggest that the 1859 Carrington Event was close to a 1-in-100 year event. The threshold of 50-55° geomagnetic latitude is proposed as a feature of most major or extreme geomagnetic storms, with 50° proposed for conservative estimates and 40° for less conservative estimates. Further work by Ngwira et al. (2013) supports this conclusion. Many notable global cities including New York, London, Chicago, Paris, Frankfurt and Washington DC are above 50°
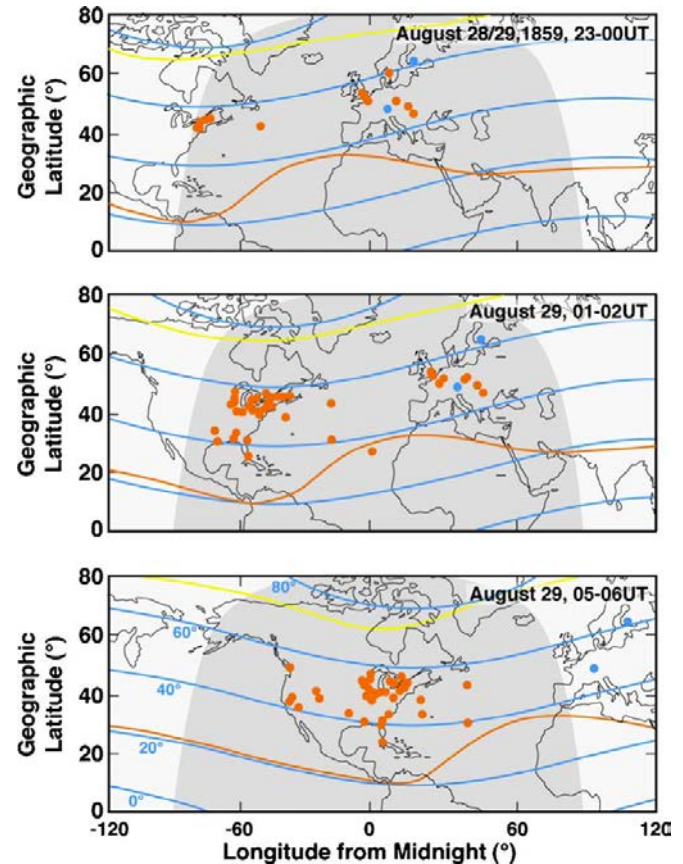
Figure 4: Carrington Event of 1859 aurora observations for 28 August. Grey shaded region represents night time area, centred at local midnight. Below lines represent geomagnetic latitude, orange line shows minimum around 20° and yellow line shows maximum around 70-75° (Image: Green and Boardsen, 2006).

geomagnetic latitude. However, increasingly there is awareness that GIC-risk is still present and a threat to low- latitude regions such as Australia (Marshall et al. 2011; 2013), Brazil (Barbosa et al. 2015; Trivedi et al. 2007), China (Zhang et al. 2015; Liu et al. 2008; 2009), Japan (Watari et al. 2009; Watari, 2015; Fujii et al. 2015), South Africa (Gaunt and Coetzee, 2007), Spain (Torta et al. 2012), and Turkey (Kalafatoğlu et al. 2015).

Table 2 (page 10) shows the probability of extreme geomagnetic activity based on geomagnetic latitude. Figure 5 (page 11) illustrates the global geomagnetic storm threat map. A more detailed threat map of the US and Europe is available in Appendix 1. 38% of the world population resides in zones unlikely to experience geomagnetic activity.

Table 1: Summary of geomagnetic latitude observations. (Silverman, 2008 and Pulkkinen, 2012)

Date	Estimated minimum Dst index values	Geomagnetic Latitude of Aurora Observations, most equartorward latitudes unless otherwise stated
August-September 1859	-850 nT	22-23°, through must activity was observed in this range 30-35° (Silverman, 2008); around 41-48° (Pulkkinen, 2012); 18-25° (Green and Boardsen, 2006)
October 1870	(ΔH at St. Petersburg 457 nT) (Ptitsyna et al. 2012)	28° (Silverman, 2008)
February 1872	(ΔH at Bombay 1,020 nT) (Lakhina et al. 2005)	20°, though an aurora was seen as low as 10° (Silverman, 2008)
September 1909	(ΔH at Potsdam >1,500 nT) (Lakhina et al. 2005)	30-35° (Silverman, 1994)
May 1921	~-900 nT (Kappenman, 2006)	30-35° (Silverman and Cliver, 2001) or at 40° (Pulkkinen, 2012)
March 1989	-589 nT	40° (Pulkkinen, 2012)
October 2003	-383 nT	30-35° (Pulkkinen, 2012)

Table 2: Probability of geomagnetic activity by geomagnetic latitude during an extreme event

| Geomagnetic Latitude Band	Colour	Description
70-85°	Various	Activity less likely to occur around magnetic poles
60-70°	Brown	Auroral oval zone where aurorae typically occur
50-60°	Dark orange	Extreme geomagnetic activity
40-50°	Medium Orange	Severe geomagnetic activity
20-40°	Light Orange	Moderate geomagnetic activity
0-20°	Cream	Unlikely zone for geomagnetic activity

The impact of extreme space weather

Given the range of space weather phenomena previously identified, there are three key effects on Earth which include geomagnetic storms, radio blackouts and radiation storms, as outlined in Table 3.

Presently, the largest risk posed is from extreme geomagnetic activity on the electric grid. There are several factors which influence the severity of effects from GICs from increased load on EHV transformers. The probability of induced damage leading to customer disruptions depends on, firstly, geophysical factors which determine the size of the electric fields in the system and, secondly, the technological characteristics that affect how a system responds to the generated electric field (Boteler et al. 1998; Molinski, 2002). On the one hand, these include the effect of ionospheric currents, the deep-earth ground conductivity structure and geomagnetic latitude while, on the other, also include physical power system characteristics such as the voltage and electrical resistance of the transmission lines, transformer type, transformer connections, and station grounding. Those characteristics which increase the risk posed from a large geomagnetic disturbance include (Gaunt, 2014):

- Severity of storm
  - The mass, density and speed of the CME
  - The strength and direction of the interplanetary magnetic field of the CME relative to Earth's magnetic field
  - Recent CME activity already interacting with the magnetosphere
- Geographic Location
  - High geomagnetic latitudes (with the exception of the polar caps)
  - Highly resistive deep-earth ground conductivity structure
  - Proximity to the coast line (<100km)
  - Those assets at the edges of the electricity network
  - Low population densities and its impact on network topology resilience and investment
- Asset and network characteristics
  - Transmission lines with very high voltages (influencing resistance)
  - Engineering or system protections to prevent GICs

Table 3: Probability of geomagnetic activity by geomagnetic latitude during an extreme event

Impact of Space Weather on Earth	Warning Time	Duration	Primary Extreme Event Impact
Geomagnetic Storm	17 to 90 hours	1 to 2 days	• Possible bulk electricity power grid voltage collapse and damaged to electrical transformers • Interference or loss of satellite and sky wave radio communications due to scintillation • Interference or loss of GPS navigation and timing signals • Satellite operations impacted
Radio Blackout	None (speed of light)	Minutes to 3 hours	• Loss of high-frequency (HF) radio communications on Earth's daylight side • Short-lived (minutes to an hour) loss of GPS • Interference on civilian and military radar systems
Radiation Storm	30 minutes to several hours	Hours to days	• Satellite operations impacted. Loss of satellites possible. • HF blackout in Polar Regions. • Increased radiation exposure to passengers and crew in aircraft at high latitudes
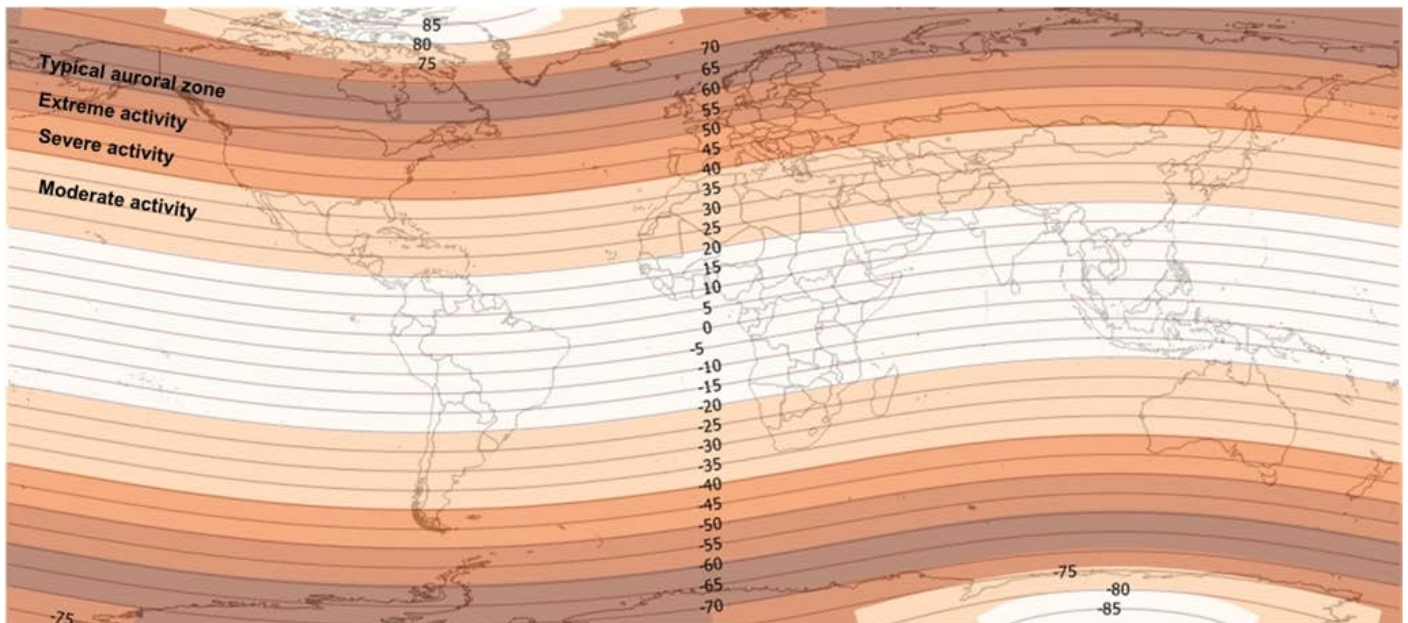
Figure 5: Geomagnetic latitude threat map following a shift in the auroral oval[5]

- ▫ Design of the transformer
  - • Age of transformers
- ▫ Position of transformers within the grid
- ▫ Number of transformers at a transmission station sharing the load
- ▫ Past exposure from previous storms
- ▫ Orientation of transmission lines
- • System operation – does the region run its electricity system at maximum capacity?
- • Geomagnetic storm mitigation/operational planning – what plans are currently in place? Is there a policy to shut the system off or leave it on during a storm?

Areas of risk are related to bands of auroral activity. The two key geophysical factors affecting the production of GIC are geomagnetic latitude and the deep-earth ground conductivity structure. In general, the areas at risk are those in higher geomagnetic latitudes, as they are closer to the band of auroral activity. The more resistive the deep-earth ground conductivity structure, the less likely that GICs will be able to dissipate through Earth, and instead follow the path of least resistance by flowing into the electricity transmission network.

[5] The contour lines on these maps were generated using the World Magnetic Model (WMM) 2015 shape file from NOAA (Chulliat, 2014).

However, calculating reliable estimates of GICs and the geoelectric field require accurate knowledge of the local geological conditions which are not always well known, preventing comprehensive estimation for entire continents (Savani et al. 2013). Often this information is only available for those regions which have previously experienced GIC activity.

Effects of GICs on systems

The potential consequences of extreme space weather are illustrated in the impact tree found in Appendix 2. This schematic outlines the different types of extreme space weather that can affect Earth and cause ground effects in many of our critical infrastructure systems. To validate the information illustrated in this diagram, a summary is provided which reviews each potential consequence. Many of the consequences are those immediate effects which can occur from space weather, with less emphasis being placed on the more uncertain cumulative long-term effects.

Other blackouts can serve as proxies for the potential costs from power losses that could arise from extreme space weather events. The North American blackout in August 2003 caused considerable disruption in the Northeastern US and Ontario, Canada, with economists estimating that this led to a $4-10 billion loss to the economy, affecting 50 million people and leaving almost 62 GW of unserved electricity (Anderson and Geckil, 2003; Anderson et al. 2007).

The following sections explore the possible damage of an extreme space weather event affecting various systems on Earth.

Electricity transmission network

Power grids are the primary assets that can be affected by GICs. It is specifically the alternating current (AC) performance of electrical networks that can be disrupted, particularly those assets associated with the Extra High Voltage (EHV) transmission system. Space weather has been cited as a cause of a wide variety of malfunctions in electrical equipment (Schrijver et al. 2014). Both EHV transmission transformers and generation step-up transformers are at risk, as seen in the Salem nuclear power plant incident during the 1989 storm (NRC, 1990). Additionally, step-down transformers to rail networks are at risk (Atkins, 2014). The key pathway to damage is illustrated in Figure 6, as certain risk factors influence the probability of a transformer asset being susceptible to half-cycle saturation.

The speed of change in Earth's magnetic field affects the magnitude of the electrical current generated, which can lead to immediate or cumulative damage in transformer components (Hutchins & Overbye,

When considering the recorded impact of past events, there are a number of well documented recent examples.

1989 Storm

The 1989 storm which led to a widespread blackout in Quebec was caused by half-cycle saturation of power transformers and the induced harmonics tripping seven static VAR compensators (SVCs) delivering reactive power (Czech at el. 1992; Samuelsson, 2013). Massive reactive power shortage led to a voltage collapse of the Hydro Quebec grid, with the total cost of equipment damage totalling $6.5 million. The net cost of the failure is estimated to be $13.2 million (Bolduc, 2002). Six million customers were left without power for almost nine hours with a loss of 19GW of unserved power. The same storm also affected the US where half-cycle saturation of a nuclear unit transformer led to its overheating and being taken out of service at Salem, New Jersey (NRC, 1990). In this case, electricity services were maintained and no blackout occurred.

2003 Halloween Storm

During the 2003 Halloween storms roughly 50,000 customers were left without power for an hour in Malmö, Sweden when harmonic distortions produced by GIC tripped overly-sensitive protective relays (Pulkkinen et al. 2005). In this case, very high GIC of 330A caused half-cycle saturation of a transformer, with harmonics causing protection to disconnect a 130kV line. No backup was present which contributed to the blackout's occurrence. There were reports of numerous transformers being badly affected with significant damage occurring in South Africa (Gaunt and Coetzee, 2007; Ngwira et al. 2011).

2011). Molinski (2002) states that this gives rise to half-cycle saturation in transformers, potential system voltage collapse, a loss in reactive power, as well as the generation of harmonics and excessive transformer heating. Studies have shown that these issues can affect electrical networks in countries in a range of latitudes (Viljanen et al. 2013; Bolduc, 2002; Erinmez et al. 2002; Marshall et al. 2011; Marshall et al. 2013).

The number of transformers at risk is highly debated and estimates vary widely. A worst-case scenario conveyed in the form of a Metatech report estimated 365 transformers were potentially at risk from a 4800 nT/min storm in the USA (Kappenman, 2010). The author suggested the possibility of there being millions

without power for months to years as a consequence, because replacement EHV transformers take such a long time to be manufactured. In response, the Department of Homeland Security tasked JASON to study the potential effects of space weather on the electricity transmission network, with their conclusion being that "we are not convinced that the worst-case scenario of [Kappenman] is plausible" (JASON, 2011:2). To put this work into perspective, a recent Royal Academy of Engineering report (Cannon et al. 2013) estimated that 13 out of 600 transformers are at risk in the UK. However, it was identified that although the technical means to protect the network exist, the steps have not necessarily been taken in order to protect the US grid, and more risk assessment needs to be undertaken, especially given the time it takes to manufacture new EHV transformers (DOE, 2014) (see breakout box). Ultimately, it is not clear what the potential damage distribution from an extreme space weather event might be, and therefore it is an area in need of further research.

If an extreme event occurred which led to a blackout, the direct economic impact would be a loss of power for businesses and consumers within the storm footprint. Indirect economic effects arise outside of the storm footprint, as disruption to supply chain linkages prevents normal economic activities taking place. Inoperability in critical infrastructure sectors is one key way in which disruptions can ripple through the global economy. Consequently, extreme space weather events have the potential to disrupt the production, distribution and consumption of both goods and services around the world, as demonstrated in Schulte in den Bäume et al. (2014).

The secondary effect of transformer damage and delayed failure in weeks or months (Gaunt and Coetzee, 2007; Moodley and Gaunt, 2012) would cause problems in energy constrained economies, since the transformers most likely to be affected are Generator Step-Up units, for which the loss of the transformer usually causes loss of the generator capacity until the transformer is replaced. Transformers outside the footprint of a system collapse will not be protected from damage by the collapse and their subsequent failures will add to the pressure on manufacturing.

Although it is agreed that extreme space weather is a threat to the global economy, it is not yet understood how severe the impact from such threats could be.

Undersea cables

Undersea cables have been affected by GICs for over a century. Indeed, during the Carrington Event of 1859, many telegraph operators reported strange electrical effects whereby communications could still
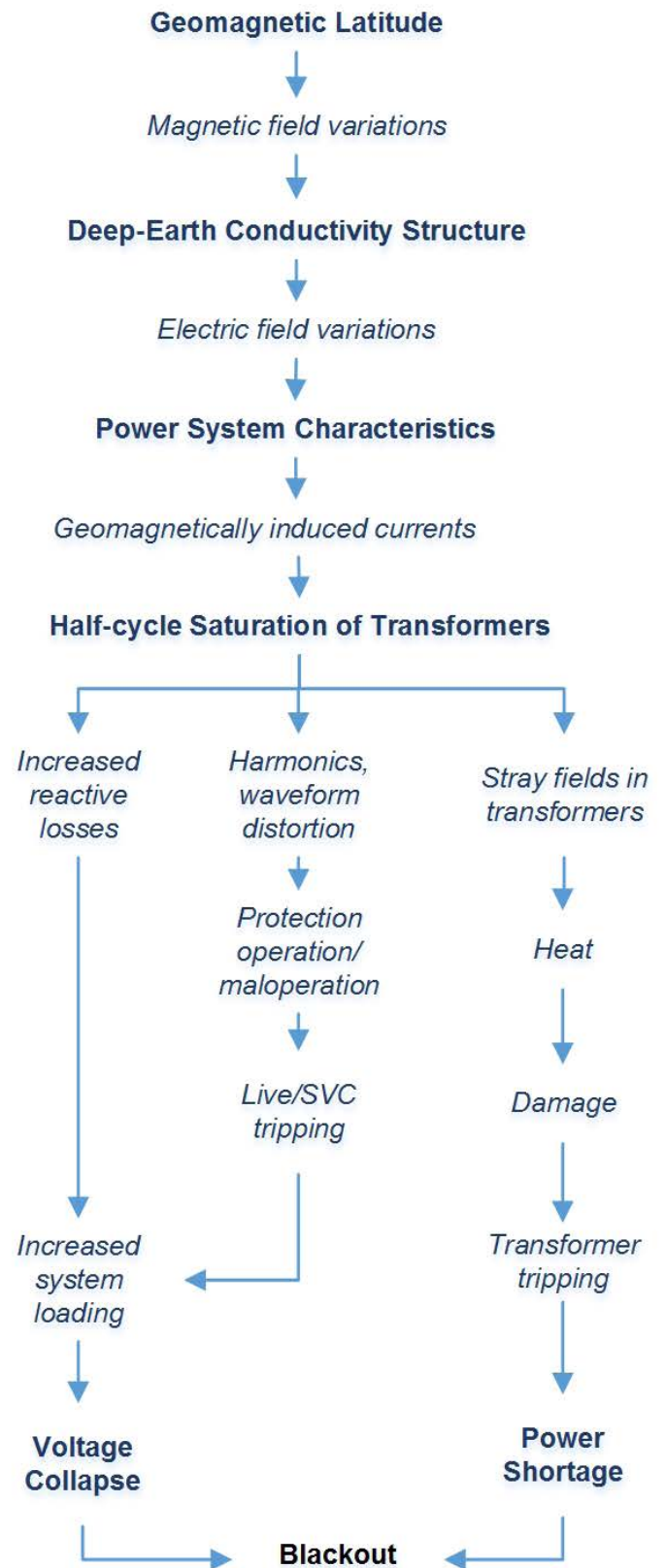

Figure 6: Pathway to damage (adapted from Boteler, 2015 and Samuelsson, 2013)

Transformer manufacturing and repair lead times

A 2014 US Department of Energy review estimates that there are 2,000 EHV transformers in the US. The average lead time of a domestically manufactured transformer is five to 12 months, internationally manufactured transformers is six to 16 months and can be up to 18 to 24 months in high demand periods (DOE, 2014). Large amounts of copper or electrical steel are required for their manufacture yet these resources are in limited supply and their price can fluctuate considerably.

In the US, international producers are the primary supplier of EHV transformers. In 2010, the US relied on international suppliers for 85% of its transformers (<60MVA), which complicates the grid's resilience to equipment damage as it requires longer transportation periods. New domestic production facilities have been opened in Georgia, Alabama, Tennessee and Wisconsin, which could help to at least alleviate part of this long supply chain issue.

Furthermore, moving EHV transformers is an involved procedure requiring special road or rail transport, a Goldhofer truck, or a Schnabel rail car. The route that a transformer takes must be preapproved in its entirety by a civil engineer to ensure that all roads meet the load requirements. Special permits must be approved and road closures may be required.

The Royal Academy of Engineering (RAE) report recommends that it will take at least eight weeks to transport, install and commission a spare transformer in the UK (Cannon et al. 2013).

There have been recent developments however, particularly with regard to a report by the US Board on Energy and Environmental Systems (2012), which recommended instigating a stockpile of easily transported EHV recovery transformers. Subsequently, the Electric Power Research Institute (2014) reported the outcome of the Recovery Transformer or RecX project, which successfully designed, manufactured, tested, transported, installed, energised and field tested a set of rapid deployment high-powered 345kV emergency spare transformers. In this project, three EHV transformers were transported in 20 hours from St. Louis, and made operational in less than six days (106 hours), which included a 25-hour road journey from a temporary storage site at ABB (St Louis, Missouri) to a CenterPoint Energy substation near Houston, Texas. The Recovery Transformers were subsequently monitored closely during a one-year prototype live demonstration, where they operated successfully within design specifications. It may be some time before this approach is made fully operational and able to adequately respond to an extreme event which affects the entirety of the US.

In addition to this, the Edison Electric Institute has been operating the Spare Transformer Equipment Program (STEP) for over a decade, which is aimed at primarily sharing spare transformers if dam age occurred from a terrorist attack, and this may be a way of redistributing stockpiled transformers and parts to locations in need. A recent US Federal Energy Regulatory Commission (FERC), North American Electric Reliability Corporation (NERC) and Regional Entity review (2016) of restoration, response and recovery plans for nine key operators responsible for the US bulk electricity sector, identified the importance of black- start equipment for restoring power. This includes portable diesel, hydro, and combustion turbine-generators which can provide power for starting other types of generation facilities.

be transmitted and received, even after systems were disconnected from the power supply. More recently, a documented case attempts to understand the problems caused by a large storm in 1958 whereby businesses and consumers in Finland were disrupted by the failures of two coaxial phone cable systems in the southern part of the country (Nevanlinna et al. 2001). The event was caused by blown fuses associated with the AC power supplies at repeater stations. Much like power grids, the submarine equivalent is equally affected by certain geographic and technical factors which, in this case, include the depth of the cable (Meloni et al. 1983).

However, we have seen in recent decades a revolution in the technologies used in the transmission of digital communications networks. Modern systems rely on fibre optics, and therefore these glass fibres are far less conductive than their coaxial copper predecessors.

As a consequence, there has been little GIC damage to submarine cables in recent years. Far more at risk are the electrical cables which often run side-by-side with fibre optic cables. Regardless, a potential loss of electricity to power these cables could still cause immediate, short-term inoperability but would be unlikely to cause any long-term damage.

Pipelines

Pipelines may be at risk of cumulative long-term damage due to GICs. The likelihood of increased corrosion could shorten an asset's life (Pulkkinen et al. 2001a; Pulkkinen et al. 2001b; Gummow & Eng, 2002). Boteler & Trichtchenko (2015) state that the telluric electric fields produced by geomagnetic field variations drive currents along engineered structures including pipelines. The specific electrical properties of a pipeline are affected by the network topology, the series impedance of the steel used, and the parallel admittance through the coating. Modern pipelines using higher resistance coatings have led to an increase in the size of telluric pipe-to-soil potential (PSP) variations potentially leading to increased corrosion. Uncertainty exists regarding the magnitude of repeated exposure and the amount of time before an asset becomes affected by PSP variations. Pirjola et al. (2000) state that significant GICs can flow near the ends and bends of the pipeline and, while the voltages can only be of the order of a few volts, can still exceed the cathodic protection potential. Effects to pipelines would not lead to immediate failure, instead shortening an asset's lifetime. It may not be possible to attribute the damage causes by exposure to high GIC to a space weather event, if the asset eventually fails many years after.

Railway signals and tracks

Railway signals and tracks can be affected by GICs in two main ways. Firstly, signalling and train control system anomalies can occur during periods of high geomagnetic activity whereby failures not related to recognised technical malfunctions can be up to five to seven times more likely on average (Ptitsyna et al. 2008; Eroshenko et al. 2010; Wik et al. 2009). Secondly, the structural integrity of rail infrastructure could also be affected if repeatedly subjected to extreme conditions, as this may increase the rate of corrosion. However, less evidence has been found to support the latter impact. Similar to pipelines, it may not be possible to link the shortening of an asset's lifetime to an extreme geomagnetic event.

Communications

The practical effects of solar-induced disturbances on radio communications have been documented for over a century (Lanzerotti, 2001; 2007). In particular, high-frequency (HF) radio communications can be temporarily disrupted due to radio absorption; a problem that is particularly prevalent in the Polar Regions (Neal et al. 2013; Rodger et al. 2008). During large electromagnetic radiation bursts released from the surface of the Sun, HF radio blackouts may occur on Earth lasting for up to 24 hours or more, although these effects would be unlikely to last more than a couple of days depending on the size of the solar flare.

Little evidence has been found to suggest that there would be any serious geomagnetic effects on mobile telephony but there is no guarantee that these technologies could continue to operate effectively during potential power outages and disruptions to the mobile location-based services on which over 3 billion mobile applications rely (European GNSS Agency, 2015) (see Spacecraft and Satellites below).

Aviation

During a period of extreme space weather, aviation routes may need to be rerouted to avoid high latitude regions due to probable disruption to HF communications (Neal et al. 2013). Moreover, airline operations also suffer problems with avionics and GPS navigation systems during extreme events (Jones et al. 2005). This could potentially cause delays at major airports around the globe, particularly where there are a large number of flights that use the high latitude regions as an aviation corridor (e.g. New York to Tokyo, or Toronto to Hong Kong). Contact may also be consequently lost with mariners already in transit in these regions. Importantly, analysis of the US National Transportation Safety Board database found no relationship between space weather factors and aviation incidents (Lyakhov and Kozlov, 2012). Radiation exposure for aviation crew is also a serious issue, particularly for pregnant personnel (Hapgood et al. 2012).

Spacecraft and satellites

Spacecraft and satellites, including those enabling Global Positioning Systems, could be affected from radiation bursts and other extreme space weather phenomena (Astafyeva et al. 2014). A study of on-orbit spacecraft failures by Tafazoli (2009) found that over 10% of spacecraft anomalies were due to solar or magnetic storms.

Short-term issues include problems with signal propagation and transmission. These can occur from ionospheric storms and scintillation causing interference and preventing normal signal propagation and transmission (Horne et al. 2013; Hapgood et al. 2012). This can disrupt many economic sectors which rely on GNSS for navigation and timing services, such as financial services (Krausmann et al. 2014) or aviation.

Potential long-term issues include catastrophic spacecraft drag or spacecraft charging to satellite assets. Increased spacecraft drag can cause uncontrolled re-entry for those satellites in low orbits (Horne et al. 2013). For satellites in higher orbits

(e.g. geosynchronous), issues arise from both solar array damage and spacecraft charging (Hastings and Garrett, 2004, Garrett and Whittlesey, 2012; Lai and Tautz, 2006). Solar arrays can be degraded when cosmic rays and solar energetic particles penetrate them and other electronic components (see Koons and Fennell, 2006). Power failures are often critical for spacecraft as 45% result in complete loss of spacecraft mission and 80% significantly affect the mission (Tafazoli, 2009).

Both the temperature and density of the satellite materials is decisive in regard to the issue of surface spacecraft charging (Huang et al. 2015). Although satellites are built with fault-tolerant software and recovery mechanisms to ensure they can continue to operate after radiation-induced errors in the memory or processors, there is no guarantee this can solve all problems, particularly in extreme radiation environments (Gorbenko et al. 2012).

Mitigation – operational and engineering

Operational mitigation plans are in place in the USA which attempt to prevent damage to key assets and keep essential infrastructure systems in full operation. These plans rely on early notification and typically call for an increase in spinning reserve and reactive power, while reducing load on key transformers.

The North American Electric Reliability Corporation (NERC) manages eight reliability regions across the US and oversees the delivery of power. NERC is currently accepting feedback on proposed engineering mitigations that would require utilities to complete an engineering assessment to help harden transmission equipment to prevent or reduce the flow of GICs over key assets. Installing capacitors, replacing solid earthing, and selecting improved key component during the equipment design phase are possible engineering mitigations against increased GICs (Samuelsson, 2013; JASON, 2011).

The Federal Energy Regulatory Commission (FERC) is the federal agency that regulates various aspects of the energy sector, electricity, oil and gas. FERC has the jurisdiction to impose fines for violation of federal acts and FERC/NERC reliability standards. The FERC has required all US utilities to develop and implement a GMD operational plan as of April 2014 based on FERC Order 779 (FERC, 2014). Operational planning can help limit or avoid power outages during a GMD by spreading the load over multiple lines, ensuring excess spinning reserve and reactive power is available should equipment trip or need to be taken off-line, returning circuits to service and possibly reducing load on at risk transformers (Samuelsson, 2013). Operational mitigation plans

rely on early notifications systems. It is unlikely that equipment will be turned off.

Notification systems

The National Oceanic Atmospheric Association (NOAA) Space Weather Prediction Center (SWPC) monitors sunspots and predicts the likelihood that a solar event will occur (NOAA).

The average CME speed measured by LASCO is 489km/s-1, making the average travel time to Earth roughly

3.5 days (Webb and Howard, 2012). However, this ranges from 100km/s-1 to more than 3000km/s-1 (Green and Baker, 2015). They are several satellites that monitor the Sun's activity, such as the advanced composition explorer (ACE), the solar terrestrial relations observatory (STEREO A and B), deep-space climate observatory (DSCOVR) and the solar and heliospheric observatory (SOHO). There are two primary positions for these satellites, rotating around the Sun and in the L1 (Langarngian point) position between the Sun and Earth. These satellites enable real-time measurements and monitoring of the Sun. The ACE satellite is able to give a 15 to

30 minute warning as to whether a CME will hit Earth (Cannon et al. 2013). NOAA reports the likelihood and severity of the space weather daily using three scales for geomagnetic storms (G1-5), solar radiation storms (S1-5) and radio blackouts R1-5).

4 Defining the Scenario

This scenario is a hypothetical example of an extreme event, based on historical and contemporary evidence. As already outlined, there is ongoing debate within the engineering community about the susceptibility of EHV transformers to extreme geomagnetic disturbances and there is still considerable work to be undertaken in verifying the expected damage levels to these key assets. We have incorporated the differing perspectives put forward by different subject matter experts within the three scenario variants explored and will demonstrate how the direct and indirect economic costs accrue for different levels of damage.

We do not present definitive economic costings for an extreme space weather event. This is not a prediction but rather a scenario that is designed to challenge the assumptions of operators, regulators, insurers and other key stakeholders. This enables us to produce more robust emergency management procedures and be better prepared to deal with potentially disruptive extreme space weather events. Here, we outline key parts of the scenario and its methodology before describing the actual scenario in Chapter 5, and presenting the results in Chapter 6.

Likelihood and severity

Estimating the likelihood of an extreme geomagnetic disturbance is a challenging task due to the short time-series of available data (Hapgood, 2011). One widely quoted statistic is that there is a 12% probability that a Carrington-sized extreme space weather event (Disturbance Storm Time (Dst) < -850 nT) might take place within the next decade (Riley, 2012).

In more recent research, Love et al. (2015) show that a storm larger than Carrington (Dst ≥ -850 nT) occurs about 1.13 times per century (although there is a wide confidence interval ranging from 0.42 – 2.41). However, the recent report by the Royal Academy of Engineering (Cannon et al. 2013) states that these events are ultimately the result of a random process, therefore the potential for extreme space weather does not increase as time passes since the last major event. In this scenario, we propose that a Carrington-sized storm hits Earth, with the CME having similar characteristics to the ejection which occurred and narrowly missed Earth in 2012.

State-level risk factors

We develop risk factors at the state-level which direct sequential customer disruptions. For each US state, the geomagnetic latitude of the population centroid is used to provide the most robust metric of population location. The coordinates of the 2010 population centroid were obtained from the US Census Bureau and were converted into geomagnetic coordinates for 2015 using the International Geomagnetic Reference Field (IGRF) Model from the World Data Centre for Geomagnetism, Kyoto.

Using data from the US Geological Survey on deep-earth ground conductivity, the weighted vertical average is calculated down to 80 km for each conductivity region in the USA. This takes into account the high amplitude variations (from tens of seconds to tens of minutes) in the production of GICs that are most damaging to EHV transformers. As these regions do not directly align with man-made boundaries, the intersection of these geological regions is taken in relation to current US state boundaries using GIS software. This then allows the weighted average of deep-earth ground conductivity to be calculated, providing a single number representing the GIC risk for each state.

These continuous values are then converted into a normalised minimum-maximum scale so that each observation falls between 0 and 1 for both risk factors. The state with the lowest risk for each variable takes the value 0 and the highest risk takes the value 1. Finally, these two variables are converted into one combined risk factor for each state by multiplying each value by its relative weighting (where each factor is treated as having equal influence). This value was also normalised based on a minimum-maximum scale so all values sit between 0 and 1.

Number of EHV transformers by state

Following detailed analysis of raw data from Electric Utility Annual Reports submitted by major utilities to FERC (2014), we estimate that there are 2,339 grid-connected EHV (<345KV) transmission transformers in the USA, with a further 222 spare transformers stored locally to connected transformers. Grid-connected and spare transformers were also estimated at the state level.

We do not address every single risk factor outlined previously, instead focusing on the most important. For example, modelling the topology of the electricity transmission network is outside of the scope of this work but is recognised as an important factor in determining the likelihood and extent of cascade failures and the population experiencing a power

outage.[6] In lieu of comprehensive topological and asset-level data for the transmission network, we make the simplifying assumption that each transformer serves a share of the state population relative to the overall number of transformers in a given state. For example, if there are ten transformers allocated to a state with a population of ten million, then we assume that damage to a given transformer would lead to a power outage affecting one million customers. The duration of the outage depends on the damage level sustained (as discussed next), and the time it takes to become operational again, as outlined in the scenario.

It is recognised that resilience measures like NERC power sharing pools transcend state boundaries and may offset power outages in a single state, but this adds an additional level of complexity which is beyond this report. Hence, the analysis produced here represents the upper bound, most extreme case, when in reality there may be technical measures and governance structures which aim to mitigate the actual impact.

Parameterising damage level distributions

In any natural catastrophe event there will always be a range of damage caused to key fixed capital assets. After a major natural catastrophe (earthquake, hurricane etc.), considerable empirical effort is put into categorising these assets, be they buildings or critical infrastructure, by damage type. This provides an understanding of the damage distribution for different event magnitudes. In the case of extreme space weather, these events occur much less frequently than in terrestrial weather systems, leaving very limited post-disaster empirical data. Moreover, today we are far more reliant on the EHV transmission of electricity than during the Carrington Event of 1859, widely regarded as the largest extreme space weather event of modern times. As a consequence we have a very limited understanding of the potential damage distribution across key EHV assets. In this report we therefore apply a methodology which enables us to examine the economic impact of different theoretical damage distributions across EHV transformers.

Following the theoretical techniques used in catastrophe loss estimation and risk assessment for other extreme natural hazards, a binomial distribution (with parameters n and p) is employed as a way of mapping the risk factors for individual spatial areas (i.e., US states) to different discrete levels of transformer damage. We consider five

damage levels (n = 5) of increasing severity from 'Not Affected', through 'Tripped Off', 'Minor Damage', and 'Major Damage', to 'Destroyed'. It is assumed that a transformer assigned to the 'Tripped Off' category incurs no physical damage but does become temporarily disconnected from the grid. Minor, major and destroyed damage levels imply physical damage and disconnection until either the damage can be repaired or a spare transformer can be substituted. By assigning a particular value of the binomial p parameter to a given risk factor, the population of EHV transformers in a state can be distributed across the five damage levels: for example, assigning p = 0 would allocate all transformers to the 'Not Affected' damage level; conversely, assigning p = 1 would see all transformers destroyed; and, assigning p = 0.5 would yield 6.25% of transformers 'Not Affected', 25% 'Tripped Off', 37.5% 'Minor Damage', 25% 'Major Damage' and 6.25% 'Destroyed'.

Parameterising damage level outage durations

The duration of the catastrophe results from the extent of damage caused to EHV transformer assets, and therefore how quickly they can either be (i) reconnected following a trip-off, (ii) repaired onsite, (ii) have spares transported to and installed at relevant transmission substations, or as a last resort (iii) have bespoke transformers manufactured from scratch. The description of the scenario in the following section provides specific restoration times for each damage level.

Estimating state-level restoration curves

Combining the outputs from the aforementioned steps defines state-level restoration curves, which indicate the estimated share of a state population experiencing a power outage in the days, weeks and months following an extreme space weather event for each of the scenario variants. The restoration curves are determined by the time it takes to replace key transformer assets following the exploration of different damage distributions. These time estimates for assessing and repairing transformer damage at different levels were obtained from subject- matter experts. Restoration times and damage distributions by scenario are outlined in the following section.

If a state of ten million people, served by ten transformers (and no spares), incurs minor damage in one transformer, while a further four are tripped off (and five are unaffected), then we assume that half the state population experiences an outage for the first five days of both the S1 and S2 scenarios. Following the inspection and reconnection of the four tripped transformers, the outage ends for 4/5th

---

[6] Much of the data required for this task is owned by the network operators and therefore is treated as commercially sensitive, making it hard to obtain.

of the affected population. The remaining 10% of the population remains without power for a further 16 days while the single transformer with minor damage is repaired onsite. Overall, the restoration period for the state lasts three weeks (dictated by the most severely damaged transformer). If we assume a spare replacement is locally available for the transformer with minor damage, then this restoration period would be shortened (factoring in the time needed to manoeuvre, connect and commission the spare).

Using our understanding of the share of transformers with spares in a given state (derived from the previous analysis of transformers), we allocate the distribution of transformers proportionally by damage level across the categories of restoration infrastructure, namely: transformers with spares and those without. Using the outage durations and power restoration figures for all variants of the solar storm scenario, we can then generate the bottom-up state-level restoration curves.

The particular parameterisation for the three scenario variants has been selected to explore both the impact of variation in the amount of damage caused by the solar storm and the duration of the subsequent outage, as shown in Table 4. S1 and S2 share the same restoration times for EHV assets, but capture different levels of damage. S2 and X1 share the same damage distribution but utilise different restoration times.

Table 4: Transformer damage distribution and restoration time ranges captured in scenario variants

Sustained damage to EHV transformers	Base Restoration Time	Prolonged Restoration Time
Low	S1	-
High	S2	X1

Further details on the methodology used in this scenario can be found in Appendix 3.

5 The Scenario

Phase 1 – Activity at the Sun

Over a 48 hour period, a large number of sunspot groups display heightened activity on the Sun. The Solar Terrestrial Relations Observatory (STEREO) detects these changes and heliophysicists at the National Oceanic and Atmospheric Administration (NOAA) take special interest in the sunspot group. Eruptions from this region, close to the solar disk centre, are usually expected to hit Earth.

A relatively moderate CME (~450 km/s ± 500 km/s) and a solar flare (less than a M5 storm, with a speed ≤ 5 x 10-5 W/m2) are detected as leaving the Sun's corona. These are not large enough to cause alarm for utility operators. Travelling close to the speed of light, large quantities of X-ray and UV radiation reach the STEREO observatory (and Earth) roughly eight minutes after it is emitted from the Sun's surface. NOAA issues a category R2 radio blackout. Lasting roughly 30 minutes, this severely affects the use of HF communications in the Polar Regions on the sunlit side of Earth. The moderately-sized CME has now entered the solar wind and has begun travelling towards Earth. NOAA scientists estimate a moderately-sized geomagnetic storm (category G2) is likely to begin in four days' time. Geomagnetic storm warnings are issued.

However, this active sunspot region continues to show signs of very high activity. Three days later a large build-up of energy takes place and due to an efficient magnetic reconnection process, a very high-mass, large CME is thrown outwards towards Earth. The CME reaches a very high speed (2,000 km/s ± 500km/s) that is sustained in its path towards Earth. The interaction effect between the moderately-sized CME a number of days earlier, the consequential preconditioning of the interplanetary space, lowers the ambient solar wind density, producing very little deceleration. A massive solar flare (X20 = 2 x 10-3 W/m2) accompanies this event releasing a large burst of electromagnetic radiation. A severe solar energetic particle event (104 megaelectron volt (MeV)) also takes place producing a radiation storm.

Phase 2 – Arrival at Earth

The hot gas cloud of charged particles from the first moderately-sized CME is identified by The Solar and Heliospheric Observatory (SOHO), The Advanced Composition Explorer (ACE), Global Geospace Science (GGS) Wind satellite and Deep Space Climate Observatory (DSCOVR) providing 30-60 minutes warning of its impact. First, the CME bombards Earth's magnetosphere until it forces a reconfiguration of the magnetic field lines. The southward-directed interplanetary magnetic field and Earth's geomagnetic field connect efficiently. Overall, the shock forces Earth's magnetic field lines to drape away from the Sun.

Then the first charged particles from the second much larger and faster CME arrive at Earth, emitted only 20 hours earlier. Consequently, billions of tonnes of gas containing charged particles intensify the shock compression, deforming Earth's magnetosphere further.

Ultimately, this mechanism causes unprecedented amounts of charged particles to be accelerated along the magnetotail, back towards Earth where they are deposited in the auroral ionosphere and magnetosphere on the night side of Earth, directly above North America. Preliminary Dst measurements of the distortion to Earth's magnetic field exceed approximately -1,000 nT and dB/dt measurements are recorded of 5,000 nT/m at 50° geomagnetic latitude.

Table 5: Total US transformer damage distribution for scenario variants S1, S2 and X1

S1	D0 Not affected	D1 Tripped off	D2 Minor damage	D3 Major damage	D4 Destroyed
No. of transformers with spare	159	53	6	0	0
No. of transformers without spare	1,432	559	115	11	0
Total no. of transformers damaged	1,595	612	121	11	0
S2 and X1	**D0**	**D1**	**D2**	**D3**	**D4**
No. of transformers with spare	118	67	22	3	0
No. of transformers without spare	1,006	703	313	74	5
Total no. of transformers damaged	1,152	770	335	77	5
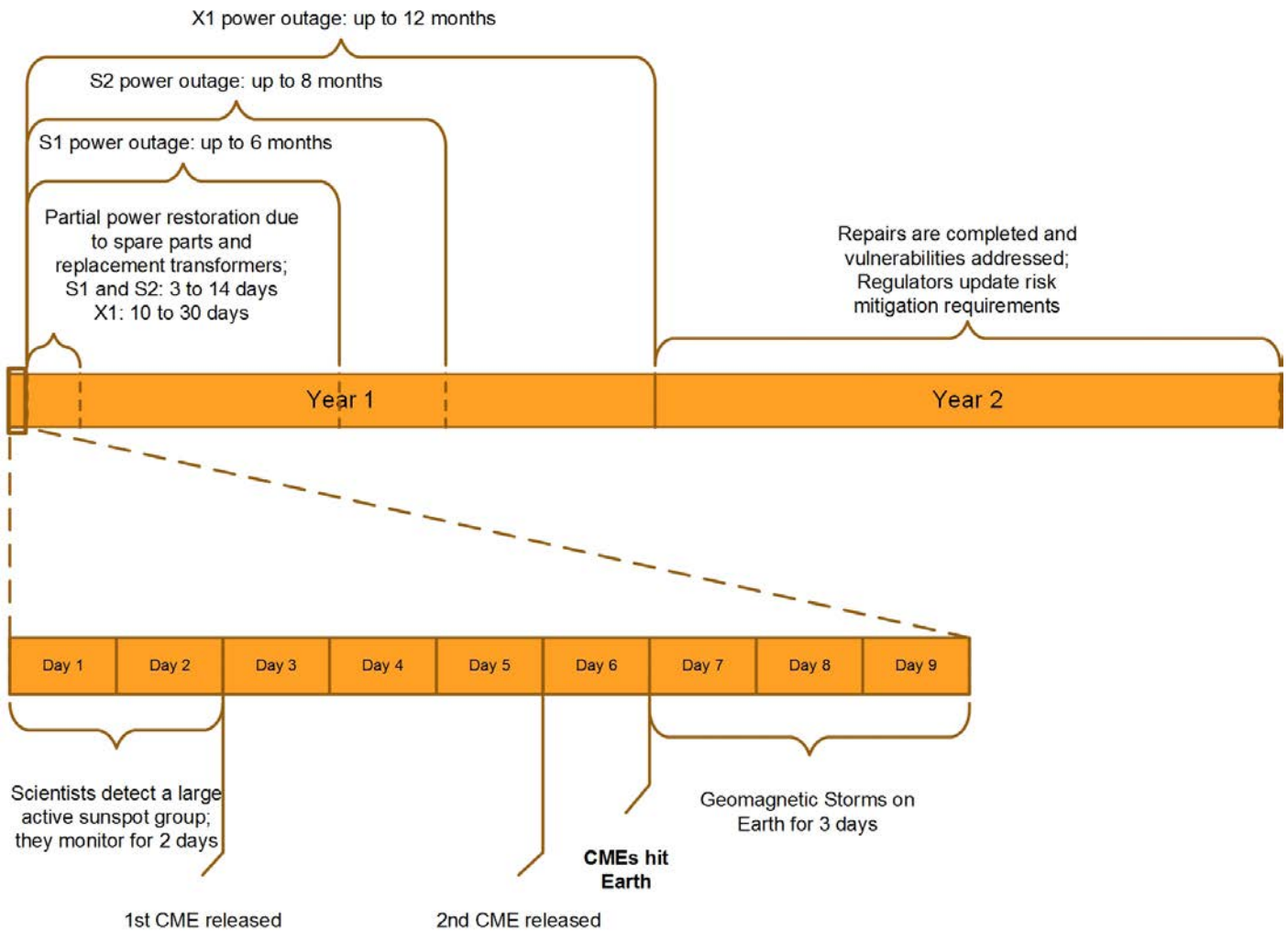
Figure 7: Timeline of the Helios Solar Storm scenario

Beneath the overall distortion of Earth's magnetic field, numerous substorms begin to take place every few hours on the dawn-to-dusk side of Earth due to the highly dynamic nature of the auroral electrojet roughly 100km above ground. This causes rapid change in the magnetic field rate-of-change down to 50° geomagnetic latitude. Ring current intensifications take place down to 20° geomagnetic latitude.

Phase 3 – Effects on the ground

Key electricity network assets experience considerable disruption and are placed under significant strain. Due to the very high speed at which the large CME arrives at Earth, utilities operators do not have time to fully implement emergency procedures. Substorms expose many assets to excessive heating. Certain electricity systems are calibrated to automatically trip offline as GIC activity reaches a certain threshold level. For those assets that do not, operators are left with no option but to manually trip off certain specific EHV transformer assets. This leads to instabilities in the grid, causing a complete voltage collapse of the entire system. Table 5 outlines the damage distribution of EHV transformers across a range of potential damage outcomes.

Many EHV transformers continue to function but have either minor or major damage. Some are completely destroyed. Degradation to the windings and insulation of destroyed transformers does not cause immediate failure, however, but occurs over the following 48 hours.

Major damage sustained to transformers leads to a period of inoperability lasting between 2-8 weeks after the event. Minor damage can lead to transformers being taken off-line over the coming years. Table 6 (page 22) outlines the number of days it takes for an EHV transformer to be brought back on-line after sustaining a specific level of damage and have been assumed following expert consultation.

A tripped transformer can be brought back online relatively quickly once an engineer has been able to undertake a visual inspection. When a transformer sustains damage and a spare is available, a replacement can be brought in from a central storage facility within 14 days. However, when a spare is not available, it may take a considerable amount of time to resolve.

Table 6: Restoration times (days) for damaged EHV transformers for all scenario variants

S1 and S2	D0	D1	D2	D3	D4
	Not affected	Tripped off	Minor damage	Major damage	Destroyed
Outage for transformers with spare (days)	0	3	14	14	14
Outage for transformers with spare (days)	0	3	91	182	243
X1	D0	D1	D2	D3	D4
Outage for transformers with spare (days)	0	10	30	30	30
Outage for transformers with spare (days)	0	10	152	304	365

Minor and major damage transformers are transported to a workshop for repair and the length of restoration relates to the time taken to replace key components. There can be considerable supply chains issues involved in the replacement of a destroyed transformer that can take many months to resolve.

Phase 4 – Aftermath

Disruption to the electricity transmission network cascades to other interdependent infrastructure systems which rely on power, causing interruption to transportation, digital communications, water, waste, health and financial services.

Satellite operations have been affected since the heightened activity on the Sun was first detected due to increased electromagnetic activity from solar flares. This causes disruption to those industrial sectors which rely on GNSS systems for timing, positioning, communications, and synchronisation, including high-frequency financial trading, transportation systems, oil and gas exploration, agriculture and utilities. The aviation and maritime sectors lose contact with many planes and vessels for a number of hours. There is chaos at airports around the world as navigation systems fail. Astronauts and aviation flight crews are subjected to high levels of radiation.
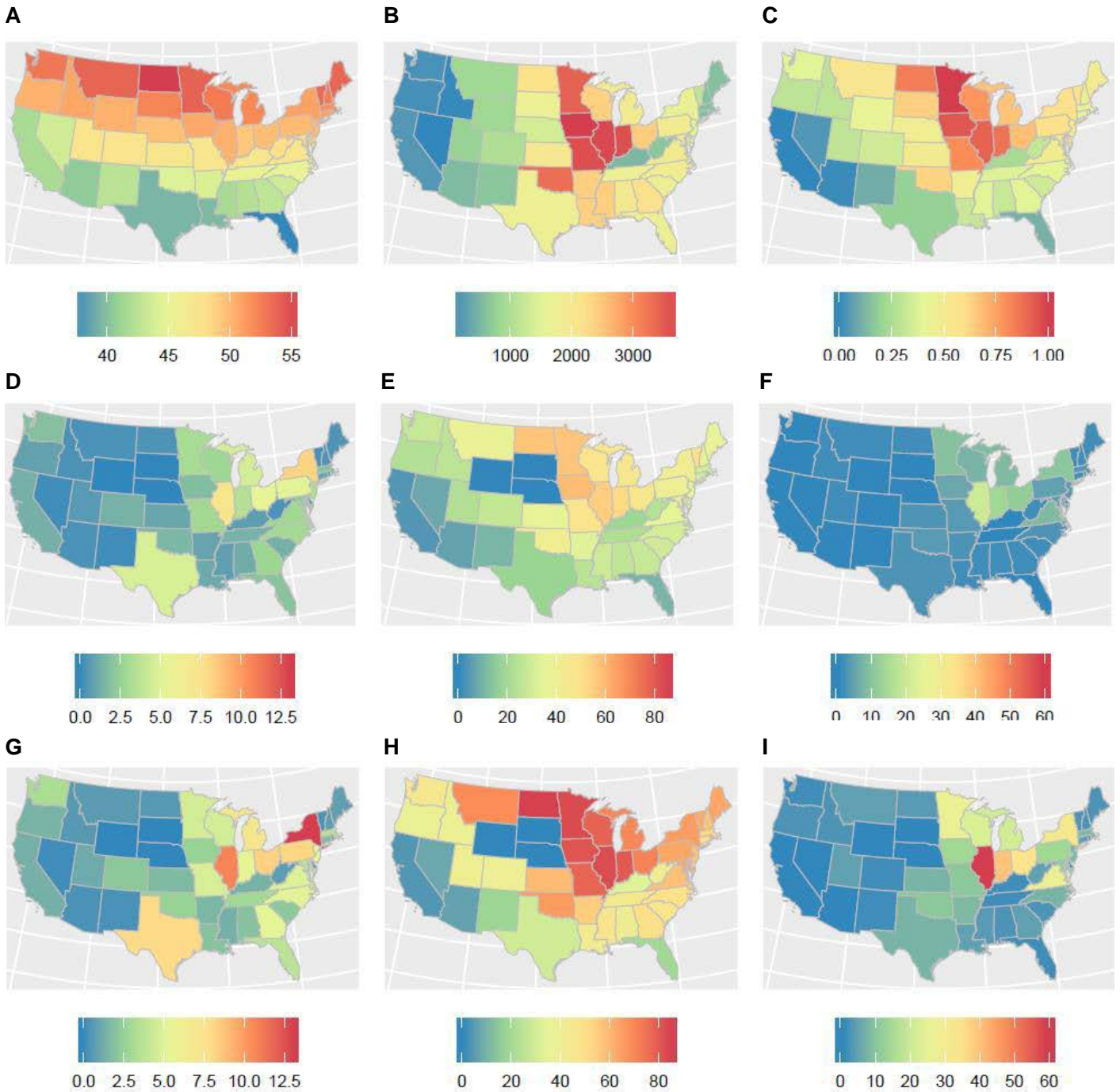
A Geomagnetic latitude of population centroid, **B** Deep-earth ground conductivity structure (<80km), **C** Combined normalised risk factor, **D** S1 day 1 total customer disruptions, **E** S1 day 1 customer disruptions as proportion of population, **F** S1 damaged EHV transformers, **G** S2/X1 day 1 total customer disruptions, **H** S2/X1 day 1 customer disruptions as proportion of population, **I** S2/X1 damaged EHV transformers

Figure 8: Risk factors, customer disruptions and EHV transformer damage by scenario

6   Direct Scenario Impacts

Approximately 121 EHV transformers suffer minor damage while 11 undergo major damage in the S1 scenario, but no transformers are destroyed. The effects are most considerable in areas where there is both a high geomagnetic latitude and highly resistive deep-earth structure. The loss of these assets leads to a power outage initially affecting 90 million US citizens (28% of the US population). Cascading failure within the electricity transmission network has happened in the past, such as during the 2003 Northwest Cascading Power Failure, and therefore this is anticipated to take place. The large number of inactive transformers in the damage distribution reflect this.

It takes three days to restore power to the majority of those affected, thus by day 4 only 14 million citizens are without power (4.6% of the US population). As our modelling uses state-level restoration curves we are able to estimate the rate at which the population is reconnected at a sub-national level. Figure 9 illustrates the aggregated length of the power outage associated with each scenario variant for the whole of the US and Table 7 shows the approximate time periods where power is restored.

The estimation of direct costs provides insight into the losses in sales revenue suffered by businesses in all economic sectors within the geographically affected area of the storm. This step is calculated

using real GDP data by state (2011) for twenty broad industrial groups available from the US Bureau of Economic Analysis. The data is reported in the 2012 North American Industry Classification System (NAICS). To align with the most recent World Input Output Database (WIOD) statistics (Timmer et al. 2015) used in Chapter 7. 2011 is selected for analysis.

Two key assumptions are utilised here. Firstly: all economic activities are dependent on electricity. Therefore, when no electricity is served there is a comparative loss in value-added. This acts as a revealed preference metric of the Value of the Lost Load (VoLL) of electricity, which has recently been identified in a Royal Academy of Engineering report (2014) as the most reliable and robust proxy for estimating economic losses in relation to electricity supply security. As this method has been favoured in the literature, we use it here to estimate the sectoral costs following the exact method used in the Netherlands and Ireland by de Nooij et al. (2007), Tol (2007) and Leahy & Tol (2011).

The second key assumption is that the state-level restoration curves for population disruptions can be interpreted equivalently as state-level production restoration curves (independent of sector). For example, if 5% of the population suffer a blackout at a particular period of time, that relates to a 5% loss
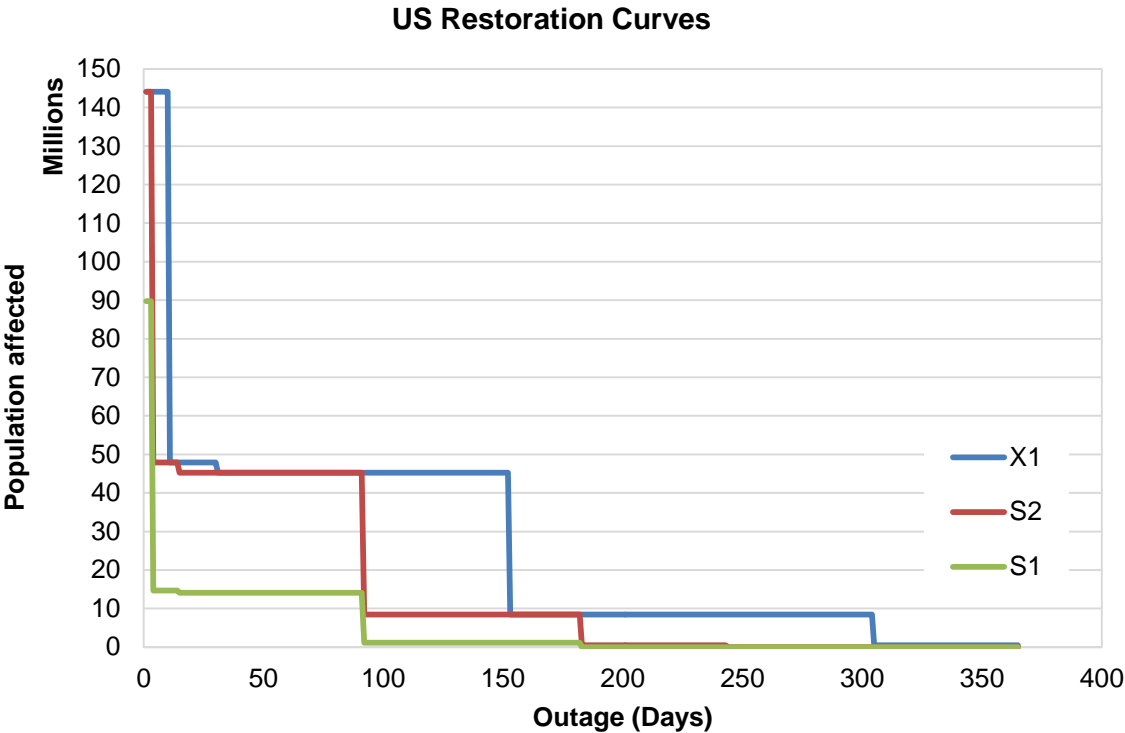

Figure 9: Power restoration curves for all variants of the scenario

in value-added across all industrial sectors in the relevant state.

Once the state-level production restoration curves have been estimated we aggregate those by economic sector to reflect direct economic costs nationally. This shows that, for each individual time period, and the total event, an estimated upper bound of the potential economic losses could be incurred for each industrial sector. Once complete we have to address the fact that the 2012 NAICS do not identically map to the sectoral categorisation system used in

the WIOD data. In which case a concordance table is used to map the relevant NAICS sectors to the WIOD sectoral categorisation which is based on the *Nomenclature Statistique des Activités économiques dans la Communauté Européenne* (NACE) revision 1 (corresponding to the ISIC revision 3) (Dietzenbacher et al. 2013). Figure 10 outlines the state-level direct costs by broad industrial sector. The largest losses are seen in the tertiary (services) and secondary (manufacturing) sectors. Smaller losses are seen in Government and Agriculture (primary) sectors.

Table 7: Power restoration for all variants of the scenario

Point in time where approximately:	S1	S2	X1
95% of population affected has power restored	3 days	3 months	5 months
99% of population affected has power restored	3 months	6 months	10 months
100% of population affected has power restored	6 months	8 months	12 months

Direct economic losses by broad industrial sector (top 15 states) (S1)
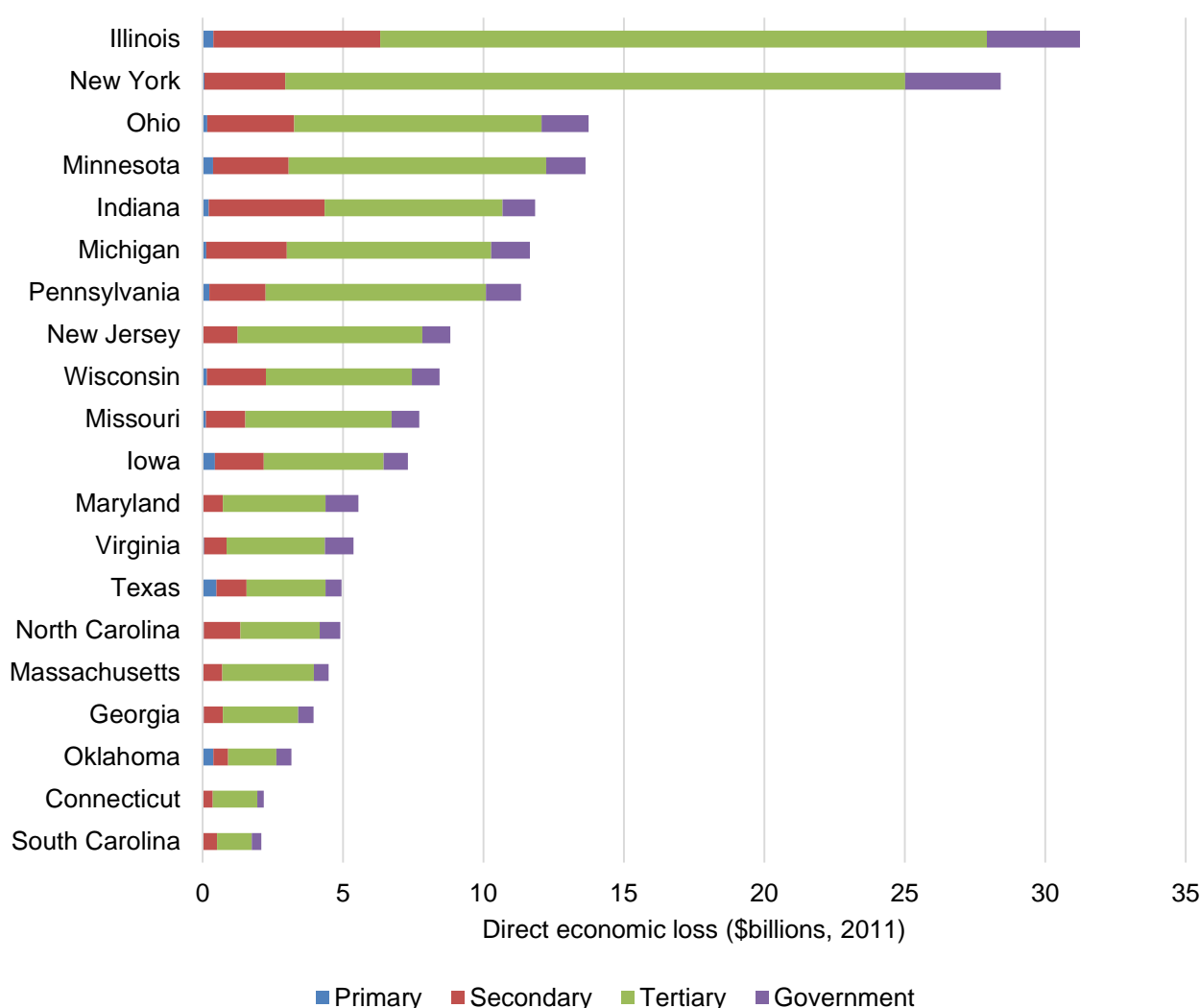
Figure 10: State-level direct costs by broad sector (S1)

7   Indirect Supply Chain Impacts

Measuring indirect supply chain impacts

The indirect consequences of direct scenario impacts are explored in this chapter from a supply chain perspective at an aggregate, sectoral level.

We assume that, in key production sectors, the supply of electricity cannot, at least in the short term, be substituted for an alternative energy source and that electricity is critical for all production activity. Therefore, if 10% of facilities in the automotive industry are without power, we assume there to be a 10% reduction in the quantity of goods and services produced by the sector. By assuming, again in the short term, that prices do not respond in the short-term, then this loss in the quantity of production corresponds to a 10% reduction in the (monetary) total output of the sector, that is, in the value of all goods and services produced by the sector.

Here, we consider three consequences of such a shock: first, there would be a reduction in the value added to the economy by the sector itself (profits, taxes, labour costs, etc., would fall in relation to the lost production activity); second, there would be a reduction in the sector's intermediate consumption of, and hence demand for, goods and services produced by other sectors (i.e., fewer orders would be placed with immediate, first-tier, suppliers); and third, there would be a reduction in the sector's ability to meet demand from its existing customers (i.e., fewer sales would be made with intermediate customers in other sectors and with household and government end customers).

We interpret the reduction in a sector's value added as: a manifestation of the direct shock; the reduction in the sector's intermediate consumption as upstream indirect shocks to other sectors; and, the reduction in the sector's sales as downstream indirect shocks to other sectors. Both upstream and downstream indirect shocks are considered to propagate along tier after tier of suppliers and customers respectively, which collectively constitute the supply chains of the economy.

The economy would dynamically respond to the value-added, upstream and downstream dimensions of a direct shock. Rather than seeking to assess the likely overall economy-wide costs of each scenario, in this section we aim to assess how different sectors and non- US countries might be initially affected relative to one another, based on an understanding of static supply chain interdependencies. We employ a relatively simple methodology based on Multi-Regional Input-Output data and techniques, discussed in detail in Appendix B. Using a system of linear equations, the Input-Output framework represents each economic sector's dependence (as monetary flows) on all other sectors of the domestic and global economy. This is a useful tool because it enables the interdependencies between economic sectors to the quantified thereby providing insight into the upstream and downstream supply chain linkages in the production and consumption of goods and services.

An in-depth overview of the Input-Output approach can be found in Miller and Blair (2009).

Key methodological assumptions

The key underlying assumptions of the methodology are as follows:

- Dynamic responses such as economies of scale, substitution effects, price elasticities and other non- linear behaviours are not captured.

- Upstream indirect impacts are assessed under the assumption that the ratios of intermediate products and value-adding activities (or the 'production recipe') required to make a unit of sector output are fixed.

- Downstream indirect impacts are assessed under the assumption that the ratios of sector output sold to other sectors and end customers (or the 'sales recipe') are fixed.

- Overall indirect impacts induced by direct shocks to other sectors can be assessed by combining isolated upstream and downstream impacts from the set of direct shocks. Overall indirect impacts cover a range: the lower bound assumes that direct and indirect shocks maximally align along common supply chains; and conversely, the upper bound assumes that shocks minimally align along common supply chains.

The lower bound on indirect impacts reflects the possibility that direct shocks could render certain facilities non-operational but which would otherwise have seen their production halted regardless due to either a reduction in output demand or input supply, indirectly caused by other direct shocks.

Conversely, the upper bound reflects the possibility that while production in certain facilities may have been halted due to indirect shocks, these may unfortunately not be the facilities experiencing a

Table 8: Summary of scenario indirect supply chain impacts

Scenario variant	Direct shock		Indirect shock				Total shock	
	US ($Bn)	% US GDP	US ($Bn)	% US GDP	Non-US ($Bn)	% Non-US GDP	Global ($Bn)	% Global GDP
S1	217	1.4	202	1.2	55	0.1	474	0.7
S2	701	4.6	652	4.3	178	0.3	1,532	2.2
X1	1,232	8.1	1,147	7.6	314	0.6	2,693	3.9

power outage themselves. As the scale of direct shocks approaches significant shares of sector total output, a greater share of the indirect impacts of these shocks will align along common supply chains. In reality, supply chains can and do reconfigure over time, but this concept of supply chain alignment allows us to assess the likely range of short-term indirect impacts facing different sectors.

Given the relatively small direct shocks applied to US sectors in the three scenario variants (less than 10% even in the most extreme variant, X1), however, we focus on upper bound indirect impacts as they provide the most conservative estimate of supply chain impacts in the exposition of results in Table 8.

In addition to the assumptions outlined above, it should be noted that there are a number of general sources of uncertainty in Input-Output models and data that affect the accuracy of analysis results, including: errors in the underlying source data; errors from the aggregation of economic activity according to broad sectors; and, uncertainties introduced in the process of constructing multi-regional models via temporal discrepancies in national data, the concordance of sectoral aggregation schemes, currency adjustments, and balancing procedures. However, these uncertainties are considered relatively insignificant compared to the overarching uncertainty, explored across all three scenario variants, in our understanding of how the electricity transmission system might respond to severe space weather.

Overview of scenario supply chain impacts

The underlying data required to perform the analysis takes the form of a balanced Multi-Regional Input-Output (MRIO) table. Specifically the 2011 MRIO table from the World Input-Output Database (WIOD) is used, which characterises interdependencies between 40 countries (and an aggregate Rest of World region) and 35 economic sectors (Timmer et al. 2015).

This data is derived from National Accounts, Supply and Use Tables and International Trade Statistics. Although only a recent development in the field of IO research, there are now several providers of MRIO data with global coverage (for a comparison

of available databases see Tukker and Dietzenbacher, 2013; Inomata and Owen, 2014 or Moran and Wood, 2014, for analysis). However, WIOD places a relatively high reliance on official national accounts statistics (rather than computational estimation techniques) and provides the greatest transparency over underlying data sources and methodologies used to construct the tables. Hence, the WIOD is one of the most frequently utilised databases in the literature (Baldwin and Lopez-Gonzalez, 2014; Trimmer et al. 2014; Johnson, 2014; Kucukvar and Samadi, 2015; Kucukvar et al. 2015; Fujii and Managi, 2015). Once the concordance table has been utilised, the direct economic loss is shown relative to the NACE (revision 1) categorisation at the national level.

The results of the indirect supply chain impacts analysis are summarised in Table 8. The direct shocks applied to US sector total outputs manifest firstly as direct shocks to the value-adding activities of these sectors, this amounts to between $217bn for scenario variant S1 and $1,232bn for X1, which corresponds to 1.4% and 4.6% of US GDP (in 2011), respectively.

Taking the upper bound on indirect impacts (i.e., minimally aligned supply chains), we estimate considerably greater indirect shocks in the domestic economy than in non-US regions: indirect US supply chain shocks amounting to 93% of overall direct shocks are found ($202bn in S1 to $1,147bn in X1), while international supply chain shocks are estimated at 25% of overall direct shocks ($55bn in S1 to $314bn in X1).

Combined together, indirect domestic and global supply chain impacts give rise to total (direct and indirect) global shocks that are more than two-fold the original direct shock ($474bn in S1 to $2,693bn in X1). With global total shocks estimated to be between 0.7% and 3.9% of global GDP, the overall economic impact of these scenarios is likely to be very significant, potentially leading to major policy intervention, such as interest rate adjustments and short-term stimulus measures.

The following sections explore firstly US sector-level results and secondly global supply chain impacts in more detail.
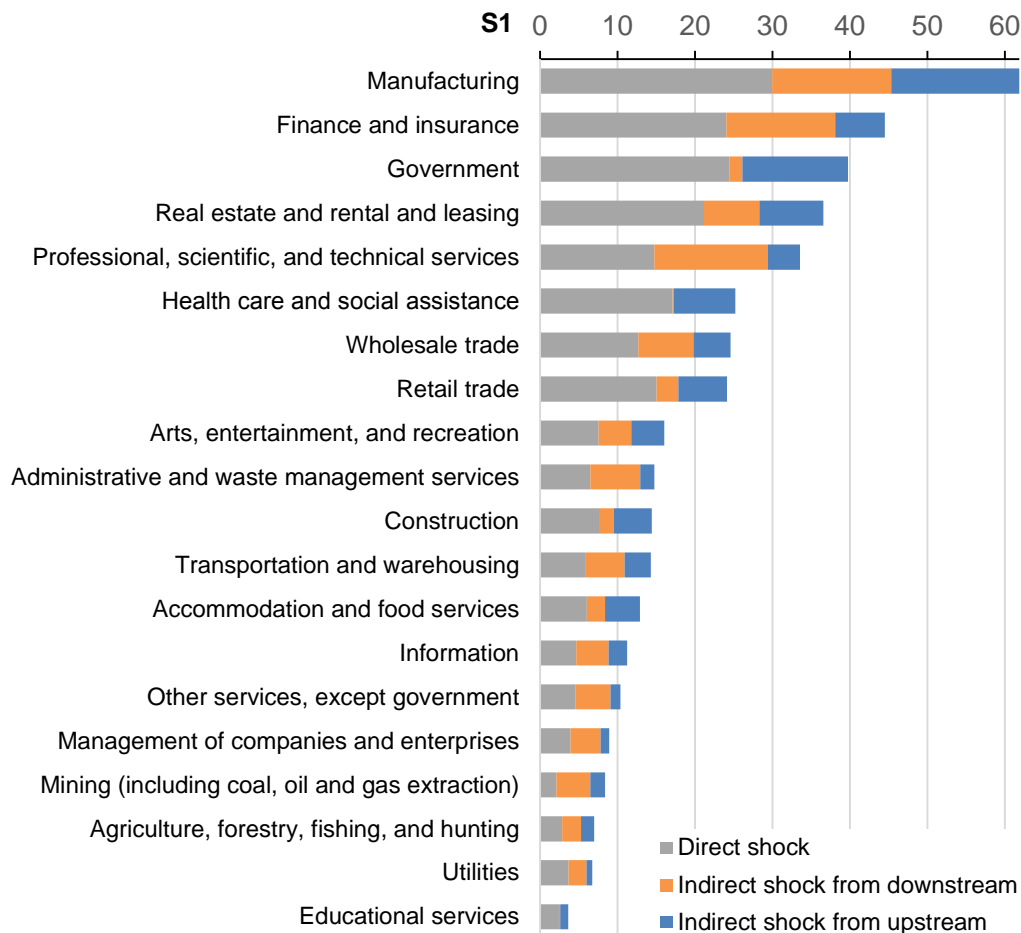
Figure 11: Scenario indirect supply chain impacts on US sectors
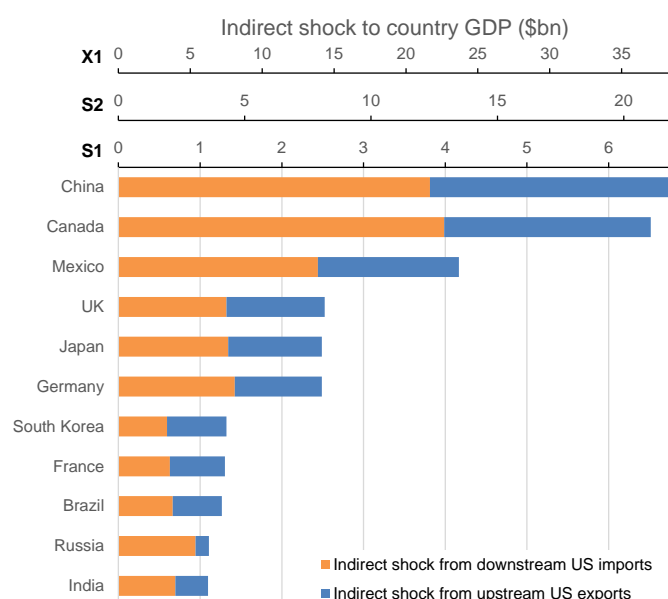
US sectoral supply chain impacts

Results for the direct and indirect shocks facing individual US sectors are presented in Figure 11. Here, we separate indirect shocks into two sub-components: impacts that have been instigated by downstream shocks, giving rise to reduced demand for a sector's output of goods and services and a corresponding reduction in value-adding activities; and, impacts that have been instigated by upstream shocks, giving rise to reduced availability of a sector's necessary inputs and, again, a corresponding reduction in value-adding activities. The choice of sectoral aggregation matches that of the BEA data used to estimate the extent of direct shocks in the previous section.

Sectors involved mainly in the production of goods and services for end-consumption, such as Construction, Retail Trade, Health Care & Social Assistance, Accommodation & Food Services, and Government can be seen receiving greater impacts from upstream supply constraints. Conversely, sectors that provide support services to the rest of the economy, such as Finance & Insurance, Professional, Scientific, & Technical Services, and Administrative

& Waste Management Services, receive a greater share of their overall indirect impact from changes in downstream demand.

The Manufacturing sector, with the largest US sector GVA ($1,891bn), is found to have both the greatest direct ($30bn in S1 to $170bn in X1) and indirect ($32bn in S1 to $181bn in X1) shocks, with indirect shocks having a roughly equal split between those that have been induced upstream and those induced downstream. The Mining sector is found to have the highest indirect shock as a share of total shock (75%). This is due to that sector having a particularly low direct shock relative to its GVA (0.7% in S1 to 5.5% in X1) as a consequence of its geographical distribution, favouring states with relatively low risk factors (e.g., oil and gas from the Gulf of Mexico), and its importance in supplying intermediate products to many other sectors.

Health Care & Social Assistance, Educational Services, and Government each have a relatively high direct shock as a share of total shock (68%, 67% and 62%, respectively), partly due to their relatively high value-added factors (primarily in the form of labour costs) and insulation from downstream shocks.

Figure 12: Scenario indirect impacts on international supply chains

International supply chain impacts

Results for the indirect shocks facing individual countries linked to the US via global supply chains are presented in Figure 12. Again, indirect shocks are separated into upstream and downstream sub-components, which in this context correspond to a country's dependence on US exports and imports, respectively. Overall, non-US regions are estimated to experience both considerable upstream and downstream indirect shocks from the US; changes in US demand for foreign goods and services (i.e., downstream import shocks) account for slightly greater share (57%) of overall indirect impacts, reflecting the general position of the US in the global value chain. However, this overall figure varies from country to country; for example, Russia, India and Canada have a higher than average impact from downstream US import shocks (85%, 64% and 61%, respectively), while South Korea and France have a higher than average impact from upstream US export shocks (45% and 48%, respectively).

China, Canada and Mexico, as the three largest trade partners of the US, collectively account for 32% of all indirect international supply chain impacts, ranging from $17bn in S1 to $99bn in X1.

8 Macroeconomic Analysis

The macroeconomic analysis quantifies both the direct and indirect macroeconomic consequences from critical interdependent infrastructure systems. It focuses on understanding how failures in the electricity sector can lead to wider indirect effects elsewhere in the global economy. Although direct shocks are only modelled for countries falling under the storm footprint, indirect effects are felt globally due to disruptions in international trade.

Direct economic shocks are initially estimated for the US based on a set of three scenario variant restoration curves (Figure 9, page 29). Each restoration curve reflects the assumed share of the national population without power each week following the storm. The least severe restoration curve (S1) is parameterised on the Bottom- up Restoration Curves, which considers around 5.2% of the US population to be affected in the first quarter, with the majority of the population being restored in the second quarter. The intermediate restoration curve (S2) considers about 15% of the population to be initially affected, with an overall duration of restoration of 2 Quarters. Finally, the most severe curve (X1) sees 17.8% initially affected and a restoration process lasting 4 Quarters. Although the restoration curves reference population affected, they are also assumed to reflect the share of business/production activity in the economy experiencing electricity supply disruption.

The immediate aftermath of the storm is assumed to give rise to a range of serious consequences, including:

- **Consumption and production** decline as the lack of electricity disrupts business operations (ranging from production activities, logistics and distribution, and financial transactions), household and government expenditure patterns, and labour supply and productivity (thus reducing potential output in the economy). There would be a fall in aggregate demand (AD=C+I+G+X-M) and a slowdown in the private and public sectors of the economy. On the consumption side of the equation, as panic sets in, there would be an initial increase in consumption however as people run out of cash due to failure of electronic methods of payment such as credit cards, eventually there would be a fall in consumption. Only necessary purchases would be made until the power returns. On the production side of the equation, power loss would result in a fall in business productivity as people are unable to access their workplace or

perform duties to an ordinary standard, causing inoperability in some businesses. In reality, some manufacturing and commercial facilities usually have backup generators but these typically provide only partial replacement. While some businesses may be able to operate without electricity, many, particularly those in busy cities, would face significant disruptions.

- **International trade** would be negatively affected as a result of power outage. Currently, about 90% of international trade (volume) and 60% (value) is conducted via sea. Maritime port operations would have to be suspended during the power outage since it would be considered unsafe or even impossible to load and unload container ships without electricity and thus import and export flow would be impacted. Goods that are already in the port and are awaiting to be exported would be put on hold, prompting a halt in production activity overseas and causing a cascading impact along the supply chain as the buyer would not be able to obtain necessary inputs for their production process. A similar story would play out with imports and the domestic economy.

- **Transportation disruption** significantly affects trade and travel. Land traffic signals cease as a consequence of the power outage resulting in a spike in traffic accidents. Government advises people to stay at home and only travel in the event of an emergency in order to prevent any further accidents. Aviation and maritime navigation signals fail as radio communications are severely disrupted by the geomagnetic waves. Airports and ports without power see activity grind to a halt. Even after power is regained, transportation companies such as railways and airports spend at least another week dealing with the aftermath chaos.

- **Digital communications** malfunction with the loss of reliable GPS timing and synchronisation, interrupting normal daily communications through mobile phones, internet, financial markets trading, etc.

- **Confidence shock** arising among the general public and financial services communities due to the uncertain outlook following power outage and corresponding effects on other industry sectors translates into weakened market sentiments. Confidence shock is also affected

by secondary effects of power outage such as social unrest and criminal activity. Criminals exploit the lack of lighting and security systems coupled with overstretched police forces. Looting intensifies as people face shortages in food and water. This spirals out of control a week after the power outage with many people scared to leave their houses after dark. The consequences of the power outage fall mostly on the most vulnerable people in the society. Many people who require constant medical supervision or drugs would be unable to obtain them resulting in a number of deaths. There would also be a long term impact on consumer confidence. As a result of significant amount of damage to many individuals and businesses, many would be pursuing a litigation process costing the US economy billions of dollars. This would force the US government to rethink its strategy on the power generation sector with additional funds appropriated towards research in better understanding extreme space weather events and the prevention mechanisms, policies and strategies required.

Estimating macroeconomic losses

Oxford Economics' Global Economic Model (GEM)

The macroeconomics model used in this analysis, the Oxford Economics' GEM, is one of the most widely used international macroeconomics models with clients including the IMF and the World Bank. The model provides multivariate forecasts and describes the systemic interactions for the largest 47 economies of the world, with headline information on a further 34 economies. Forecasts used in this study are updated monthly for a 10-year projection.

The GEM is best described as an eclectic model, adopting Keynesian principles in the short run and a monetarist viewpoint in the long run. In the short run output is determined by the dem and side of the economy, and in the long term, output and employment are determined by supply side factors. The Cobb-Douglas production function links the economy's capacity (potential output) to the labour supply, capital stock and total factor productivity. Monetary policy is endogenised through the Taylor rule, where central banks change nominal interest rates in response to changes in inflation. Relative productivity and net foreign assets determine exchange rates, and trade is the weighted average of the growth in total imports of goods (excluding oil) of all remaining countries. Country competitiveness is determined from unit labour cost.

Simulating economic impacts

Table 9 summarises the shocks applied to the Oxford Economics Model in each scenario variant. In the S1 and S2 scenarios, the shock is applied for two quarters and is tapered according to the scaling ratios. In the X1 scenario, the shock is applied to all four quarters.

Shocks are applied to specific economic variables, namely, consumption, potential output, government consumption, investment, exports and imports, and confidence shock on the basis of empirical evidence to measure the economic impact on GDP (or GDP@ Risk). For instance, there is a strong tendency for consumption (both private and government) to decline following major negative economic shocks: for example, Hurd and Rohwedder (2010) find that between 2007 and 2009 (i.e. during the height of the Great Financial Crisis) there was an average

Table 9: Shocks applied to Oxford Economics' GEM variables (Q1)

	Average population without power	Consumption	Potential Output	Government Consumption	Investment	Exports	Imports	Confidence Shock
Scaling factors		0.5	0.5	0.5	0.5	0.8	0.8	1.0
S1								
Q1	5.2%	2.6%	2.6%	2.6%	2.6%	4.16%	4.16%	5.2%
Q2	0.4%	0.2%	0.2%	0.2%	0.2%	0.32%	0.32%	0.4%
S2								
Q1	15.3%	7.65%	7.65%	7.65%	7.65%	12.24%	12.24%	15.3%
Q2	2.6%	1.3%	1.3%	1.3%	1.3%	2.08%	2.08%	2.6%
X1								
Q1	17.8%	8.9%	8.9%	8.9%	8.9%	14.24%	14.24%	17.8%
Q2	10.4%	5.2%	5.2%	5.2%	5.2%	8.32%	8.32%	10.4
Q3	2.6%	1.3%	1.3%	1.3%	1.3%	2.08%	2.08%	2.6%
Q4	0.99%	0.495%	0.495%	0.495%	0.495%	0.792%	0.792%	0.99%

decline of eight percentage points in US expenditure. Similarly potential output and international trade fall following an adverse shock due to less production and consumption taking place (Gassebner et al. 2006).

Macroeconomic modelling of the scenario

The model assumes the shock begins in the first quarter of 2016 (although it should be noted that the exact timing of the extreme space weather event is not specified in the scenario). The macroeconomic consequences of this scenario are modelled using the Oxford GEM. The output from the model is a five-year projection for the world economy. The impacts of the three scenario variants are compared with the baseline projection of the global economy under the condition of the extreme space weather event not occurring.

The overall impact of this catastrophe can be captured by the GDP@Risk metric, which represents the total difference in GDP between the baseline projections and the scenario projections. The total GDP loss over five years, beginning in the first quarter of 2016 during which the shock of the extreme space weather event is applied and sustained through to the last quarter of 2020, defines the GDP@Risk for this scenario. This is expressed as a percentage of the total GDP projection for the five years without the crisis occurring.
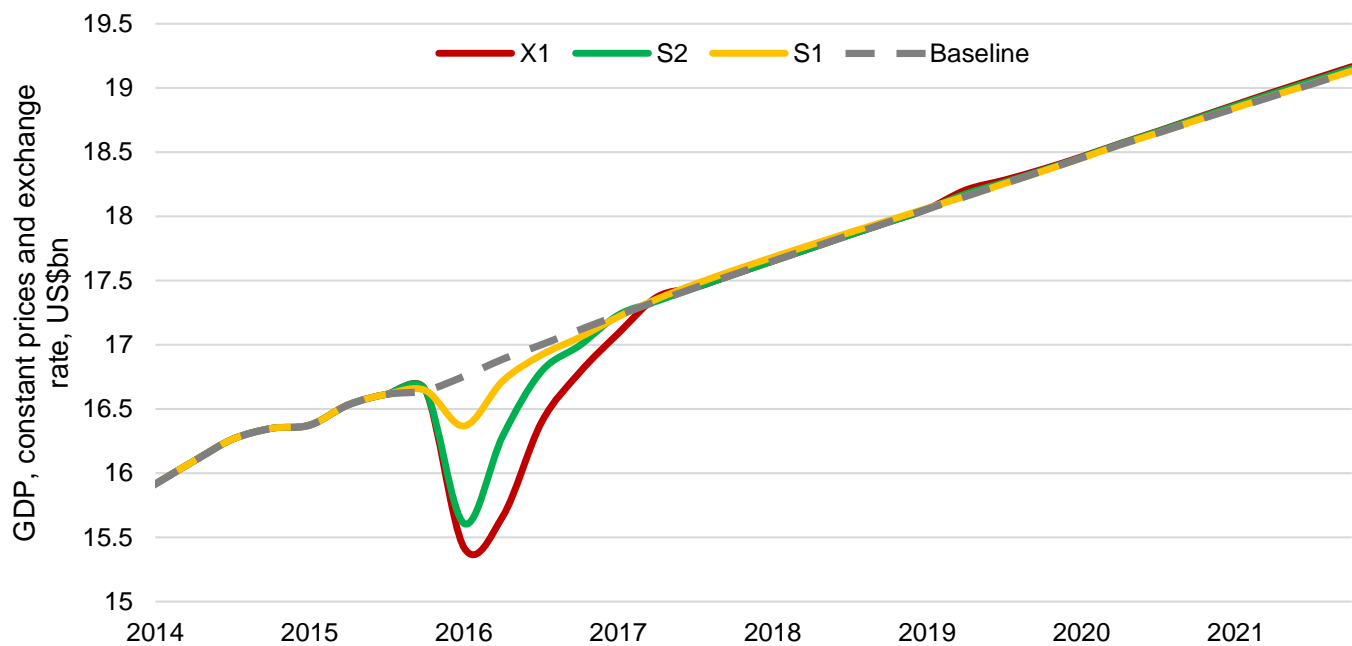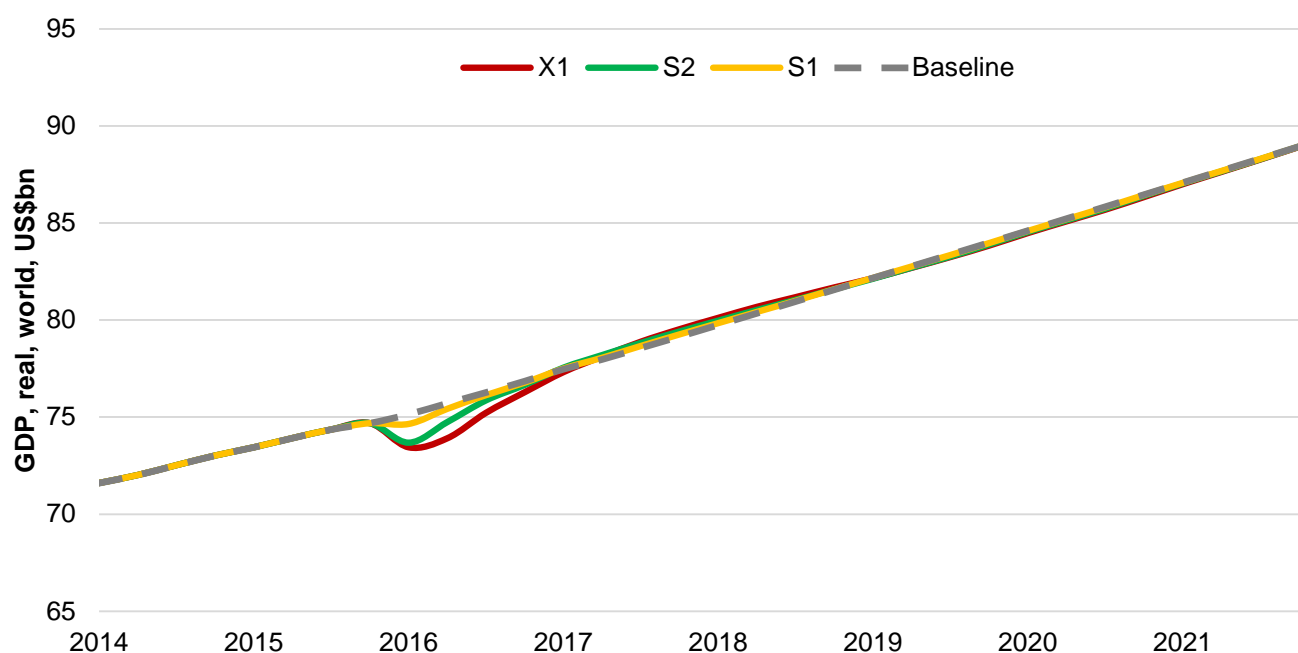

Figure 13: Estimated loss in US GDP

Figure 14: Estimated loss in global GDP

Table 10: Summary of scenario indirect supply chain impacts

Location	Baseline	S1		S2		X1	
	5-Yr GDP (US$ Bn)	GDP@Risk (US$ Bn)	GDP@Risk (%)	GDP@Risk (US$ Bn)	GDP@Risk (%)	GDP@Risk (US$ Bn)	GDP@Risk (%)
Canada	9569.8	2.5	0.03%	11.7	0.12%	24.8	0.26%
China	52586.2	-2.8	-0.01%	34.0	0.06%	48.9	0.09%
Mexico	6642.2	0.6	0.01%	5.4	0.08%	12.6	0.19%
Germany	19417.5	1.1	0.01%	9.0	0.05%	18.0	0.09%
Japan	29384.8	-1.6	-0.01%	14.2	0.05%	23.8	0.08%
United Kingdom	14303.5	0.2	0.002%	5.6	0.04%	10.9	0.08%
Russia	8243.4	-0.6	-0.01%	8.3	0.10%	14.1	0.17%
India	13647.7	0.7	0.01%	37.4	0.27%	64.9	0.48%
Brazil	11720.1	-0.08	-0.001%	22.6	0.19%	38.5	0.33%
France	14509.9	0.8	0.01%	7.7	0.05%	15.3	0.11%
South Korea	6903.8	1.1	0.02%	13.2	0.19%	18.5	0.27%
Spain	7648.8	0.05	0.001%	5.6	0.07%	12.8	0.17%
United States	88944.5	135.9	0.15%	319.7	0.36%	613.0	0.69%
World	403556.5	141.0	0.03%	575.9	0.14%	1067.2	0.26%

The results shown in Figure 13 suggest that the initial shock to the US economy is severe, especially in the X1 variant scenario when the full restoration of the power outage takes up to four quarters. However, recovery takes place between 2017 and 2018. This can be attributed, in part, to a sharp increase consumption spending as soon as the power supply is reinstated. Figure 14 illustrates the dip in global GDP modelled to occur as a result of the scenario, in all its variants.

Table 10 summarises the OEM outputs. In S1, the total estimated US GDP@Risk is US$136 billion, or 0.15% of the five-year baseline GDP projection of the US economy. Similarly, the global GDP@Risk amounts to $141 billion, or 0.03% of the five-year baseline GDP projection of the global economy. The negative signs in the S1 scenario for China, Japan, Russia and Brazil indicate that there might be a substitution effect in play. Some suppliers may decide to switch from US producers to those in China, Japan, Russia and Brazil, benefiting these countries.

9   Insurance Impacts

Insurers could see a large number of claims across many lines of business resulting from an extreme space weather event. In recent years there have been a number of industry reports on space weather and insurance including those by SCOR, Aon Benfield, CRO Forum and Lloyds (Launay, 2014; Aon Benfield, 2013; CRO Forum, 2011; Lloyd's 2013). None of these reports has attempted to estimate insurance loss from an extreme space weather event. Schrijver et al (2014) analyse a proportion of US insurance claims over an 11 year period between January 2000 and December 2010 and find that on average 500 claims can be attributed to large- scale geomagnetic variability in the low-voltage power distribution network even during a relatively calm period of space weather.

There is increasing interest in understanding extreme space weather as an emerging risk in the insurance industry. The Bank of England Prudential Regulation Authority included a solar flare/geomagnetic storm as one of the 11 stress tests recommended for insurers to estimate losses against (Bank of England, 2015). Lloyd's of London offer a space weather event scenario as part of its realistic disaster scenarios (RDS) that is not part of the compulsory scenarios, meaning an insurer only has to report on the space weather scenario if losses are above a certain value (Lloyd's, 2016). More specifically, the Lloyd's space weather RDS focuses on satellite risks and not the impact that could result from a long-term power outage.

In this section, we estimate the losses that the US insurance industry are likely to sustain due to a hypothetical extreme space weather event. Table 11 shows the losses for the main areas of insurance business that are likely to drive the total payouts. We describe the main assumptions in this section.

Claimant types

We have estimated the loss based on seven categories of claimants:

1. **Power transmission operators** – owners of EHV transformers (>345 kV).

2. **Power generation companies** – owners of generator step-up transformers.

3. **Companies that lose electricity supply** – those that suffer losses as a result of the blackout interrupting business-as-usual operations. These include companies who suffer property losses (principally to perishable contents), or who experience a service interruption due to a blackout.

4. **Satellite** – increased radiation and charging issues cause damage to a small portion of satellites.

5. **Homeowners** – power outages at individual households cause fridge and freezer contents to spoil resulting in claims on contents insurance.

6. **Speciality** – the power outage is likely to cause claims under event cancellation coverage.

Table 11: Estimated insurance industry losses resulting from the three variants of the scenario ($millions)

Claimant Type	Coverage	S1	S2	X1
Power transmission companies	Property damage (EHV transmission transformers)	466	1,845	1,845
	Incident response	29	92	92
	Fines FERC/NERC8	4	8	24
	Directors & Officers Liability	600	1,867	1,867
Power generation companies	Property damage (Generator step-up transformers)	84	539	880
	Business Interruption	423	2,424	3,825
	Incident response	4	21	28
	Fines FERC/NERC*	4	8	16
	Directors & Officers Liability	95	533	729
Companies that lose power	Perishable contents	1,079	1,727	1,790
	Service interruption	50,983	161,584	318,861
Satellite	Property damage (satellites)	218	435	645
Homeowners	Household contents	449	720	720
Specialty	Event cancellation	603	1,206	2,411
Total		**55,040**	**173,009**	**333,732**

[*] Federal Energy Regulatory Commission (FERC), North American Electric Reliability Council (NERC)Homeowners

Table 12: Estimated insurance industry losses resulting from the three variants of the scenario ($millions)

Damage Scale	Damage Scale Description	% of transformers			Damage factor
		S1	S2	X1	
D0	Not Affected	68%	49%	49%	0%
D1	Tripped Off	26%	33%	33%	0%
D2	Minor Damage	5%	14%	14%	30%
D3	Major Damage	0%	3%	3%	100%
D4	Destroyed	0%	0.2%	0.2%	100%

Power transmission and generation companies

Property damage (EHV transmission transformers)

Damage could arise from the overheating of components due to increased GICs in the network, leading to a machinery breakdown, fire or explosion. Overheating is generally covered under all-risk property policies and may fall under machinery breakdown.

There are approximately 2,300 EHV transformers in the US (Electric Utility Annual Reports, 2014). In order to develop detailed restoration curves, we assigned transformers to a damage scale (D1-D5). Table 12 shows the percentage of transformers assigned to each damage scale by scenario variant and the damage factors used. For minor damage, D2, we assume a 30% loss in asset value and for major damage and destroyed, we assume a 100% loss. Using asset values from DOE (2014) and adjusted for 2016 dollars, we estimate that the average cost of a 345kV transformer is $11.25 million, inclusive of 25% inflation for transportation and installation costs. We also assume a deductible of $0.5 million and a limit of $11 million.

Property damage (Generation step-up transformers)

There are over 7,400 generation plants in the US with 10% reporting grid connections over 345 kV (Energy Information Administration, 2015). We assume that each generation plant has at least one EHV transformer. We assume that, from the total number of generation plants, only 10 to 20% of their transformers get damaged, thus 20 (S1 variant) and over 150 (X1 variant) generation transformers are assumed to be damaged. Using asset values from DOE (2014) and adjusted for 2016 US dollars, we estimate that the average cost of a 345kV generation transformer is $6.25 million, inclusive of 25% inflation for transportation and installation costs. Generator step-up transformers are normally operated at nameplate capacity without any redundancy, thus we assume a damage factor of 75 to 100% for each scenario variant. We also assume a deductible of $0.5 million and a limit of $7 million.

Business Interruption (Generation step-up transformers)

The damage to the generation step-up transformers prevents the selling of electricity to the grid while these assets are repaired/replaced and brought back on-line. They claim a business interruption loss under their property cover. Given that large regulated power generation companies typically self-insure, we assume that only 50% of the generation transformers belong to companies that purchase BI coverage. Using data from S&P Capital IQ, we estimate the average annual revenue of a US transmission/generation company is $1.9 billion and we assume a 25% loss of daily revenue in our estimates. We assume a range of deductibles from 30 to 60 days with a limit of $5 million. We assume that each generation transformer is out for 3 to 6 months.

Incident response costs

The incident will generate additional costs for the power transmission and generation companies in their emergency response to the event, the clean-up and making safe process. Companies would employee specialists to inspect the transformers prior to returning them to service. These specialists will complete test to ensure that the transformer is sage to turn back on. For those they may have caught on fire, special foam extinguishers will be used to put out the fire. These costs are sub-limited to $100,000-250,000.

Fines FERC/NERC

The power transmission and generation companies face civil penalty fines from their regulators for failing to have robust operational mitigation plans and for not being up to the reliability standards. Fines can be levied by FERC based on Reliability Standards written by the NERC standards. Fines of up to $25 million have been levied on power companies and we have assumed similar fines would occur in this scenario (see breakout box). If these fines are completely covered by insurance they would be sublimited.

Directors and Officer Liability

There are many areas where possible liability claims could arise, such as worker safety concerns, General Liability, and Directors and Officers (Lloyd's, 2013 and CRO Forum, 2012). The main area we consider for liability claims relating to generation and transmission companies is directors and officers. Owners of the transformers that cause the power outages owe a duty of care to their shareholders to maintain operational mitigation plans to deal with adverse situations such as an extreme space weather event. Companies who lose power may underperform compared to their competitors and could see share price devaluation. This could result in legal action by the shareholders.

Using the same number of generation and transmission companies impacted by transformer damage, we assume that 5% have liability insurance and file a successful claim, we also assume a 5% loss in valuation in order to estimate the insurance payout.

Other Liabilities

Historically, mass torts against power companies for failure to supply electricity resulting in property damage have not gone favourably for the plaintiffs.

The burden of proof of gross negligence is on the plaintiff. The economic loss doctrine of tort law requires the plaintiff to show that significant property damage or personal injury occurred as a direct consequence of the outage. They also must demonstrate that they have taken every precaution to prevent the loss themselves, such as installing uninterruptible power supplies. Given these requirements for torts, the most successful tort actions have been for food spoilage and mould remediation (Standler, 2011).

Companies that lose power

Although, the direct damage from the storm is to the physical assets, there is an even larger loss potential from companies that lose power, because they either have to cease production/operation and for some their perishable contents spoil (CRO Forum, 2012; Rose and Huyck, 2016). The percentage of companies impacted by the power outage is assumed to be equivalent to the state power affect from the state level restoration curves, see Figure 9 (page 24). We use a data set from the US Census Bureau (2016) for number of establishments and revenue by NAICS sector by US state. There are just over 1.1 million establishments in the US that have over 500 employees.

FERC Regulation and Fines

FERC Order No. 779 outlines a two part process that requires NERC to implement operational and engineering reliability standards. The operational reliability standards went into effect in 2014 and require a utility to have an operational plan to mitigate the impact of a GMD on their systems (FERC,

2014). In the second part, utilities will be required to perform engineering assessments of their systems to determine how they will be affected by geomagnetic storms (Kemp, 2014).

NERC conducts annual audits of various electric utilities over the course of the year, either randomly or after a major outage event. FERC can then impose fines on electricity companies for violating these NERC reliability and CIP standards and can be as high as $1 million per day (Tripwire). The CIP fines focus in particular on cyber security standards.

Typically, a portion of these fines is paid to the US Treasury and NERC, while the remainder is used by the electricity company to make improvements in keeping with reliability and security standards. Although civil penalty fines for violation of NERC reliability standards typically range from $50,000 to $350,000, there are recent examples of fines greater than $1 million, especially in cases where an outage has occurred. (J. DeJesus and J. Halpern)

- Florida Power and Light Company (FPL) was asked to pay a $25 million fine for violating reliability standards in 2009. (J. DeJesus and J. Halpern)

- PacifiCorp was required to pay $3.9 million for a 2011 outage. (J. DeJesus and J. Halpern)

- Arizona Public Service Company (APS) was forced to pay $3.3 million in fines for 2011

- Southwest outage that affected 5 million people. (R. E. Peace and C. Tweed)

There is also a precedent of FERC fining an entire NERC region. A 2008 outage in the Florida Reliability Coordinating Council (FRCC) left almost one million people without power and FRCC was asked to pay a $350,000 fine (E. M. Daly).

Business Interruption Insurance

There are two main forms of business interruption coverage (Berry, 2000).

Insurance Coverage	Definition	Example
Business interruption (BI)	1st party coverage for lost income due to physical damage at the insured's location	Power generation companies with damaged generator step-up transformers
Contingent business interruption (CBI)	3rd party coverage for lost income due physical damage at a suppliers, providers or consumer of its product or services	Companies that lose power due to the physical damage to transformers

An extension available for CBI is service interruption, which covers the loss of key utilities such as electricity, gas and water.

The legal side of power outages and insurance

The courts seem undecided on the definition of "physical damage" when it comes to service interruption coverage. In *American Guarantee & Liability Insurance Co. v. Ingram Micro, Inc. (2010)*, the courts ruled that "physical damage" occurred when a power outage shut down a microcomputer manufacturing plant. "The Court finds that 'physical damage' is not restricted to the physical destruction or harm of computer circuitry, but includes loss of access, loss of use and loss of functionality" (Samson).

In *Wakefern Food Corp v. Liberty Mutual (2009)* the Courts ruled that Liberty Mutual must pay service interruption claims to Wakefern for food spoilage that occurred at their supermarkets during the Northeast 2003 power outage (McCarter; FindLaw).

In *Ferraro v. North Country Insurance (2005)* The courts held that the insurer should have been more clear in the policy wording regarding 'physical damage' wording and sided with the insure for losses from the 2003 blackout (Suriano and Haas, 2012)

Finally, in *Fruit and Vegetable Supreme Inc. v. The Hartford Steam Boiler Insp.* (2010) and *Lyle Enterprizes, Inc. v. Hartford Steam Boiler Inspection and Insurance Co., 399 F.Supp.2d 821* (E.D.Mich. 2005) the courts seemed to have changed their definition of 'physical damage' given the insurance policies in question and denied the requested service interruption payment for food spoilage during the 2003 outage (Jackson, 2012).

Perishable contents

We estimate from the US Census Bureau (2016) that approximately 29% of US industry sectors are associated with perishable contents business, including Wholesale and Retail, Transportation, Warehousing, Accommodation, Food Services, and Manufacturing. Of these sectors, 95% have purchased insurance that covers loss or damage to these contents. We assume that 20% of their daily revenue is claimed and that the deductibles range from 24 to 72 hours with limits ranging from $10 - 25 million.

Contingent Business Interruption –Service Interruption/Suppliers Extension/

Service interruption cover is widely purchased by large corporations and covers the outages of key utility service providers, such as electricity, gas and water (Launay, 2014).

Taking into account key assumptions about the number of companies with service interruption insurance covering a loss of power and with policies that have wording such that claims are paid out, we estimate from data drawn from the US Census Bureau (2016) that approximately 19% are eligible for claims.[7]

---

[7] To estimate the number of companies experiencing a loss, we first assume that on average 25% of all large (500+ employee) US companies have supplier's interruption insurance. Then we take another cut to keep only companies without back-up generators. Using a dataset of electricity generators and power plants in the US from EIA.gov, we have calculated the number of back generators per US NAICS sector for each state (Energy Information Administration, 2015). Finally, we assume another 25% reduction for policy wording that prevents or limits successful claims. With all these reductions, the total company's eligible for a service interruption claim is just over 222,000 out of the 1.1 million in the original dataset , or j ust 19%. We then take a future reduction by using the state restoration curves as a proxy of the business affected in each state, estimating the only 63,000 companies or 5% experience an outage and are eligible for a claim in the S1 scenario variant.

Table 13: Summary of satellite orbits characteristics

Satellite Type	Purpose	Typical Users	Examples	Space Weather Concerns	Insured
Low Earth Orbit (LEO)	Imaging, Earth observation, data services	Commercial	ISS, Iridium	Most affected by space weather, potential damage to solar panels or imaging sensors	Insured
Mid Earth Orbit (MEO)	GPS,GNSS, Military	Government	Galileo	Most government owned assets	Typically not insured
Geostationary (GEO)	Communications, TV, Broadband	Commercial	DirecTV/Sky	Possible exposure	Insured
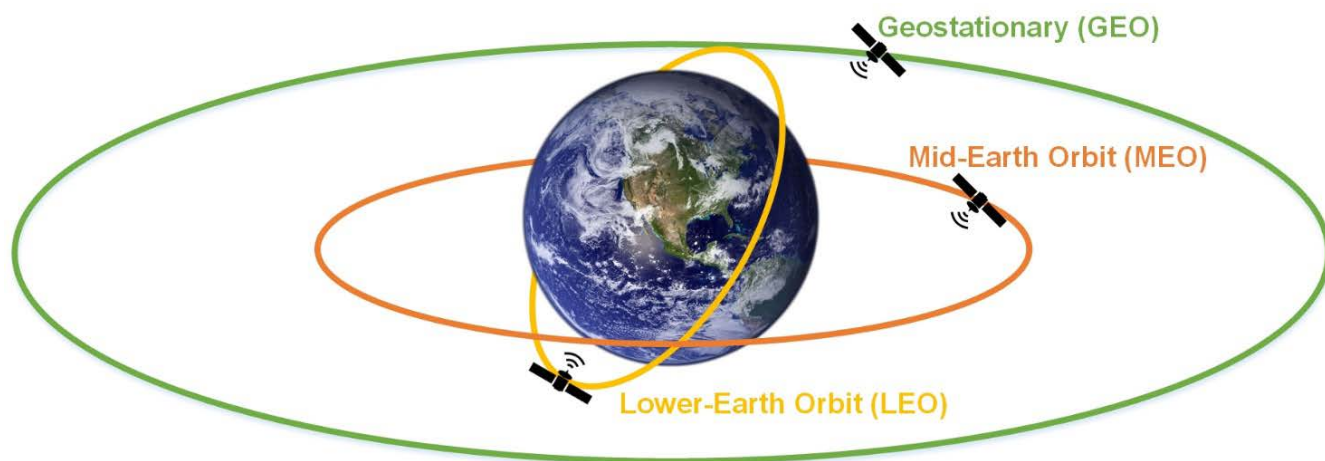
Figure 15: Satellite orbits (Source: Harris CapRock**)**

We use the US restoration curves to again estimate the percentage of companies that experience a power outage. We assume that the average deductible is 24 hours with a sublimit of $15 million.

Products could have to be scrapped for production processes that are running at the time the outage hits. Or emergency shut procedures could be activated and cause additional safety issues at the time of the blackout , such as an environmental release, as was the case with a Marathon Oil Plant in Michigan during the 2003 Northeast Cascading outage (CRO Forum, 2011). This could result in additional claims.

Satellite insurance

Due to increased radiation damage and charging issues, satellites could experience a permanent loss of functionality. There are three orbits for satellites: Low Earth Orbit (LEO), Mid Earth Orbit (MEO) and Geostationary (GEO), see Figure 15. The MEO satellites are primarily GPS/GNSS satellites which are owned by various governments and thus not insured.

Satellites are insured for pre-launch, launch and in-orbit phases. In-orbit insurance is purchased with launch insurance as launch plus one year in-orbit coverage and can be purchased for subsequent years as an additional coverage. Some satellite operators choose to self-insure after the first year (Swiss Re, 2011). Uninsured commercial satellites tend to be either very small or beyond their design life. In-orbit insurance typically only covers permanent loss of functionality, i.e. machinery breakdown.

The Royal Academy of Engineering Report (Cannon et al. 2013) recommended that extreme space weather could potentially damage or disrupt service to 10% of the satellite population and all satellites will experience premature ageing along with increased failure and anomaly rates.[8] Newer satellites have increased vulnerabilities due to standard off the shelf component designs that are not radiation-hardened (Horne et al, 2013).

Odenwald et al (2006) developed a simple method to estimate the loss of 80 satellites during a Carrington-like event; reporting the economic loss to be under $70 billion from lost revenue and satellite damage/ replacement. Wade et al (2012) reports that from 1994 to 2011, only 3% of the all space insurance

---

[8] Satellite failure is a result of complete loss of operation of the asset, i.e. damage that can't be repaired. This type of loss is less common with satellites. Abnormal operation is a result of partial damage or damage that is repairable, this is a more common event for satellites. Abnormal operation does not necessary lead to an insurance claim, as a satellite must suffer a permanent loss of functionality.

claims (or $274.5 million) from satellite operators were unambiguously attributable to space weather.

There are over 1,200 operational satellites in space as of year-end 2014 and 38% are for commercial use (SIA, 2015). Additionally, we assume that half of those are owned by US satellite operators. We also assume that of the entire satellite fleet that about 180 are insured, this is about 14% of the entire fleet (Swiss Re, 2011).

The Royal Academy of Engineering Report (Cannon et al. 2013) states that their "best engineering estimate, bases on the 2003 storm, is that around 10% of spacecraft will experience an anomaly leading to an outage of hours to days but most if these will be restored to normal operation in due course." For the S1 scenario variant, we extend the recommendation from the Royal Academy of Engineering Report (Cannon et al. 2013) and assume that 10% of satellite fleet suffers a 10% permanent loss of functionality.[9] This factor is increased for the S2 and X1 variants to 20% and 30% respectively. The insurance loss estimates are for 18 (S1), 36 (S2) and 54 (X1) satellites damaged.

We assume the average asset value for an LEO satellite is $75 million and a GEO satellite is $150 million. We apply no deductibles as space insurance policies typically don't offer them.

Further research is required to accurately estimate the exact number of satellites damaged during an extreme space weather event.

Homeowners

Homeowners could be accepted to claim a loss of fridge and freezer content spoilage under their homeowner policy. HO-3 is a common extension to a homeowner's policy that covers such spoilage with up to $500 limit and $100 deductible (Agrella, 2015). A 24 hour outage is likely to cause spoilage. We assume a 30% insurance penetration, with only 10% having the HO-3 wording.

Speciality

Given the length and widespread severity of the possible power outages resulting from extreme space weather, a number of public and private events will inevitably be cancelled. We assume that the affected US outage area has, in a typical month, an average of 300 significant events which would incur insurance payouts following forced cancellation or delay due to a loss of power, including public sporting events,

music concerts and festivals, large conferences, trade shows, political conventions, art shows and theatrical productions.

Event attendance in this calibre range from 500 to 90,000. Typically, baseball stadium such as the Yankee Stadium holds over 50,000 people. Average ticket price is assumed to be $70; given the range for an average New York Yankees game is $30 to $250. Cancellation costs incur loss of ticket sale profits and event advertising costs.

Additional areas of insured loss not included in estimate

Extreme space weather would likely cause claims across many other areas of insurance. For example:

- **Natural gas lines and oil pipelines** – Pipelines may be at risk from GICs due to cumulative long-term damage. The likelihood of increased corrosion could shorten an asset's life (Pulkkinen et al. 2001a; Pulkkinen et al. 2001b; Gummow & Eng, 2002). Gas lines are typically insured as part of an electric utilities physical assets.

- **Underground/underwater cables/fibre optic cables** – Undersea cables have been affected by GICs for over a century. However, modern systems rely on fibre optics, and therefore these glass fibres are far less conductive than their coaxial copper predecessors. As a consequence, there has been little GIC damage to submarine cables in recent years. Far more at risk are the electrical cables which often run side-by-side with fibre optic cables. Regardless, a potential loss of electricity to power these cables could still cause immediate, short-term inoperability but would be unlikely to cause any long-term damage.

- **Transformer manufacturers** – The manufactures of the transformers that fail or are damaged during the event could potential face litigation from the owners/operators of the assets under product liability coverage part of a general commercial liability excess liability policy.

- **Telecommunications** – Global communication systems could be impacted if a radio blackout occurs.

- **GPS/GNSS failure** – Companies that rely on GPS information could have a business interruption. It is still being debated as to who is liable for a GPS/GNSS outage (Baumann, 2015).

- **Rail transportation** - Step-down transformers in rail electrical networks are vulnerable to damage from extreme space weather.

---

[9] We understand that the degree of damage will vary based on satellite type; for example imaging satellites are less robust than communication satellites. We assume an average 20% damage factor for simplicity of calculations.

- **Goods in transit** – Shipments of goods could slow down or come to a stop during extend power outages due to the lack of traffic signals.

- **Auto** – There could be an increase in the number of automotive accidents during the power outage due to the lack of traffic signals. As the outage drags on, people will be less likely to travel and thus this risk could reduce greatly.

- **Aviation** – In 2012, extreme space weather caused increased radiation, forcing airlines to reroute flights. (Johanson, 2012).

- **Travel** – There could be reduced reduction in tourism as people cancel their travel plans due to lack of local transportation or hotels turning away guests due to lack of power and thus file claims against travel insurance policies.

- **Property fire** – As individuals and companies turn to diesel powered back-up generators during the outage, there is an increased risk of property fires.

- **Industrial accidents and environmental liability** – industrial companies that have to execute power outage operational procedures have an increased risk of industrial accidents and/or environmental releases.

- **Bodily injury** – There could be a possible increase in accidents during the power outage. Aviation workers could have increased radiation exposure during the storm. This would cause a rise in insurance payouts under accident and health, worker's compensation covers, general liability, healthcare insurance and life insurance.

- **Social unrest** – Prolonged power outages are likely to lead to social unrest as the population loses straightforward access to food and other key emergency services. In excessively long outages looting is likely as people become desperate for food and water.

Ambiguity in space weather coverage

All-risk vs. named peril policies

Space weather related losses will most likely be covered under an "all-risk" policy as very few, if any, exclusions exist. However, for a "named peril" policy to cover this event type, the loss will have to be caused by one of the perils, typically fire, lighting, explosion, or aircraft impact (FLEXA).

Electricity supplier and physical damage

As discussed in Launay (2014), the notion of electricity supplier may be challenged as part of a

---

Space Weather Exclusion Clause

It is not common for a policy to explicitly exclude space weather from coverage. Below is an example of a policy wording that excludes space weather.

"The following causes of loss are excluded whether or not insurance for such causes of loss is being maintained by you at the time of the loss and whether or not such loss or damage is directly or indirectly caused by or contributed to by a cause of loss covered under this policy:

Geomagnetic storms, solar flares, solar eruptions or bursts including plasma bubbles or ejections, magnetic field or magnetosphere fluctuations or disruptions, comets, asteroids, meteorites, or any falling spacecraft, part or fragment thereof" (ISO).

---

service interruption claim. If a company that directly loses power has a contract with the transmission company for electricity services, then an insurer is not likely to dispute the claim. However, if the company does not have an insurance policy directly with the transmission company but has a contract with the distribution company instead, then the insurer may dispute the claim. The grounds for this dispute are that the physical damage did not occur in the electrical distribution company, but instead at the transmission company. The US courts are not in aggregable as to the definition of physical damage and whether it has to occur in order for a service interruption claim to be paid, see breakout box.

Companies indirectly affected by power outage

Several other companies could be impacted via a disruption in their supply chains. For example, a manufacturer affected by the power outage could be a nominated Tier 1 critical vendor for another manufacturer not affected by the blackout. For a contingent business interruption (CBI) "coverage is usually triggered by physical damage to customers' or suppliers' property or to property on which the insured company depends to attract customers" (Torpey, 2003). In most cases, CBI claims will not be possible unless physical damage occurs.

Equipment degradation instead of failure

Degradation of transformers over time is likely to occur if the transformers are exposed to increased GICs without being damaged (Moodley and Gaunt, 2012). This raises the question as to whether the owner of this asset is insured. If the owner has cover for machinery breakdown, then yes, but if the

owner is hoping to rely on their traditional property insurance policy, it is not clear whether this would pay out for premature ageing of transformers caused by space weather.

The results in context

We estimate a US insurance industry loss of $55.0 to $333.7 billion for the Helios Solar Storm scenario described in this report. Looking at other estimates of insurance loss helps put the loss estimates into context. Swiss Re studies estimated the loss from Hurricane Katrina and Sandy as $45 to $35 billion, respectively (Swiss Re, 2006; Swiss Re 2013).

Additionally, all losses from catastrophes in 2015 were estimated as $85 billion (Swiss Re, 2015). Another angle to evaluate the insurance loss and comparing it to the total economic loss, both direct and indirect, see Table 14. The insurance estimates from an extreme space weather scenario account for about 12% of the total economic loss.

Table 14: Insurance loss in comparison with economic loss from IO modelling ($billions)

Scenario Variant	Total Outage Duration	Direct Shock for US, $ Bn	Indirect Shock for US, $ Bn	Total Shock for US, $ Bn	US Insurance Industry Loss Estimate, $ Bn	Insurance Loss as a % of economic loss
S1	6 months	$217	$202	$474	$55	13%
S2	8 months	$701	$652	$1,532	$173	13%
X1	12 months	$1,232	$1,147	$2,693	$333.7	14%

10   Investment Impacts

The macroeconomic effects of the hypothetical extreme space weather scenario will inevitably have an effect on the capital markets. This section considers the capital market impact of the scenario and the consequence for investors therein.

The performance of bonds, alternatives and equities in different markets are estimated from the macroeconomic outputs, and compared with a baseline projection of their expected performance had the scenario not occurred.

Valuation fundamentals

Note that this is an estimate of how the fundamentals of asset values are likely to change as a result of these market conditions, as directional indication of valuation. This analysis is not a prediction of daily market behaviour and does not take into account the wide variations and volatility that can influence asset values due to trading fluctuations, sentiment and the mechanisms of the market.

Passive investor assumption

A fundamental assumption we make in our analysis is that of considering a passive investment strategy. This assumption is unrealistic, as we expect an asset manager to react to changing market conditions in order to reduce losses and large fluctuations in returns. It is, however, a useful exercise to consider what would happen to a fixed portfolio, in particular because this represents a benchmark against which to compare the performance of dynamic strategies. Understanding what drives the behaviour of the fixed portfolio at different times gives useful insight towards the design of an optimal investment strategy.

A standardised investment portfolio

We access the performance of four typical high-quality investment portfolios under the extreme space weather scenario.

We built a fictional representative portfolio that mimics features observed in the investment strategies of insurance companies, titled High Fixed Income Portfolio and three others that mimic the investment strategies of pension funds titled Conservative, Balanced and Aggressive. For example the Conservative Portfolio structure has 55% of investments in sovereign snd corporate bonds, of which 95% are rated A or higher (investment grade). Residential Mortgage Backed Securities (RMBS) make up 5% of the Conservative Portfolio structure.

Investments are spread across the US, UK, Germany and Japan. Equities compose 40% of the Conservative Portfolio. We will assume for simplicity that equity investments correspond to investments in stock indexes. The Wilshire 5000 Index (W5000), FTSE 100 (FTSE), DAX (DAX) and Nikkei 225 (N225) stocks are used to represent equity investments in the US, UK, Eurozone and Japan, respectively. We assume a maturity of 10 years for long-term bonds, while short-term bonds have a maturity of 2 years in each country.

Details of the High Fixed Income Portfolio are shown in Table 15, Figure 16, Figure 17, and Figure 18.

Computation of returns

The estimation of portfolio returns is carried out using the following method. Market price changes or Mark to Market (MtM) are calculated for all government bonds using equation (1) and for corporate bonds and RMBS using equation (2).

(1) $\Delta\text{MtM}_{\text{Gov,t}} = (D_b)(-\Delta I/100)$,

(2) $\Delta\text{MtM}_{\text{Corp,t}} = (D_b)(-\Delta I/100) + (SD_b)(-\Delta CS/100)$

Where D_b is the bond duration, for which we assumed the following values: D_b=7 for ten years bonds and D_b=1.8 for two years bonds. SD_b represents the spread duration. The change in interest rates, ΔI on government and corporate bonds and the change in credit spreads, ΔCS are taken from the output of the macroeconomic analysis discussed in the previous chapter.

Government bond yields are estimated using a representative quarterly yield. While corporate and RMBS yields are estimated using a representative quarterly yield and the period averaged credit spread.

Equities market prices are calculated using the change in equity value from the macroeconomic modelling. The equity dividends are estimated using a representative quarterly yield.

Exchange rate affects are taken into to account to ensure that all reported portfolio returns are with respect to US dollars. Inflation rates are used to discount the nominal portfolio returns into real portfolio returns.

Portfolio Returns

Figure 19 shows the scenario variant impacts by portfolio structure. For the extreme space weather scenario, we see the aggressive portfolio structure underperform compared with the other structures.

Table 15: Composition of the High Fixed Income Portfolio Structure

	USD	GBP	Euro	Yen	Total
Government 2 yr	8.0%	6.0%	5.0%	3.0%	22.0%
Government 10 yr	8.0%	7.0%	6.0%	2.0%	23.0%
Corporate Bonds 2 yr	4.0%	4.0%	4.0%	2.0%	14.0%
Corporate Bonds 10 yr	6.0%	7.0%	3.0%	2.0%	18.0%
RMBS 2 yr	2.0%	1.0%	1.0%	1.0%	5.0%
RMBS 10 yr	1.0%	1.0%	1.0%	1.0%	4.0%
Equities	2.0%	3.0%	3.0%	2.0%	10.0%
Cash	4.0%	0.0%	0.0%	0.0%	4.0%
Total	35.0%	29.0%	23.0%	13.0%	100.0%
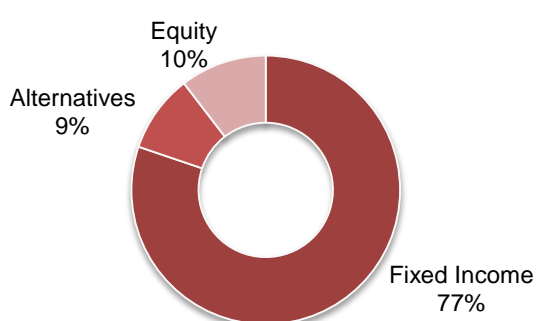
Figure 16: Asset classes in High Fixed Income Portfolio Structure
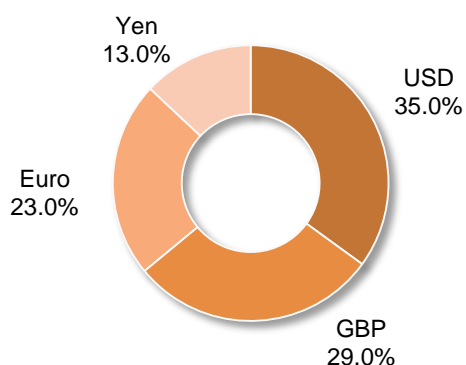
Figure 17: Geographic market spread of High Fixed Income Portfolio Structure
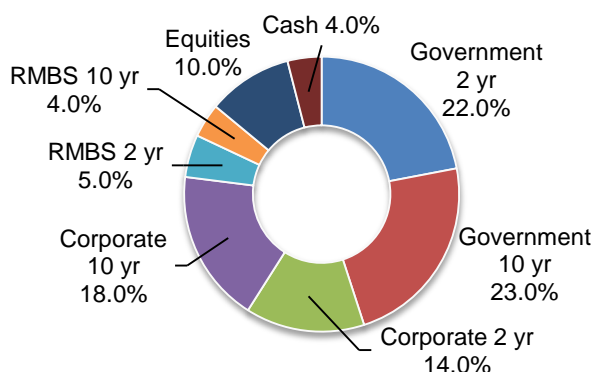
Figure 18: Detailed asset class breakdown of High Fixed Income Portfolio Structure
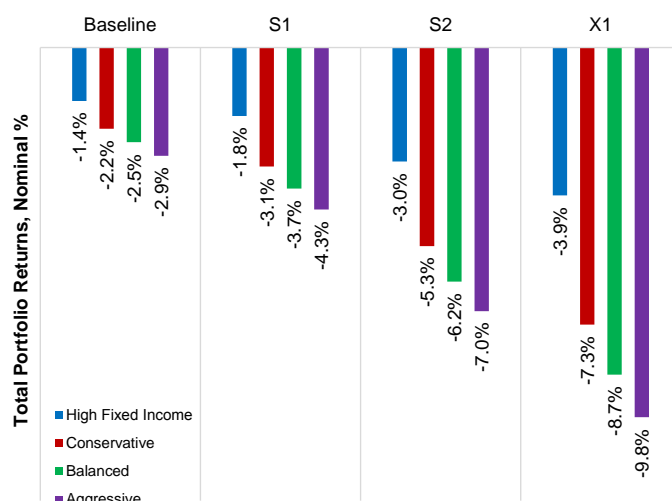
Figure 19: Extreme Space Weather Max Downturn by portfolio structure in nominal %.

Summary of investment portfolio analysis

In this part of the scenario analysis we have taken the output from the macroeconomic model and used it as an input to assess the performance of the four different portfolio structures. We have estimated the performance of the portfolio under the different variants of the scenario and compared it with the business as usual performance or baseline. The Aggressive portfolio structure performs the worst in this scenario, with a loss of -4.3% in the least extreme variant, S1.

The analysis presented in this section assumes a passive investment strategy. Nonetheless, it represents a useful benchmark to compare more asset management strategies. In particular, it can be used to discuss strategies that improve portfolio performance on a counterfactual basis under the scenario. Table 16 summarises the max downturn by portfolio structure and scenario variant.

Table 16: Summary of portfolio performance (max downturn) by structure and scenario variant, nominal %.

Portfolio Structure	S1	S2	X1
High Fixed Income	-1.8%	-3.0%	-3.9%
Conservative	-3.1%	-5.3%	-7.3%
Balanced	-3.7%	-6.2%	-8.7%
Aggressive	-4.3%	-7.0%	-9.8%

An important issue that we have not addressed in our analysis is that of systematically testing the stability of the results with respect to the parameter settings used in the earlier stages of the scenario development. This is to a certain degree taken into account given that we considered different variants of the scenario, but a more systematic analysis will be needed in this respect.

11 Conclusions

There is considerable ongoing debate around the risk extreme space weather poses to the global economy. In undertaking the research within this report, engagement with a range of stakeholders from industry and government showed that there are many different schools of thought on this subject. Indeed, we do not offer comprehensive and definitive economic assessment of extreme space weather because we do not believe that it is yet possible with our current level of scientific understanding. More resources need to be placed into refining the estimates presented here.

In light of this, however, what we have been able to accomplish is the exploration of different theoretical damage distributions for EHV transformers, at the same time as using scenarios of different event durations. By being transparent about the modelling assumptions applied and making use of only openly-accessible data, we have been able to provide new insight into the direct and indirect economic costs associated with extreme space weather. This includes providing estimates for the impact on insurance and asset portfolios for each of the scenarios.

Given the range of views put forward by the subject matter experts engaged in this research, the next major task is to determine the actual expected damage distribution of EHV transformers in space weather events. Indeed, with a large range of loss estimates for these scenario variants, it is important to again reiterate that we do not present a prediction or a definitive estimate of the potential costs of extreme space weather. What we instead present is a scenario-driven approach utilising theoretical damage distributions for EHV transformers, where we are able to (i) demonstrate an methodology for estimating the economic impact, and (ii) show how the potential costs stack-up under the outlined constraints. This hypothetical approach hence provides risk management teams with the ability to undertake stress testing activity to assess their exposure to this threat over each of the scenarios presented. This is an important contribution for both the academic and industry stakeholders.

Recapping on the research, the damage distributions explored in the S1 scenario saw 26% of US transformers tripped off-line with only 5% suffering any form of damage. In the S2/X1 scenarios 33% tripped off-line, 14% sustained minor damage, and 3% sustained major damage. 0.2% were completely destroyed. The loss of these assets led to a power outage initially affecting between 90 – 145 million US citizens for the S1 and S2/X1 scenarios. The majority of those affected had power restored relatively quickly. Only a smaller proportion of those affected from the grid collapse, approximately 5 – 15% of the total US population, were disconnected for more than three days between the S1 and X1 scenarios. The US states most directly affected were Illinois and New York which had economic losses of $31bn and $28bn in S1, and $171bn and $148bn in X1 respectively.

The total direct shock to value-added activities in affected economic sectors amounted to $217bn for S1 and $1,232bn for X1, corresponding to 1.4% and 4.6% of US GDP (in 2011), respectively. Taking the upper bound on the estimated indirect impacts, the domestic economy was more affected than non-US regions. The total indirect US supply chain shock was comparative to the direct shock, albeit slightly smaller ($202bn in S1 - $1,147bn in X1). The international supply chain shock was estimated at being roughly 25% the size of the overall direct shock ($55bn in S1 to $314bn in X1).

Combined together, indirect domestic and global supply chain impacts give rise to total (direct and indirect) global shocks that are more than two-fold the original direct shock ($474bn in S1 to $2,693bn in X1). With global total shocks estimated to be between 0.7% and 3.9% of global GDP, the overall economic impact of these scenarios is likely to be very significant, potentially leading to major policy intervention, such as interest rate adjustments and short-term stimulus measures.

The Manufacturing sector, with the largest US sector GVA ($1,891bn), is found to have both the greatest direct ($30bn in S1 to $170bn in X1) and indirect ($32bn in S1 to $181bn in X1) shocks, with indirect shocks having a roughly equal split between those that have been induced upstream and those induced downstream. China, Canada and Mexico, as the three largest trade partners of the US, collectively account for 32% of all indirect international supply chain impacts, ranging from $17bn in S1 to $99bn in X1.

In S1, the total estimated US GDP@Risk was US$ 135.99 billion, or 0.15% of the five-year baseline GDP projection of the US economy, whereas the global GDP@Risk is US$ 141.07 billion, or 0.03% of the five-year baseline GDP projection. In X1, the total estimated US GDP@Risk was US$ 613.03 billion, or 0.69% of the five- year baseline GDP projection of the US economy, whereas the global GDP@Risk is US$ 1067.22 billion, or 0.26% of the five-year baseline GDP projection.

We estimated the range of US insurance industry losses for the scenarios described in this report to be between $55.0 and $333.7 billion. Looking at other estimates of insurance loss helps put the loss estimates into context. Swiss Re studies estimated the loss from Hurricane Katrina and Sandy as $45 to 35 billion, respectively (Swiss Re, 2006; Swiss Re 2013). Additionally, all losses from catastrophes in 2015 were estimated as $85 billion (Swiss Re, 2015).

We see a number of benefits which can result from this work. Firstly, it is relevant for government and emergency planning agencies that are able to understand which economic sectors may be affected under the conditions of an extreme space weather event. This supports the decision-making processes associated with allocating limited resources. It is likely that there will be a desire to preference those sectors which experience the largest loss in economic output. Secondly, in terms of the relevance of these findings for private industry, the results can be of use to both network operators of critical national infrastructure, as well as those financially responsible in the insurance industry for paying out claims for personal, property and business interruption damages. Using these results, utility companies can understand the commercial (and potential litigious) consequences that can filter through the economy should they fail to protect critical infrastructure assets such as EHV transformers correctly. To date, there has been relatively little research carried out which considers the additional impact of indirect supply chain losses resulting from extreme space weather.

Further research is needed to understand how much redundancy lies in the power grid. Moreover, we do not yet have a scientifically robust way to link together extreme space weather, the expected response of the power grid, and finally how this may lead to lost direct and indirect economic value. Considering the level of uncertainty which persists in our understanding of the impact of space weather on modern society, space physicists, geophysicist and electrical engineers must continue now to work collaboratively on improving three main areas of research necessary for estimating the economic impacts of extreme space weather:

1. Improve the parameterisation of the risk matrix;

2. Introduce proper network asset and topology modelling of the transmission grid and the asset distribution within it to capture both asset-level vulnerability and network redundancy;

3. Empirically determine the potential damage distribution to EHV transformers from an extreme space weather event.

12   References

Agrella, R. 2015. 'Does Homeowners Insurance Cover Solar Storm Damage?' *Insuramatch*. March 19. https://www.insuramatch.com/news/does-homeowners-insurance-cover-solar-storm-damage.

Anderson, Christopher W., Joost R. Santos, and Yacov Y. Haimes. 2007. 'A Risk-Based Input–Output Methodology for Measuring the Effects of the August 2003 Northeast Blackout'. *Economic Systems Research* 19 (2): 183–204. doi:10.1080/09535310701330233.

Anderson, C. W. 1978. 'Magnetic Storms and Cable Communications'. *Solar System Plasma Physics*.

Anderson, Patrick L., and Ilhan K. Geckil. 2003. 'Northeast Blackout Likely to Reduce US Earnings by $6.4 Billion'. *Anderson Economic Group.*

Angelopoulos, V., A. Runov, X.-Z. Zhou, D. L. Turner, S. A. Kiehas, S.-S. Li, and I. Shinohara. 2013. 'Electromagnetic Energy Conversion at Reconnection Fronts'. *Science* 341 (6153): 1478–82. doi:10.1126/science.1236992.

AON Benfield. 2013. 'Geomagnetic Storms'. Minneapolis, MN: AON Benfield.

Astafyeva, E., Yu. Yasyukevich, A. Maksikov, and I. Zhivetiev. 2014. 'Geomagnetic Storms, Super-Storms, and Their Impacts on GPS-Based Navigation Systems'. *Space Weather* 12 (7): 2014SW001072. doi:10.1002/2014SW001072.

Atkins. 2016. 'Rail Resilience to Space Weather, Final Phase 1 Report'. London: Atkins Engineering Group. Accessed March 22. http://p.sparkrail.org/record.asp?q=PB021844.

Baker, D. N., X. Li, A. Pulkkinen, C. M. Ngwira, M. L. Mays, A. B. Galvin, and K. D. C. Simunac. 2013. 'A Major Solar Eruptive Event in July 2012: Defining Extreme Space Weather Scenarios'. *Space Weather* 11 (10): 585–91.

Balan, N., I. S. Batista, S. Tulasi Ram, and P. K. Rajesh. 2016. 'A New Parameter of Geomagnetic Storms for the Severity of Space Weather'. *Geoscience Letters* 3 (1): 1. doi:10.1186/s40562-016-0036-5.

Balan, N., R. Skoug, S. Tulasi Ram, P. K. Rajesh, K. Shiokawa, Y. Otsuka, I. S. Batista, Y. Ebihara, and T. Nakamura. 2014. 'CME Front and Severe Space Weather'. *Journal of Geophysical Research: Space Physics* 119 (12): 2014JA020151. doi:10.1002/2014JA020151.

Baldwin, Richard, and Javier Lopez-Gonzalez. 2015. 'Supply-Chain Trade: A Portrait of Global Patterns and Several Testable Hypotheses'. *The World Economy* 38 (11): 1682–1721. doi:10.1111/twec.12189.

Banerjee, Adrija, Amaresh Bej, and T. N. Chatterjee. 2011. 'On the Existence of a Long Range Correlation in the Geomagnetic Disturbance Storm Time (Dst) Index'. *Astrophysics and Space Science* 337 (1): 23–32. doi:10.1007/s10509-011-0836-1.

Barbosa, Cleiton, Livia Alves, Ramon Caraballo, Gelvam A. Hartmann, Andres R. R. Papa, and Risto J. Pirjola. 2015. 'Analysis of Geomagnetically Induced Currents at a Low-Latitude Region over the Solar Cycles 23 and 24: Comparison between Measurements and Calculations'. *Journal of Space Weather and Space Climate* 5: A35. doi:10.1051/swsc/2015036.

Basurah, Hassan M. 2006. 'Records of Aurora in the Islamic Chronicles during 9th–16th Centuries'. *Journal of Atmospheric and Solar-Terrestrial Physics* 68 (8): 937–41. doi:10.1016/j.jastp.2006.02.005.

Baumann, I. 2015. 'Liability for GNSS Signals and Services'. http://www.insidegnss.com/auto/novdec15-LAW.pdf.

Bergeot, N., C. Bruyninx, P. Defraigne, S. Pireaux, J. Legrand, E. Pottiaux, and Q. Baire. 2010. 'Impact of the Halloween 2003 Ionospheric Storm on Kinematic GPS Positioning in Europe'. *GPS Solutions* 15 (2): 171–80. doi:10.1007/s10291-010-0181-9.

Berry, D. 2000. "The Basics of a Business Interruption Claim". Dec 2000. https://www.irmi.com/articles/expert-commentary/the-basics-of-a-business-interruption-claim [Accessed: Feb 2016].

Board on Energy and Environmental Systems. 2012. *Terrorism and the Electric Power Delivery System.* http://www.nap.edu/catalog/12050/terrorism-and-the-electric-power-delivery-system.

Bolduc, Léonard. 2002. 'GIC Observations and Studies in the Hydro-Québec Power System'. *Journal of Atmospheric and Solar-Terrestrial Physics*, Space Weather Effects on Technological Systems, 64 (16): 1793–1802. doi:10.1016/S1364-6826(02)00128-1.

Boteler, David H., and Larisa Trichtchenko. 2015. 'Telluric Influence on Pipelines'. In *Oil and Gas Pipelines*, edited by R. Winston Revie, 275–88. John Wiley & Sons, Inc. http://onlinelibrary.wiley.com/doi/10.1002/9781119019213.ch21/summary.

Boteler, D. H. 2006. 'The Super Storms of August/September 1859 and Their Effects on the Telegraph System'. *Advances in Space Research*, The Great Historical Geomagnetic Storm of 1859: A Modern Look, 38 (2): 159–72. doi:10.1016/j.asr.2006.01.013.

———. 2015. 'The Impact of Space Weather on the Electric Power Grid'. In *Heliophysics V. Space Weather and Society*, by C. J. Schrijver, F. Bagenal, and Sojka. Palo Alto, CA: Lockheed Martin Solar & Astrophysics Laboratory.

Boteler, D. H., R. J. Pirjola, and H. Nevanlinna. 1998. 'The Effects of Geomagnetic Disturbances on Electrical Systems at the Earth's Surface'. *Advances in Space Research*, Solar-Terrestrial Relations: Predicting the Effects on the Near-Earth Environment, 22 (1): 17–27. doi:10.1016/S0273-1177(97)01096-X.

Cade, William B. 2013. 'The First Recorded Space Weather Impact?' *Space Weather* 11 (9): 489–489. doi:10.1002/swe.20091.

Cannon, P. S., et al. (2013), Extreme space weather: Impacts on engineered systems *Rep.*, ISBN 1-903496-95-0, Royal Academy of Engineering, London, UK.

Chulliat, A., S. Macmillan, P. Alken, C. Beggan, M. Nair, B. Hamilton, A. Woods, V. Ridley, S. Maus, and A. Thomson. 2015. 'The US/UK Magnetic Model 2015-2020'. Boulder, CO: National Geophysical Data Center, NOAA. http://dx.doi.org/10.7289/V5TH8JNW.

Clark, Jeff. 2013. 'Solar Flares: Risk to the Data Center'. Article. *The Data Center Journal*. July 25. http://www.datacenterjournal.com/solar-flares-risk-data-center/.

Clauer, C. R., and G. Siscoe. 2006. 'The Great Historical Geomagnetic Storm of 1859: A Modern Look'. *Advances in Space Research*, The Great Historical Geomagnetic Storm of 1859: A Modern Look, 38 (2): 117–18. doi:10.1016/j.asr.2006.09.001.

CRO Forum. 2011. 'Power Blackout Risks – Risk Management Options'. Netherlands: CRO Forum.

———. 2012. 'Solar Storm Ground Impact, Vulnerability, Mitigation and Basic Analysis of Stakeholders in the Associated Risk Arena'. Netherlands: CRO Forum.

Czech, P., S. Chano, H. Huynh, and A. Dutil. 1992. "The Hydro-Québec System Blackout of 13 March 1989: System Response to Geomagnetic Disturbances." *Electric Power Research Institute Report* EPRI TR-100450.

Davidson, W. F. 1940. 'The Magnetic Storm of March 24, 1940 – Effects in the Power System'. *Edison Electric Institute Bulletin* 8: 365–66.

de Nooij, Michiel, Carl Koopmans, and Carlijn Bijvoet. 2007. 'The Value of Supply Security: The Costs of Power Interruptions: Economic Input for Damage Reduction and Investment in Networks'. *Energy Economics* 29 (2): 277–95. doi:10.1016/j.eneco.2006.05.022.

Department of Energy. 2014. 'Large Power Transformers and the U.S. Electric Grid'. Washington D.C.: Department of Energy.

Eastwood, J. P., H. Hietala, G. Toth, T. D. Phan, and M. Fujimoto. 2014. 'What Controls the Structure and Dynamics of Earth's Magnetosphere?' *Space Science Reviews* 188 (1-4): 251–86. doi:10.1007/s11214-014-0050-x.

EIS Council. 2014. 'Geomagnetic Storms Information Sheet'. Los Angeles, CA: Electric Infrastructure Security Council. http://www.ourenergypolicy.org/wp-content/uploads/2014/01/Geomagnetic-Storms-Information-Sheet.pdf.

Electric Power Research Institute. 2014. 'Considerations for a Power Transformer Emergency Spare Strategy for the Electric Utility Industry'. Palo Alto, CA: Electric Power Research Institute.

Energy Information Administration. 2015. 'Form EIA-860 Detailed Data'. US Energy Information Administration.

Erinmez, I. Arslan, John G Kappenman, and William A Radasky. 2002. 'Management of the Geomagnetically Induced Current Risks on the National Grid Company's Electric Power Transmission System'. *Journal of Atmospheric and Solar-Terrestrial Physics*, Space Storms and Space Weather, 64 (5–6): 743–56. doi:10.1016/S1364-6826(02)00036-6.

Eroshenko, E. A., A. V. Belov, D. Boteler, S. P. Gaidash, S. L. Lobkov, R. Pirjola, and L. Trichtchenko. 2010. 'Effects of Strong Geomagnetic Storms on Northern Railways in Russia'. *Advances in Space Research* 46 (9): 1102–10. doi:10.1016/j.asr.2010.05.017.

European GNSS Agency. 2015. 'GNSS Market Report'. Luxembourg: Publications Office of the European Union. http://www.gsa.europa.eu/market/market-report.

Federal Energy Regulatory Commission. 2015. 'Documents & Filing - Forms - Form 1 - Electric Utility Annual Report'. http://www.ferc.gov/docs-filing/forms/form-1/data.asp.

Feldstein, Y. I. 1990. 'A Quarter of a Century with the Auroral Oval'. In *History of Geophysics: Volume 4*, edited by C. Stewart Gillmor, 103–8. American Geophysical Union. http://onlinelibrary.wiley.com/doi/10.1029/HG004p0103/summary.

FERC. 2014. 'RM12-22-000 Reliability Standards for Geomagnetic Disturbances'. Federal Energy Regulatory Commission. http://www.ferc.gov/whats-new/comm-meet/2014/011614/E-3.pdf.

FERC-NERC-Regional Entities. 2016. 'Report on FERC-NERC-Regional Entities Joint Review of Restoration and Recovery Plans'. Atlanta, Georgia: North American Electric Reliability Corporation.

Fletcher, L., B. R. Dennis, H. S. Hudson, S. Krucker, K. Phillips, A. Veronig, M. Battaglia, et al. 2011. 'An Observational Overview of Solar Flares'. *Space Science Reviews* 159 (1-4): 19–106. doi:10.1007/s11214-010-9701-8.

Fujii, Hidemichi, and Shunsuke Managi. 2015. 'Optimal Production Resource Reallocation for CO2 Emissions Reduction in Manufacturing Sectors'. *Global Environmental Change* 35 (November): 505–13. doi:10.1016/j.gloenvcha.2015.06.005.

Fujii, Ikuko, Takashi Ookawa, Shingo Nagamachi, and Takeshi Owada. 2015. 'The Characteristics of Geoelectric Fields at Kakioka, Kanoya, and Memambetsu Inferred from Voltage Measurements during 2000 to 2011'. *Earth, Planets and Space* 67 (1): 1–17. doi:10.1186/s40623-015-0241-z.

Garrett, Henry B., and Albert C. Whittlesey. 2012. *Guide to Mitigating Spacecraft Charging Effects*. John Wiley & Sons.

Gassebner, Martin, Alexander Keck, and Robert Teh. 2006. 'The Impact of Disasters on International Trade'. *WTO Staff Working Paper ERSD-2006-04*. http://papers.ssrn.com/sol3/papers.cfm?abstract_id=895246.

Gaunt, C.T., and G. Coetzee. 2007. 'Transformer Failures in Regions Incorrectly Considered to Have Low GIC-Risk'. In *Power Tech, 2007 IEEE Lausanne*, 807–12. doi:10.1109/PCT.2007.4538419.

Gonzalez, W. D., J. A. Joselyn, Y. Kamide, H. W. Kroehl, G. Rostoker, B. T. Tsurutani, and V. M. Vasyliunas. 1994. 'What Is a Geomagnetic Storm?' *Journal of Geophysical Research: Space Physics* 99 (A4): 5771–92. doi:10.1029/93JA02867.

Gorbenko, A, V Kharchenko, O Tarasyuk, and S Zasukha. 2012. 'A Study of Orbital Carrier Rocket and Spacecraft Failures: 2000-2009 - Proquest'. *Information & Security* 28 (2): 179–98.

Green, James L., and Scott Boardsen. 2006. 'Duration and Extent of the Great Auroral Storm of 1859'. *Advances in Space Research*, The Great Historical Geomagnetic Storm of 1859: A Modern Look, 38 (2): 130–35. doi:10.1016/j.asr.2005.08.054.

Green, Lucie, and Deb Baker. 2015. 'Coronal Mass Ejections: A Driver of Severe Space Weather'. *Weather* 70 (1): 31–35. doi:10.1002/wea.2437.

Gummow, R. A, and P Eng. 2002. 'GIC Effects on Pipeline Corrosion and Corrosion Control Systems'. *Journal of Atmospheric and Solar-Terrestrial Physics*, Space Weather Effects on Technological Systems, 64 (16): 1755–64. doi:10.1016/S1364-6826(02)00125-6.

Haimes, Y, and P Jiang. 2001. 'Leontief-Based Model of Risk in Complex Interconnected Infrastructures'. *Journal of Infrastructure Systems* 7 (1): 1–12. doi:10.1061/(ASCE)1076-0342(2001)7:1(1).

Hapgood, M. A. 2011. 'Towards a Scientific Understanding of the Risk from Extreme Space Weather'. *Advances in Space Research* 47 (12): 2059–72.

Hapgood, Mike, Richard B. Horne, David Kerridge, Bryn Jones, Paul Cannon, Keith Ryden, Mark Gibbs, et al. 2012. 'Summary of Space Weather Worst-Case Environments'. Didcot: Science and Technology Facilities Council. http://eprints.lancs.ac.uk/64441/.

Harang, Leiv. 1941. 'Maximalwerte Der Erdstromspannungen in Der Nähe Der Nordlichtzone Während Sehr Intensiver Erdmagnetischer Störungen (Maximum Values of Earth Current near the Auroral Zone during Very Intensive Geomagnetic Disturbances),(written in German, with an English Summary)'. *Gerl. Beitr. Geophys* 57: 310.

Harris CapRock. 2014. 'High Throughput Satellite Communications Systems: MEO vs. LEO vs. GEO' http://www.harriscaprock.com/blog/high-throughput-satellite-communications-systems-meo-vs-leo-vs-geo/.

Hastings, Daniel, and Henry Garrett. 2004. *Spacecraft-Environment Interactions.* Cambridge University Press.

Horne, R. B., S. A. Glauert, N. P. Meredith, D. Boscher, V. Maget, D. Heynderickx, and D. Pitchford. 2013. 'Space Weather Impacts on Satellites and Forecasting the Earth's Electron Radiation Belts with SPACECAST'. *Space Weather* 11 (4): 169–86. doi:10.1002/swe.20023.

Huang, Jianguo, Guoqing Liu, and Lixiang Jiang. 2015. 'Threshold for Spacecraft Charging in Double-Maxwellian Plasma'. *Journal of Geophysical Research: Space Physics* 120 (8): 2015JA021173. doi:10.1002/2015JA021173.

Hurd, Michael D., and Susann Rohwedder. 2010. 'Effects of the Financial Crisis and Great Recession on American Households'. National Bureau of Economic Research. http://www.nber.org/papers/w16407.

Hutchins, T.R., and T.J. Overbye. 2011. 'The Effect of Geomagnetic Disturbances on the Electric Grid and Appropriate Mitigation Strategies'. In *North American Power Symposium (NAPS), 2011*, 1–5. doi:10.1109/NAPS.2011.6025162.

Inomata, Satoshi, and Anne Owen. 2014. 'Comparative Evaluation of Mrio Databases'. *Economic Systems Research* 26 (3): 239–44. doi:10.1080/09535314.2014.940856.

Intriligator, Devrie S., Wei Sun, Murray Dryer, James Intriligator, Charles Deehr, Thomas Detman, and William R. Webber. 2015. 'Did the July 2012 Solar Events Cause a "tsunami" throughout the Heliosphere, Heliosheath, and into the Interstellar Medium?' *Journal of Geophysical Research: Space Physics* 120 (10): 2015JA021406. doi:10.1002/2015JA021406.

Jackson, S. V. 2016. 'Ensuring Service Interruption Coverage'. Accessed March 24. http://www.zelle.com/assets/htmldocuments/Ensuring%20Service%20Interruption%20Coverage.pdf.

JASON. 2011. 'Impacts of Severe Space Weather on the Electric Grid'. Mclean, Virginia: JASON. https://fas.org/irp/agency/dod/jason/spaceweather.pdf.

Johanson, M. 2012. 'Solar Storm 2012: Scientists Monitor as Airlines Divert Flights'. http://www.ibtimes.com/solar-storm-2012-scientists-monitor-airlines-divert-flights-400502.

Johnson, Robert C. 2014. 'Five Facts about Value-Added Exports and Implications for Macroeconomics and Trade Research'. *The Journal of Economic Perspectives* 28 (2): 119–42.

Jones, J. B. L., R. D. Bentley, R. Hunter, R. H. A. Iles, G. C. Taylor, and D. J. Thomas. 2005. 'Space Weather and Commercial Airlines'. *Advances in Space Research*, Space Weather, 36 (12): 2258–67. doi:10.1016/j.asr.2004.04.017.

Juusola, L., A. Viljanen, M. van de Kamp, E. I. Tanskanen, H. Vanhamäki, N. Partamies, and K. Kauristie. 2015. 'High-Latitude Ionospheric Equivalent Currents during Strong Space Storms: Regional Perspective'. *Space Weather* 13 (1): 2014SW001139. doi:10.1002/2014SW001139.

Kalafatoğlu, E. C., Z. Kaymaz, A. C. Moral, and R. Çağlar. 2015. 'Geomagnetically Induced Current (GIC) Observations of Geomagnetic Storms in Turkey: Preliminary Results'. In *2015 7th International Conference on Recent Advances in Space Technologies (RAST)*, 501–3. doi:10.1109/RAST.2015.7208396.

Kamide, Y., W. Baumjohann, I. A. Daglis, W. D. Gonzalez, M. Grande, J. A. Joselyn, R. L. McPherron, et al. 1998. 'Current Understanding of Magnetic Storms: Storm-Substorm Relationships'. *Journal of Geophysical Research: Space Physics* 103 (A8): 17705–28. doi:10.1029/98JA01426.

Kappenman, John. 2010. 'Geomagnetic Storms and Their Impacts on the US Power Grid'. Goleta, CA: Metatech: Prepared for Oak Ridge National Laboratory. http://citeseerx.ist.psu.edu/viewdoc/download?doi=10.1.1.227.2009&rep=rep1&type=pdf.

Kappenman, John G. 2006. 'Great Geomagnetic Storms and Extreme Impulsive Geomagnetic Field Disturbance Events – An Analysis of Observational Evidence Including the Great Storm of May 1921'. *Advances in Space Research*, The Great Historical Geomagnetic Storm of 1859: A Modern Look, 38 (2): 188–99. doi:10.1016/j.asr.2005.08.055.

Karsberg, A., G. Swedenborg, and K. Wyke. 1959. 'The Influences of Earth Magnetic Currents on Telecommunication Lines'. *Tele (English Edition), Televerket (Swedish Telecom)* 1: 1–21.

Kataoka, Ryuho. 2013. 'Probability of Occurrence of Extreme Magnetic Storms'. *Space Weather* 11 (5): 214–18. doi:10.1002/swe.20044.

Kemp, John. 2014. 'Time to Be Afraid – Preparing For Next Big Solar Storm'. http://www.insurancejournal.com/magazines/features/2014/08/04/336115.htm.

Koen, J., and T. Gaunt. 2003. 'Geomagnetically Induced Currents in the Southern African Electricity Transmission Network'. In *Power Tech Conference Proceedings, 2003 IEEE Bologna*, 1:7 pp. Vol.1 – . doi:10.1109/PTC.2003.1304165.

Koons, H. C., and J. F. Fennell. 2006. 'Space Weather Effects on Communications Satellites'. *Radio Science Bulletin* 316: 27–41.

Krausmann, Elisabeth, Chris Felton, William Murtagh, Neil Mitchison, and Stephan Lechner. 2014. 'Space Weather and Financial Systems: Findings and Outlook'. Italy: Joint Research Centre. http://www.researchgate.net/profile/Elisabeth_Krausmann/publication/268223307_Space_weather_and_financial_systems_findings_and_outlook/links/546640290cf2f5eb18016ae0.pdf.

Kucukvar, Murat, Gokhan Egilmez, Nuri Cihat Onat, and Hamidreza Samadi. 2015. 'A Global, Scope-Based Carbon Footprint Modeling for Effective Carbon Reduction Policies: Lessons from the Turkish Manufacturing'. *Sustainable Production and Consumption* 1 (January): 47–66. doi:10.1016/j.spc.2015.05.005.

Kucukvar, Murat, and Hamidreza Samadi. 2015. 'Linking National Food Production to Global Supply Chain Impacts for the Energy-Climate Challenge: The Cases of the EU-27 and Turkey'. *Journal of Cleaner Production* 108, Part A (December): 395–408. doi:10.1016/j.jclepro.2015.08.117.

Lai, Shu T., and Maurice Tautz. 2006. 'High-Level Spacecraft Charging in Eclipse at Geosynchronous Altitudes: A Statistical Study'. *Journal of Geophysical Research: Space Physics* 111 (A9): A09201. doi:10.1029/2004JA010733.

Lakhina, G. S., S. Alex, B. T. Tsurutani, and W. D. Gonzalez. 2004. 'Research on Historical Records of Geomagnetic Storms'. In *Null*, 2004:3–15. Proceedings of the International Astronomical Union. doi:10.1017/S1743921305000074.

Lanzerotti, Dr Louis J. 2007. 'Space Weather Effects on Communications'. In *Space Weather- Physics and Effects*, 247–68. Springer Praxis Books. Springer Berlin Heidelberg. http://link.springer.com/chapter/10.1007/978-3-540-34578-7_9.

Lanzerotti, L. J., and G. P Gregori. 1986. 'Telluric Currents: The Natural Environment and Interactions with Man-Made Systems'. *The Earth's Electrical Environment*, 232–57.

Lanzerotti, Louis J. 2001. 'Space Weather Effects on Communications'. In *Space Storms and Space Weather Hazards*, edited by I. A. Daglis, 313–34. NATO Science Series 38. Springer Netherlands. http://link.springer.com/chapter/10.1007/978-94-010-0983-6_12.

Launay, R. 2014. 'Solar Storms and Their Impacts on Power Grids – Recommendations for (re) insurers'. *SCPR Papers*, no. 28 (February). https://www.scor.com/images/stories/pdf/scorpapers/sp28.pdf.

Lazutin, L. L. 2013. 'Injection of Relativistic Electrons into the Internal Magnetosphere during Magnetic Storms: Connection with Substorms'. *Geomagnetism and Aeronomy* 53 (6): 716–32. doi:10.1134/S0016793213050113.

Leahy, Eimear, and Richard S. J. Tol. 2011. 'An Estimate of the Value of Lost Load for Ireland'. *Energy Policy* 39 (3): 1514–20. doi:10.1016/j.enpol.2010.12.025.

Liou, Kan, Chin-Chun Wu, Murray Dryer, Shi-Tsan Wu, Nathan Rich, Simon Plunkett, Lynn Simpson, Craig D. Fry, and Kevin Schenk. 2014. 'Global Simulation of Extremely Fast Coronal Mass Ejection on 23 July 2012'. *Journal of Atmospheric and Solar-Terrestrial Physics* 121, Part A (December): 32–41. doi:10.1016/j.jastp.2014.09.013.

Liu, C. M., L. G. Liu, and R. Pirjola. 2009. 'Geomagnetically Induced Currents in the High-Voltage Power Grid in China'. *IEEE Transactions on Power Delivery* 24 (4): 2368–74. doi:10.1109/TPWRD.2009.2028490.

Liu, Lian-Guang, Chun-Ming Liu, Bing Zhang, Ze-Zhong Wang, Xiang-Ning Xiao, and Li-Zhang Han. 2008. 'Strong Magnetic Storm's Influence on China's Guangdong Power Grid'. *Chinese Journal of Geophysics* 51 (4): 694–99. doi:10.1002/cjg2.1261.

Liu, Ying D., Janet G. Luhmann, Primož Kajdič, Emilia K. J. Kilpua, Noé Lugaz, Nariaki V. Nitta, Christian Möstl, et al. 2014. 'Observations of an Extreme Storm in Interplanetary Space Caused by Successive Coronal Mass Ejections'. *Nature Communications* 5 (March). doi:10.1038/ncomms4481.

Lloyd's. 2013. 'Solar Storm Risk to the North American Electric Grid'. London: Lloyd's of London.

———. 2016. 'Realistic Disaster Scenarios – Scenario Specification'. London: Lloyd's of London.

Love, Jeffrey J., E. Joshua Rigler, Antti Pulkkinen, and Pete Riley. 2015. 'On the Lognormality of Historical

Magnetic Storm Intensity Statistics: Implications for Extreme-Event Probabilities'. *Geophysical Research Letters*. http://onlinelibrary.wiley.com/doi/10.1002/2015GL064842/full.

Lyakhov, A. N., and S. L. Kozlov. 2012. 'Whether Space Weather Factors Affect the Occurrence of Aviation Accidents'. *Geomagnetism and Aeronomy* 52 (1): 129–34. doi:10.1134/S0016793212010069.

MacAlester, Mark H., and William Murtagh. 2014. 'Extreme Space Weather Impact: An Emergency Management Perspective'. *Space Weather* 12 (8): 2014SW001095. doi:10.1002/2014SW001095.

Marshall, R. A., H. Gorniak, T. Van Der Walt, C. L. Waters, M. D. Sciffer, M. Miller, M. Dalzell, et al. 2013. 'Observations of Geomagnetically Induced Currents in the Australian Power Network'. *Space Weather* 11 (1): 6–16. doi:10.1029/2012SW000849.

Marshall, R. A., E. A. Smith, M. J. Francis, C. L. Waters, and M. D. Sciffer. 2011. 'A Preliminary Risk Assessment of the Australian Region Power Network to Space Weather'. *Space Weather* 9 (10): S10004. doi:10.1029/2011SW000685.

Meloni, A., L. J. Lanzerotti, and G. P. Gregori. 1983. 'Induction of Currents in Long Submarine Cables by Natural Phenomena'. *Reviews of Geophysics* 21 (4): 795–803. doi:10.1029/RG021i004p00795.

Miller, Ronald E., and Peter D. Blair. 2009. *Input-Output Analysis: Foundations and Extensions*. Cambridge University Press.

Molinski, Tom S. 2002. 'Why Utilities Respect Geomagnetically Induced Currents'. *Journal of Atmospheric and Solar-Terrestrial Physics*, Space Weather Effects on Technological Systems, 64 (16): 1765–78. doi:10.1016/S1364-6826(02)00126-8.

Moodley, N., and C. T. Gaunt. 2012. 'Developing a Power Transformer Low Energy Degradation Assessment Triangle'. In *2012 IEEE Power Engineering Society Conference and Exposition in Africa (PowerAfrica)*, 1–6. doi:10.1109/PowerAfrica.2012.6498647.

Moran, Daniel, and Richard Wood. 2014. 'Convergence Between the Eora, Wiod, Exiobase, and Openeu's Consumption-Based Carbon Accounts'. *Economic Systems Research* 26 (3): 245–61. doi:10.1080/09535314.2014.935298.

Möstl, Christian, Tanja Rollett, Rudy A. Frahm, Ying D. Liu, David M. Long, Robin C. Colaninno,

Martin A. Reiss, et al. 2015. 'Strong Coronal Channelling and Interplanetary Evolution of a Solar Storm up to Earth and Mars'. *Nature Communications* 6 (May): 7135. doi:10.1038/ncomms8135.

National Science and Technology Council. 2015. 'National Space Weather Action Plan'. Washington D.C.: Executive Office of the President of the United States. https://www.whitehouse.gov/sites/default/files/microsites/ostp/final_nationalspaceweatheractionplan_20151028.pdf.

Neal, Jason J., Craig J. Rodger, and Janet C. Green. 2013. 'Empirical Determination of Solar Proton Access to the Atmosphere: Impact on Polar Flight Paths'. *Space Weather* 11 (7): 420–33. doi:10.1002/swe.20066.

NERC. 2012. 'Effects of Geomagnetic Disturbances on the Bulk Power System'. Atlanta, Georgia: North American Electric Reliability Corporation. https://www.frcc.com/Public%20Awareness/Lists/Announcements/Attachments/105/GMD%20Interim%20Report.pdf.

Nevanlinna, Heikki, Pentti Tenhunen, Risto Pirjola, Jaakko Annanpalo, and Antti Pulkkinen. 2001. 'Breakdown Caused by a Geomagnetically Induced Current in the Finnish Telesystem in 1958'. *Journal of Atmospheric and Solar-Terrestrial Physics* 63 (10): 1099–1103. doi:10.1016/S1364-6826(01)00021-9.

Ngwira, Chigomezyo M., Lee-Anne McKinnell, and Pierre J. Cilliers. 2011. 'Geomagnetic Activity Indicators for Geomagnetically Induced Current Studies in South Africa'. *Advances in Space Research* 48 (3): 529–34. doi:10.1016/j.asr.2011.03.042.

Ngwira, Chigomezyo M., Antti Pulkkinen, M. Leila Mays, Maria M. Kuznetsova, A. B. Galvin, Kristin Simunac, Daniel N. Baker, Xinlin Li, Yihua Zheng, and Alex Glocer. 2013. 'Simulation of the 23 July 2012 Extreme Space Weather Event: What If This Extremely Rare CME Was Earth Directed?' *Space Weather* 11 (12): 671–79. doi:10.1002/2013SW000990.

NOAA. 2016. 'Space Weather: Storms from the Sun'. Boulder, CO: National Oceanic and Atmospheric Administration. Accessed March 22. http://www.srh.noaa.gov/srh/jetstream/downloads/space_weather_booklet.pdf.

NRC. 1990. 'Information Notice No. 90-42: Failure of Electrical Power Equipment Due to Solar Magnetic Disturbances'. United States Nuclear Regulatory Commission. http://www.nrc.gov/

reading-rm/doc-collections/gen-comm/info-notices/1990/in90042.html.

Odenwald, Sten F., and James L. Green. 2007. 'Forecasting the Impact of an 1859-Caliber Superstorm on Geosynchronous Earth-Orbiting Satellites: Transponder Resources'. *Space Weather* 5 (6): S06002. doi:10.1029/2006SW000262.

Odenwald, Sten, James Green, and William Taylor. 2006. 'Forecasting the Impact of an 1859-Calibre Superstorm on Satellite Resources'. *Advances in Space Research*, The Great Historical Geomagnetic Storm of 1859: A Modern Look, 38 (2): 280–97. doi:10.1016/j.asr.2005.10.046.

OECD. 2011. 'Geomagnetic Storms'. Paris: Organisation for Economic Co-operation and Development.

Ouyang, Min. 2014. 'Review on Modeling and Simulation of Interdependent Critical Infrastructure Systems'. *Reliability Engineering & System Safety* 121 (January): 43–60. doi:10.1016/j.ress.2013.06.040.

Pirjola, R, A Viljanen, A Pulkkinen, and O Amm. 2000. 'Space Weather Risk in Power Systems and Pipelines'. *Physics and Chemistry of the Earth, Part C: Solar, Terrestrial & Planetary Science* 25 (4): 333–37. doi:10.1016/S1464-1917(00)00027-1.

Ptitsyna, N. G., V. V. Kasinskii, G. Villoresi, N. N. Lyahov, L. I. Dorman, and N. Iucci. 2008. 'Geomagnetic Effects on Mid-Latitude Railways: A Statistical Study of Anomalies in the Operation of Signaling and Train Control Equipment on the East-Siberian Railway'. *Advances in Space Research* 42 (9): 1510–14. doi:10.1016/j.asr.2007.10.015.

Ptitsyna, N. G., M. I. Tyasto, and B. A. Khrapov. 2012. 'Great Geomagnetic Storms in 1841–1870 according to the Data from the Network of Russian Geomagnetic Observatories'. *Geomagnetism and Aeronomy* 52 (5): 613–23. doi:10.1134/S0016793212040123.

Pulkkinen, A., E. Bernabeu, J. Eichner, C. Beggan, and A. W. P. Thomson. 2012. 'Generation of 100-Year Geomagnetically Induced Current Scenarios'. *Space Weather* 10 (4): S04003. doi:10.1029/2011SW000750.

Pulkkinen, Antti, Sture Lindahl, Ari Viljanen, and Risto Pirjola. 2005. 'Geomagnetic Storm of 29–31 October 2003: Geomagnetically Induced Currents and Their Relation to Problems in the Swedish High-Voltage Power Transmission System'. *Space Weather* 3 (8): S08C03. doi:10.1029/2004SW000123.

Pulkkinen, Antti, Risto Pirjola, David Boteler, Ari Viljanen, and Igor Yegorov. 2001. 'Modelling of Space Weather Effects on Pipelines'. *Journal of Applied Geophysics* 48 (4): 233–56. doi:10.1016/S0926-9851(01)00109-4.

Pulkkinen, Antti, Ari Viljanen, Kari Pajunpää, and Risto Pirjola. 2001. 'Recordings and Occurrence of Geomagnetically Induced Currents in the Finnish Natural Gas Pipeline Network'. *Journal of Applied Geophysics* 48 (4): 219–31. doi:10.1016/S0926-9851(01)00108-2.

Ribeiro, P., J. M. Vaquero, and R. M. Trigo. 2011. 'Geomagnetic Records of Carrington's Storm from Guatemala'. *Journal of Atmospheric and Solar-Terrestrial Physics*, Space Climate, 73 (2–3): 308–15. doi:10.1016/j.jastp.2009.12.017.

Riley, Pete. 2012. 'On the Probability of Occurrence of Extreme Space Weather Events'. *Space Weather* 10 (2): S02012. doi:10.1029/2011SW000734.

Rinaldi, Steven M., James P. Peerenboom, and Terrence K. Kelly. 2001. 'Identifying, Understanding, and Analyzing Critical Infrastructure Interdependencies'. *Control Systems, IEEE* 21 (6): 11–25.

Rodger, Craig J., Pekka T. Verronen, Mark A. Clilverd, Annika Seppälä, and Esa Turunen. 2008. 'Atmospheric Impact of the Carrington Event Solar Protons'. *Journal of Geophysical Research: Atmospheres* 113 (D23): D23302. doi:10.1029/2008JD010702.

Rose, Adam, and Charles K. Huyck. 2016. 'Improving Catastrophe Modeling for Business Interruption Insurance Needs'. *Risk Analysis*, January, n/a – n/a. doi:10.1111/risa.12550.

Saiz, Elena, Antonio Guerrero, Consuelo Cid, Judith Palacios, and Yolanda Cerrato. 2016. 'Searching for Carrington-like Events and Their Signatures and Triggers'. *Journal of Space Weather and Space Climate* 6: A6. doi:10.1051/swsc/2016001.

Samuelsson, O. 2013. 'Geomagnetic Disturbances and Their Impact on Power Systems - Status Report 2013'. Sweden: Lund University.

Savani, N. P., A. Vourlidas, A. Pulkkinen, T. Nieves-Chinchilla, B. Lavraud, and M. J. Owens. 2013. 'Tracking the Momentum Flux of a CME and Quantifying Its Influence on Geomagnetically Induced Currents at Earth'. *Space Weather* 11 (5): 245–61. doi:10.1002/swe.20038.

Schrijver, C. J., R. Dobbins, W. Murtagh, and S. M. Petrinec. 2014. 'Assessing the Impact of Space Weather on the Electric Power Grid Based on Insurance Claims for Industrial Electrical Equipment'. *Space Weather* 12 (7): 487–98. doi:10.1002/2014SW001066.

Schulte in den Bäumen, H., D. Moran, M. Lenzen, I. Cairns, and A. Steenge. 2014. 'How Severe Space Weather Can Disrupt Global Supply Chains'. *Nat. Hazards Earth Syst. Sci.* 14 (10): 2749–59. doi:10.5194/nhess-14-2749-2014.

Sharma, Rahul, Nandita Srivastava, and D. Chakrabarty. 2013. 'Role of Filament Plasma Remnants in ICMEs Leading to Geomagnetic Storms'. In *Nature of Prominences and Their Role in Space Weather*, 8:493–94. Proceedings of the International Astronomical Union. doi:10.1017/S1743921313011708.

Shea, M. A., and D. F. Smart. 2012. 'Space Weather and the Ground-Level Solar Proton Events of the 23rd Solar Cycle'. *Space Science Reviews* 171 (1-4): 161–88. doi:10.1007/s11214-012-9923-z.

SIA. 2014. 'State of the Satellite Industry Report'. http://www.sia.org/state-of-the-satellite-industry-report/.

Silverman, S. M. 1995. 'Low Latitude Auroras: The Storm of 25 September 1909'. *Journal of Atmospheric and Terrestrial Physics* 57 (6): 673–85. doi:10.1016/0021-9169(94)E0012-C.

———. 2006. 'Comparison of the Aurora of September 1/2, 1859 with Other Great Auroras'. *Advances in Space Research*, The Great Historical Geomagnetic Storm of 1859: A Modern Look, 38 (2): 136–44. doi:10.1016/j.asr.2005.03.157.

———. 2008. 'Low-Latitude Auroras: The Great Aurora of 4 February 1872'. *Journal of Atmospheric and Solar-Terrestrial Physics* 70 (10): 1301–8. doi:10.1016/j.jastp.2008.03.012.

Silverman, S. M, and E. W Cliver. 2001. 'Low-Latitude Auroras: The Magnetic Storm of 14–15 May 1921'. *Journal of Atmospheric and Solar-Terrestrial Physics*, Interplanetary medium and geophysical phenomena during geomagnetic stroms, 63 (5): 523–35. doi:10.1016/S1364-6826(00)00174-7.

Siscoe, G., N. U. Crooker, and C. R. Clauer. 2006. 'Dst of the Carrington Storm of 1859'. *Advances in Space Research*, The Great Historical Geomagnetic Storm of 1859: A Modern Look, 38 (2): 173–79. doi:10.1016/j.asr.2005.02.102.

Sonis, Michael, Joaquim J. M. Guilhoto, Geoffrey J. D. Hewings, and Eduardo B. Martins. 1995. 'Linkages, Key Sectors, and Structural Change: Some New Perspectives'. *The Developing Economies* 33 (3): 243–46. doi:10.1111/j.1746-1049.1995.tb00716.x.

Space Studies Board. 2008. *Severe Space Weather Events–Understanding Societal and Economic Impacts:: A Workshop Report*. Washington D.C.: National Academies Press.

Sparks, R. S. J., W. P. Aspinall, B. E. Chapman, D. J. Kerridge, J. Pooley, and C. A. Taylor. 2013. 'Technological Facilities, Infrastructure and Hazardous Materials, Including Some Notes on Space Weather'. In *Risk and Uncertainty Assessment for Natural Hazards*, by Jonathan Rougier, Steve Sparks, Lisa J. Hill, and Robert Stephen John Sparks. Cambridge: Cambridge University Press.

Standler, R. 2011. 'Liability of Electric Utility in the USA for Outage or Blackout'. Dr. Ronald B. Standler.

Sugiura, M. 1963. 'Hourly Values for Magnetic Storm Variation for International Geophysical Year'. http://ntrs.nasa.gov/search.jsp?R=19650020355.

Swiss Re. 2006. 'Swiss Re Sigma, Catastrophe Report 2005'. http://www.swissre.com/media/news_releases/swiss_re_sigma_catastrophe_report_2005_catastrophes_cause_total_damage_of_usd_230_billion.html.

———. 2011. 'Space Debris: On Collision Course for Insurers?' http://media.swissre.com/documents/Publ11_Space+debris.pdf.

———. 2013. 'Natural Catastrophes and Man-Made Disasters in 2012'. http://www.swissre.com/media/news_releases/nr_20130327_sigma_natcat_2012.html.

———. 2015. 'Preliminary Sigma Estimates for 2015'. http://www.swissre.com/media/news_releases/Preliminary_sigma_estimates_for_2015.html.

Tafazoli, Mak. 2009. 'A Study of on-Orbit Spacecraft Failures'. *Acta Astronautica* 64 (2–3): 195–205. doi:10.1016/j.actaastro.2008.07.019.

Temmer, M., and N. V. Nitta. 2015. 'Interplanetary Propagation Behavior of the Fast Coronal Mass Ejection on 23 July 2012'. *Solar Physics* 290 (3): 919–32. doi:10.1007/s11207-014-0642-3.

Thomson, Alan W. P., Ewan B. Dawson, and Sarah J. Reay. 2011. 'Quantifying Extreme Behavior in Geomagnetic Activity'. *Space Weather* 9 (10): S10001. doi:10.1029/2011SW000696.

Thomson, A. W. P., C. T. Gaunt, P. Cilliers, J. A. Wild, B. Opperman, L. -A. McKinnell, P. Kotze, C. M. Ngwira, and S. I. Lotz. 2010. 'Present Day Challenges in Understanding the Geomagnetic Hazard to National Power Grids'. *Advances in Space Research*, Special Issue: Recent Advances in Space Weather Monitoring, Modelling, and Forecasting, 45 (9): 1182–90. doi:10.1016/j.asr.2009.11.023.

Timmer, Marcel P., Erik Dietzenbacher, Bart Los, Robert Stehrer, and Gaaitzen J. de Vries. 2015. 'An Illustrated User Guide to the World Input–Output Database: The Case of Global Automotive Production'. *Review of International Economics* 23 (3): 575–605. doi:10.1111/roie.12178.

Timmer, Marcel P., Abdul Azeez Erumban, Bart Los, Robert Stehrer, and Gaaitzen J. de Vries. 2014. 'Slicing Up Global Value Chains'. *The Journal of Economic Perspectives* 28 (2): 99–118.

Tol, Richard SJ. 2007. 'The Value of Lost Load'. Dublin: Economic and Social Research Institute (ESRI). http://www.econstor.eu/handle/10419/68056.

Torpey, D. 2003. "Contingent Business Interruption: Getting All the Facts". International Risk Management Institute. 3 May 2003. https://www.irmi.com/articles/expert-commentary/contingent-business-interruption-getting-all-the-facts [Accessed: Feb 2016].

Torta, J. Miquel, Lluís Serrano, J. Ramon Regué, Albert M. Sánchez, and Elionor Roldán. 2012. 'Geomagnetically Induced Currents in a Power Grid of Northeastern Spain'. *Space Weather* 10 (6): S06002. doi:10.1029/2012SW000793.

Trivedi, Nalin B., Ícaro Vitorello, Wanderli Kabata, Severino L. G. Dutra, Antonio L. Padilha, Mauricio S. Bologna, Marcelo B. de Pádua, et al. 2007. 'Geomagnetically Induced Currents in an Electric Power Transmission System at Low Latitudes in Brazil: A Case Study'. *Space Weather* 5 (4): S04004. doi:10.1029/2006SW000282.

Tsurutani, B. T., D. L. Judge, F. L. Guarnieri, P. Gangopadhyay, A. R. Jones, J. Nuttall, G. A. Zambon, et al. 2005. 'The October 28, 2003 Extreme EUV Solar Flare and Resultant Extreme Ionospheric Effects: Comparison to Other Halloween Events and the Bastille Day Event'. *Geophysical Research Letters* 32 (3): L03S09. doi:10.1029/2004GL021475.

Tukker, Arnold, and Erik Dietzenbacher. 2013. 'Global Multiregional Input–Output Frameworks: An Introduction and Outlook'. *Economic Systems Research* 25 (1): 1–19. doi:10.1080/09535314.2012.761179.

Vaquero, J. M., M. A. Valente, R. M. Trigo, P. Ribeiro, and M. C. Gallego. 2008. 'The 1870 Space Weather Event: Geomagnetic and Auroral Records'. *Journal of Geophysical Research: Space Physics* 113 (A8): A08230. doi:10.1029/2007JA012943.

Viljanen, A., R. Pirjola, E. Prácser, S. Ahmadzai, and V. Singh. 2013. 'Geomagnetically Induced Currents in Europe: Characteristics Based on a Local Power Grid Model'. *Space Weather* 11 (10): 575–84. doi:10.1002/swe.20098.

Wade, D., Hoffer, D. and R. Gubby. 23 April 2012. " Financial Impact of Space Weather Anomalies – An insurer's Perspective". NOAA Satellite Anomaly Mitigation Stakeholders Meeting, Boulder, CO. ftp://ftp.ngdc.noaa.gov/STP/publications/sam/SAM_Hoffer.pdf [Accessed: March 2016]

Watari, Shinichi. 2015. 'Estimation of Geomagnetically Induced Currents Based on the Measurement Data of a Transformer in a Japanese Power Network and Geoelectric Field Observations'. *Earth, Planets and Space* 67 (1): 1–12. doi:10.1186/s40623-015-0253-8.

Watari, S., M. Kunitake, K. Kitamura, T. Hori, T. Kikuchi, K. Shiokawa, N. Nishitani, et al. 2009. 'Measurements of Geomagnetically Induced Current in a Power Grid in Hokkaido, Japan'. *Space Weather* 7 (3): S03002. doi:10.1029/2008SW000417.

Webb, David F., and Timothy A. Howard. 2012. 'Coronal Mass Ejections: Observations'. *Living Reviews in Solar Physics* 9: 3.

Wik, M., R. Pirjola, H. Lundstedt, A. Viljanen, P. Wintoft, and A. Pulkkinen. 2009. 'Space Weather Events in July 1982 and October 2003 and the Effects of Geomagnetically Induced Currents on Swedish Technical Systems'. *Ann. Geophys.* 27 (4): 1775–87. doi:10.5194/angeo-27-1775-2009.

Willis, D. M., G. M. Armstrong, C. E. Ault, and F. R. Stephenson. 2005. 'Identification of Possible Intense Historical Geomagnetic Storms Using Combined Sunspot and Auroral Observations from East Asia'. *Annales Geophysicae* 23 (3): 945–71.

Zhang, J. J., C. Wang, T. R. Sun, C. M. Liu, and K. R. Wang. 2015. 'GIC due to Storm Sudden Commencement in Low-Latitude High-Voltage Power Network in China: Observation and Simulation'. *Space Weather* 13 (10): 2015SW001263. doi:10.1002/2015SW001263.

Appendix 1
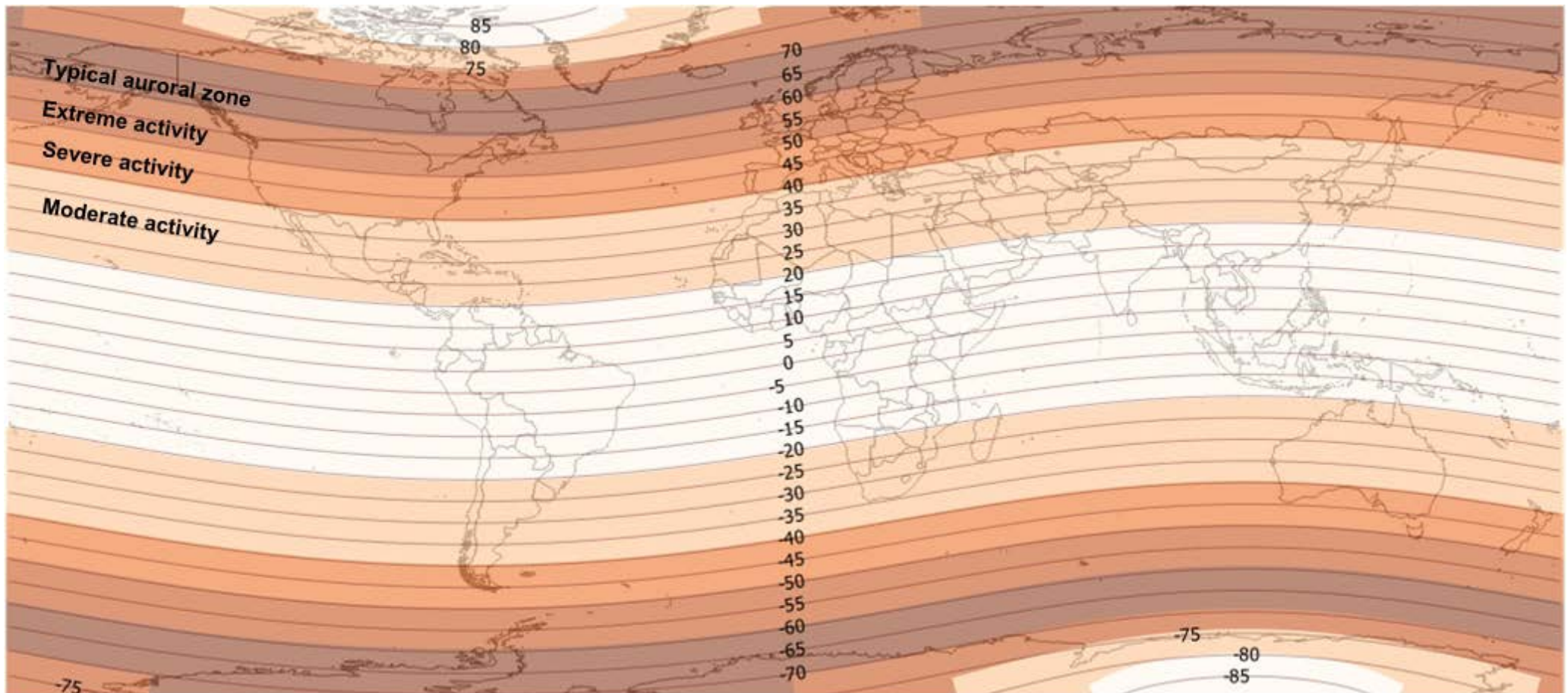
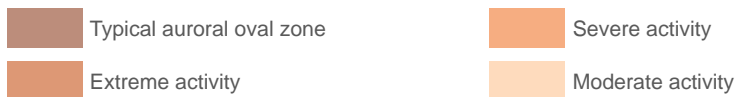Geomagnetic bands of activity following a shift in the auroral oval during an extreme event

Typical auroral oval zone

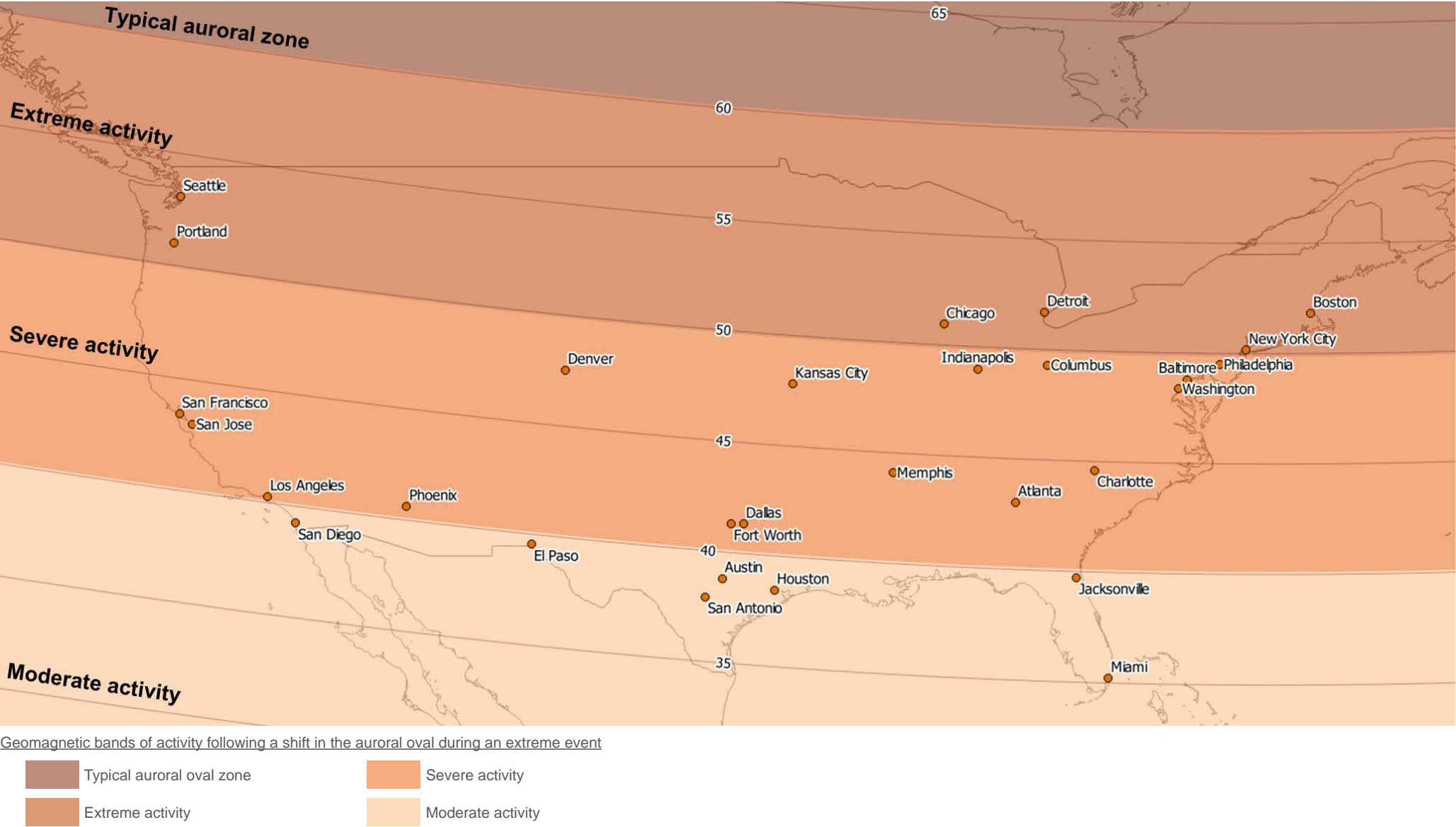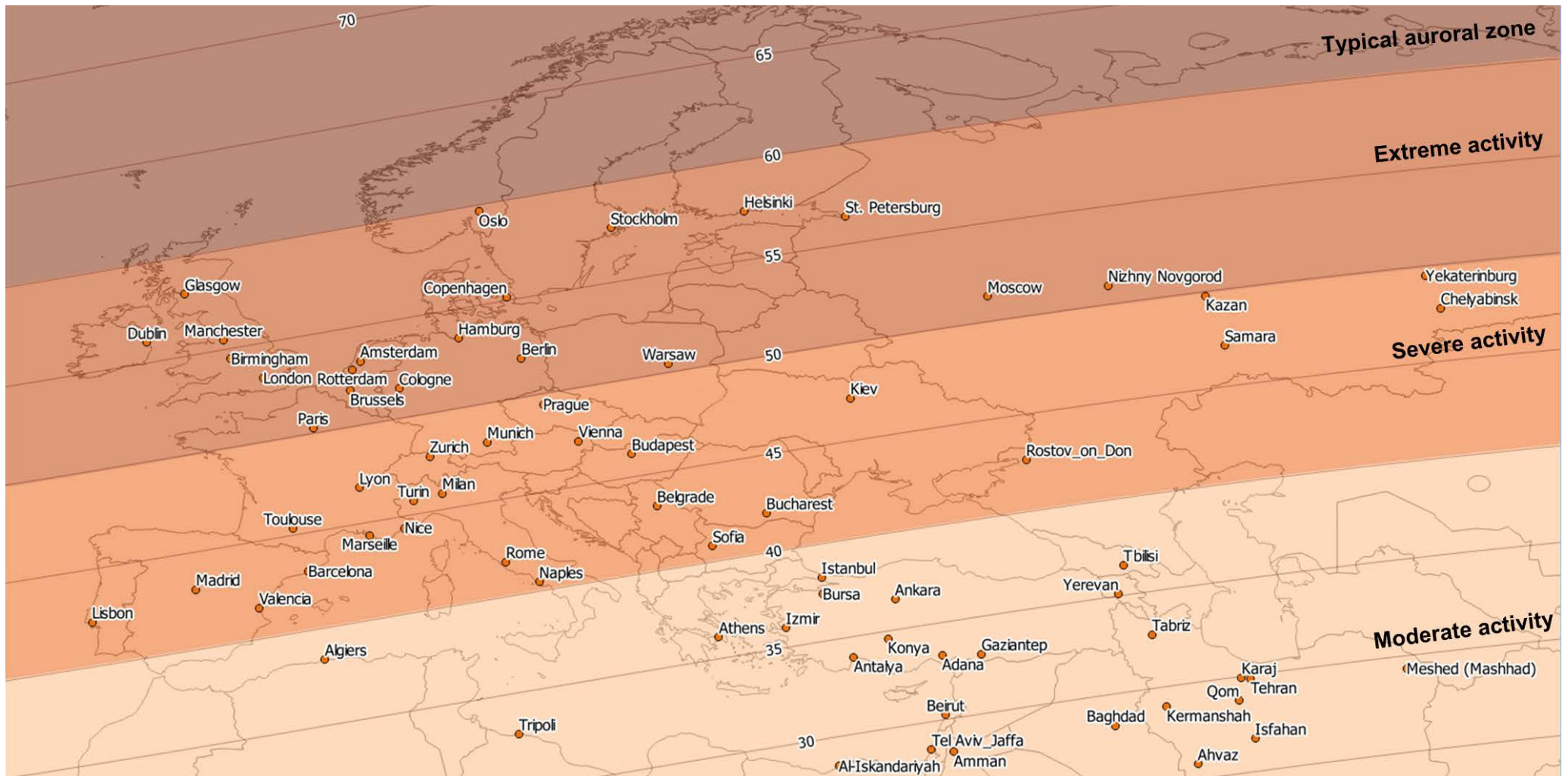Severe activity

Extreme activity

Moderate activity

Figure 20: World geomagnetic latitude threat map generated using the World Magnetic Model (WMM) 2015 (Chulliat, 2014)

Geomagnetic bands of activity following a shift in the auroral oval during an extreme event

	Typical auroral oval zone		Severe activity
	Extreme activity		Moderate activity

Figure 21: US geomagnetic latitude threat map generated using the World Magnetic Model (WMM) 2015 (Chulliat, 2014)

Geomagnetic bands of activity following a shift in the auroral oval during an extreme event

Legend:
- Typical auroral oval zone
- Extreme activity
- Severe activity
- Moderate activity
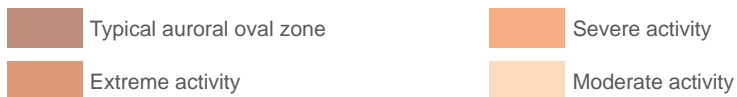
Figure 22: Europe geomagnetic latitude threat map generated using the World Magnetic Model (WMM) 2015 (Chulliat, 2014)

Appendix 2
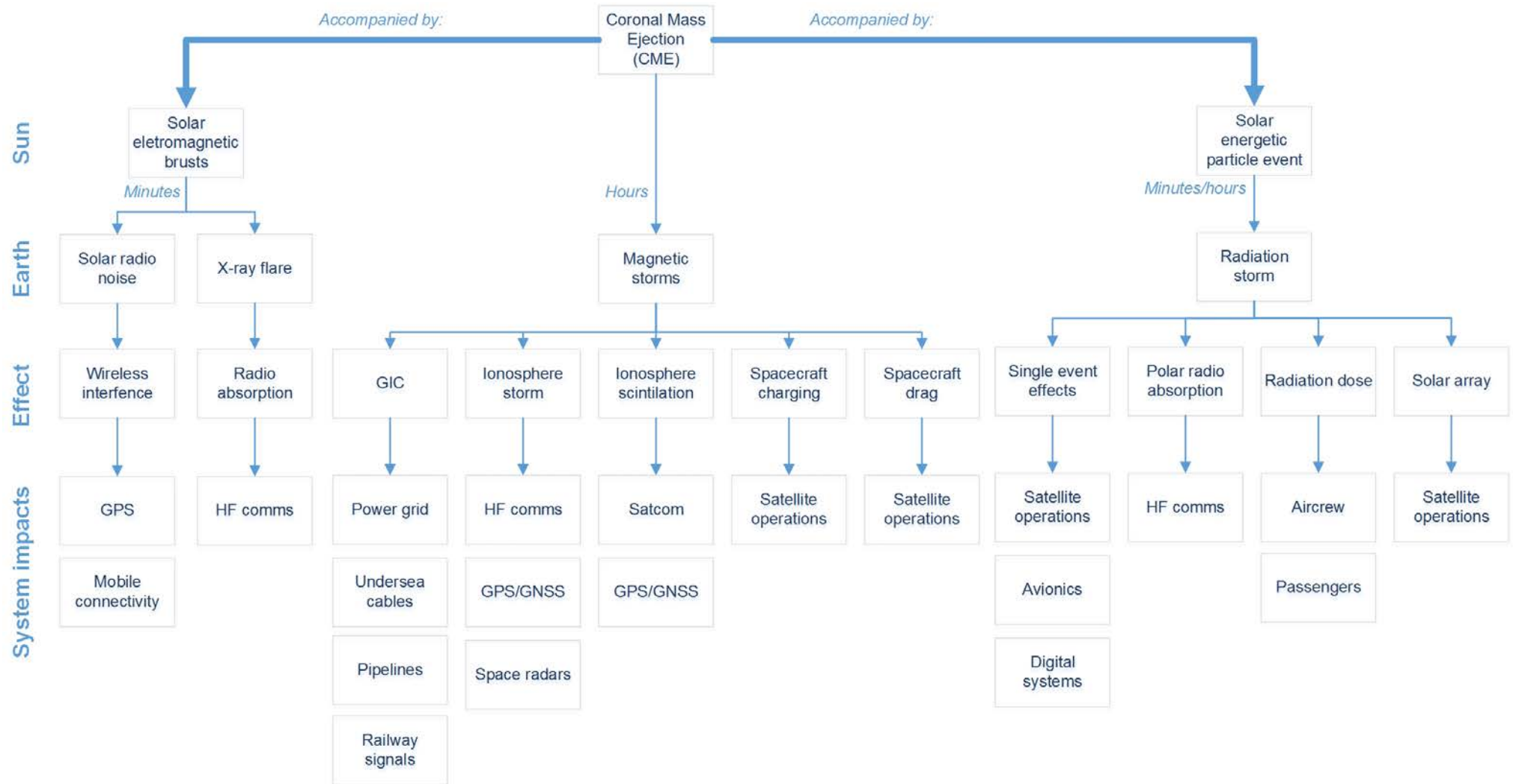
Figure 23: Scenario impact tree (Adapted from Hapgood et al. 2012)

Appendix 3

Input-Output methodology

We employ an Input-Output (IO) approach to calculate indirect economic costs. Using a system of linear equations, the IO framework represents each economic sector's dependence (as monetary flows) on all other sectors of the domestic and global economy. This is a useful tool because it enables the interdependencies between economic sectors to the quantified, thereby providing insight into the upstream and downstream supply chain linkages in the production and consumption of goods and services. An in-depth overview of the IO approach can be found in Miller and Blair (2009).

There are two main types of questions addressed using IO data : attributional questions, such as, "what is the supply chain carbon footprint of UK end consumption of goods and services?"; and 'what if' questions such as: "to what extent would the output of the US steel sector decline if there were a sudden 40% downturn in demand for automobiles?" The later can be addressed using the conventional Leontief open model (and the former using its environmental extension drawing on satellite greenhouse gas emissions inventories), given by:

$$\mathbf{x} = (\mathbf{I} - \mathbf{A})^{-1}\mathbf{y}$$

where, $\mathbf{x}$ is a vector of sector total outputs, $\mathbf{y}$ is a vector of final demand for the goods and services produced by each sector, $\mathbf{I}$ is an identity matrix, and $\mathbf{A}$ is a matrix of sector direct requirements (or technical coefficients). Each column of the direct requirements matrix represents a sector's production recipe of inputs from all other sectors that are needed to make one unit of output. This demand-side model centres on the key assumption that the ratios of a sector's production recipe are fixed, that is for example, a 10% reduction in the output of a given sector would lead to a 10% reduction in all of its intermediate demands on other sectors. As such, the model explores upstream consequences (or attributions) of a downstream impact (or consumption quantity).

The IO literature also provides a counterpoint for the investigation of downstream consequences, based on the Ghosh open model, given by:

$$\mathbf{x} = \mathbf{v}(\mathbf{I} - \mathbf{B})^{-1}$$

where, $\mathbf{v}$ is a vector of value added in each sector and $\mathbf{B}$ is a matrix of sector direct sales. Each row of the direct sales matrix represents the distribution of a unit of output from a sector across all other sectors (ie, its sales recipe). This supply-side model assumes that these sales recipes are fixed, hence a 10% reduction in the output of a given sector would lead to a 10% reduction in that sector's sales to all other sectors.

Following on with the sequential methodology, we are concerned with assessing the consequences of shocks to the production capacity of different sectors caused by power outage. It is intuitive to consider that a 10% loss in the production capabilities of say the steel sector will have both upstream and downstream consequences: since less product is being produced, both less product is available to sell to purchasing sectors and less intermediate product inputs to production will be required. A novel approach has been developed which combines features of the standard Leontief and Ghosh formulations along with insights into pure linkage measures proposed by Sonis et al. (2007). The approach provides an estimated range of indirect impacts for a disparate set of shocks across sectors; the reported range considers both the optimistic possibility, for the lower bound, that sector shocks maximally align along common supply chains and the conservative possibility, for the upper bound, that shocks are minimally aligned along supply chains.

For each sector s experiencing a shock to its production capacity (total output, Δx_s), the upstream **impact on the economy** $\Delta\mathbf{x}_s^{\text{up}}$, that is free from intra-sector demands and feedbacks from the rest of the economy, is given by:

$$\Delta\mathbf{x}_s^{\text{up}} = (\mathbf{I} - \mathbf{A}^*)^{-1} \mathbf{A}_{:s}\Delta x_s$$

where, $\mathbf{A}^*$ is a sub-matrix of the technical coefficients matrix where the row and column ascribed to sector s have been stripped out, and $\mathbf{A}_{:s}$ is a column sub-vector of the technical coefficients matrix where the row ascribed to sector s and columns ascribed to all other sectors have been stripped out (i.e., ':' denotes all sectors except sector s).

Similarly, the downstream impact on the economy $\Delta\mathbf{x}_s^{\text{down}}$ is given by:

$$\Delta\mathbf{x}_s^{\text{down}} = \Delta x_s\mathbf{B}_{s:}(\mathbf{I} - \mathbf{B}^*)^{-1}$$

where, $\mathbf{B}^*$ is a sub-matrix of the direct sales matrix where the row and column ascribed to sector s have been stripped out, and $\mathbf{B}_{s:}$ is a column sub-vector of the direct sales matrix where the column ascribed to sector s and rows ascribed to all other sectors have been stripped out.

Defining the direct total output shock vector as $\Delta\mathbf{x}^{\text{dir}}$, we can now specify the lower bound $\Delta\mathbf{x}^{\text{indir,lb}}$

and upper bound $\Delta\mathbf{x}^{indir,ub}$ for indirect impacts as follows:

$$\Delta\mathbf{x}^{indir,lb} = \min_{s} \left[\Delta\mathbf{x}^{dir}, \min_{s} \Delta\mathbf{x}_{s}^{up}, \min_{s} \Delta\mathbf{x}_{s}^{down} \right]$$

$$\Delta\mathbf{x}^{indir,ub} = \Delta\mathbf{x}^{dir} + \sum_{s} \Delta\mathbf{x}_{s}^{up} + \sum_{s} \Delta\mathbf{x}_{s}^{down}$$

Using this approach we are able to rank those economic sectors which feature the largest loss in economic output as a consequence of the extreme space weather scenario variants. This provides insight which can be used for supporting decision making in resilience planning, as limited resources can be targeted at those vulnerable sectors with the largest cascading effects. This can also help to bolster private and public investment into protecting interdependent critical infrastructure assets with the aim of avoiding catastrophic events.

Appendix 4

Additional investment portfolio details

Conservative Portfolio Structure

Details of the Conservative Portfolio are shown in Table 17, Figure 24, Figure 25 and Figure 26.

Balanced Portfolio Structure

Details of the Balanced Portfolio are shown in Table 18, Figure 27, Figure 28 and Figure 29.
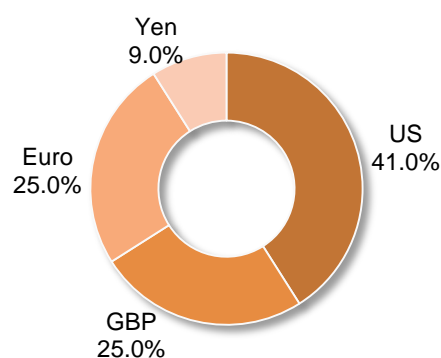
Aggressive Portfolio Structure

Details of the Aggressive Portfolio are shown in Table 19, Figure 30, Figure 31 and Figure 32.

Table 17: Composition of the High Fixed Income Portfolio Structure

	USD	GBP	Euro	Yen	Total
Government 2 yr	4.0%	3.0%	3.0%	0.0%	10.0%
Government 10 yr	3.0%	3.0%	3.0%	1.0%	10.0%
Corporate Bonds 2 yr	6.0%	5.0%	5.0%	1.5%	17.5%
Corporate Bonds 10 yr	6.0%	5.0%	5.0%	1.5%	17.5%
RMBS 2 yr	1.5%	0.5%	0.5%	0.0%	2.5%
RMBS 10 yr	1.5%	0.5%	0.5%	0.0%	2.5%
Equities	19.0%	8.0%	8.0%	5.0%	40.0%
Cash	0.0%	0.0%	0.0%	0.0%	0.0%
Total	41.0%	25.0%	25.0%	9.0%	100.0%
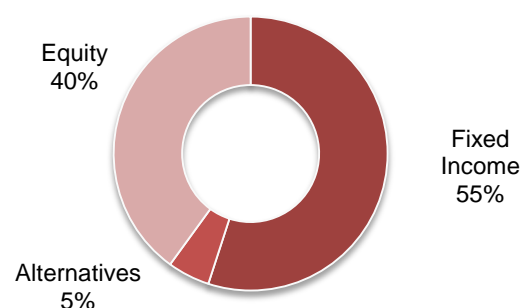
Figure 24: Asset classes in Conservative Portfolio Structure

Figure 25: Geographic market spread of Conservative Portfolio Structure
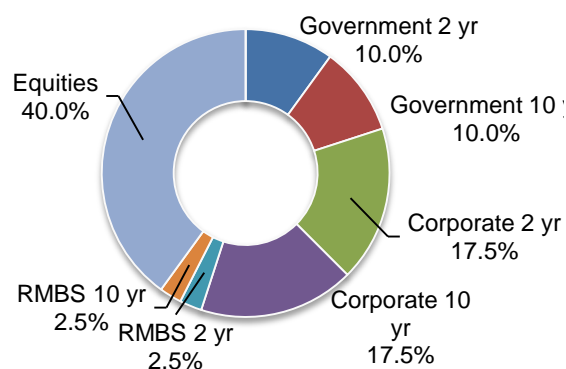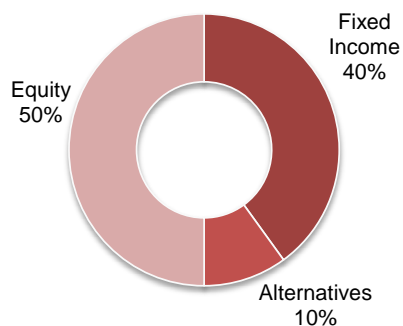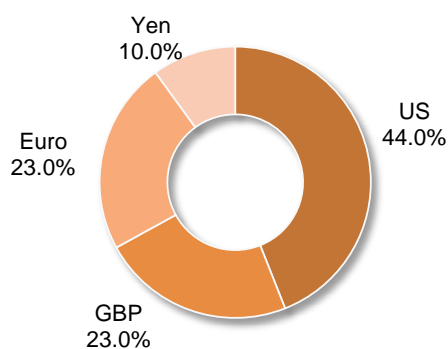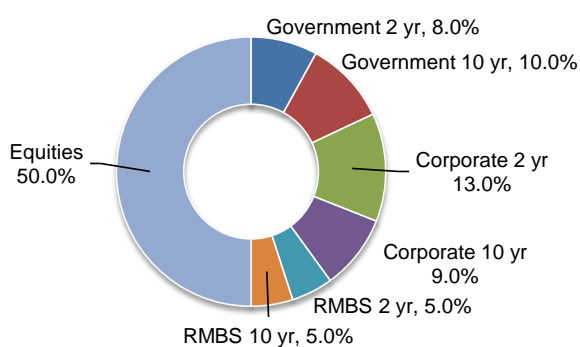

Figure 26: Detailed asset class breakdown of Conservative Portfolio Structure
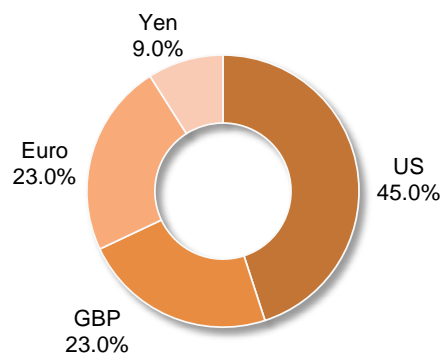
Table 18: Composition of the High Fixed Income Portfolio Structure

	USD	GBP	Euro	Yen	Total
Government 2 yr	3.0%	2.0%	2.0%	1.0%	8.0%
Government 10 yr	3.0%	3.0%	3.0%	1.0%	10.0%
Corporate Bonds 2 yr	4.0%	3.5%	3.5%	2.0%	13.0%
Corporate Bonds 10 yr	4.0%	2.5%	2.5%	0.0%	9.0%
RMBS 2 yr	2.5%	1.0%	1.0%	0.5%	5.0%
RMBS 10 yr	2.5%	1.0%	1.0%	0.5%	5.0%
Equities	25.0%	10.0%	10.0%	5.0%	50.0%
Cash	0.0%	0.0%	0.0%	0.0%	0.0%
Total	44.0%	23.0%	23.0%	10.0%	100.0%

Table 19: Composition of the High Fixed Income Portfolio Structure

	USD	GBP	Euro	Yen	Total
Government 2 yr	1.5%	1.0%	1.0%	0.5%	4.0%
Government 10 yr	1.5%	1.0%	1.0%	0.5%	4.0%
Corporate Bonds 2 yr	3.0%	2.5%	2.5%	0.5%	8.5%
Corporate Bonds 10 yr	3.0%	2.5%	2.5%	0.5%	8.5%
RMBS 2 yr	3.0%	2.0%	2.0%	0.5%	7.5%
RMBS 10 yr	3.0%	2.0%	2.0%	0.5%	7.5%
Equities	30.0%	12.0%	12.0%	6.0%	60.0%
Cash	0.0%	0.0%	0.0%	0.0%	0.0%
Total	45.0%	23.0%	23.0%	9.0%	100.0%

Figure 27: Asset classes in Balanced Portfolio Structure
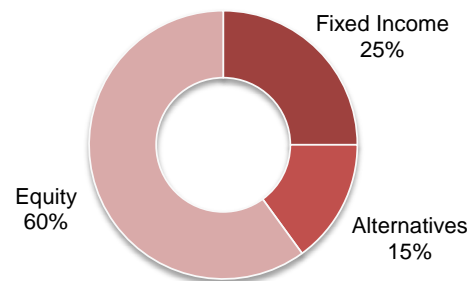
Figure 30: Asset classes in Aggressive Portfolio Structure

Figure 28: Geographic market spread of Balanced Portfolio Structure

Figure 31: Geographic market spread of Aggressive Portfolio Structure

Figure 29: Detailed asset class breakdown of Balanced Portfolio Structure
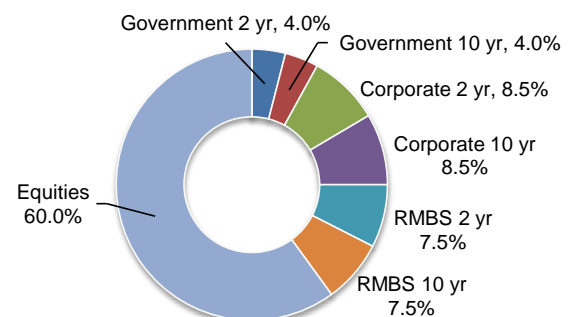
Figure 32: Detailed asset class breakdown of Aggressive Portfolio Structure